A generic rate equation for catalysed, template-directed polymerisation and its use in computational systems biology

by

Olona P.C. Gqwaka

Thesis presented in partial fulfilment of the requirements for the degree of Master of Science (Biochemistry) in the Faculty of Science at Stellenbosch University

Department of Biochemistry
University of Stellenbosch
Private Bag X1, 7602 Matieland, South Africa

Supervisors:

Prof. J.-H.S. Hofmeyr (supervisor) Prof. J.M. Rohwer (co-supervisor)

December 2011

Declaration

By submitting this thesis electronically, I declare that the entirety of the work contained therein is my own, original work, that I am the sole author thereof (save to the extent explicitly otherwise stated), that reproduction and publication thereof by Stellenbosch University will not infringe any third party rights and that I have not previously in its entirety or in part submitted it for obtaining any qualification.

Signature: .....
Olona P.C. Gqwaka

Date: 15 November 2011 .....

Acknowledgements

- Prof. Jannie Hofmeyr for your continuous supervision and patience. For igniting a passion for mathematics, and for imparting unmeasurable knowledge to me. Thank you for not giving up on this work and me but always believing that we would finish.
- Prof. Johann Rohwer for assisting with critical parts of the project.
- Dr. Brett Olivier for your invaluable help with PySCeS.
- Dr. Riaan Conradie and dr. Franco du Preez for assistance with the initial derivation of the rate equation.
- The National Bioinformatics Network (NBN) for funding.
- Mbathane no MaRhadebe for your love, guidance, patience, many funny moments and for always pushing me to never give up. Thank you for understanding that I am an academic at heart.
- Family and friends for always being there and pushing me in the right direction to finish this work. Thank you all for the love.
- God for keeping me sane throughout these years.

For Mbathane no MaRhadebe

Contents

List of Figures

List of Tables

Summary

Progress in computational systems biology depends crucially on the availability of generic rate equations that accurately describe the behaviour and regulation of catalysed processes over a wide range of conditions. Such equations for ordinary enzyme-catalysed reactions have been developed in our group and have proved extremely useful in modelling metabolic networks. However, these networks link to growth and reproduction processes through template-directed synthesis of macromolecules such as polynucleotides and polypeptides. Lack of an equation that captures such a relationship led us to derive a generic rate equation that describes catalysed, template-directed polymerisation reactions with varying monomer stoichiometry and varying chain length. A model describing the mechanism of a generic template-directed polymerisation process in terms of elementary reactions with mass action kinetics was developed. Maxima, a computational algebraic solver, was used to determine analytical expressions for the steady-state concentrations of the species in the equation system from which a steady-state rate equation could be derived. Using PySCeS, a numerical simulation platform developed in our group, we calculated the time-dependent evolution and the steady-states of the species in the catalytic mechanisms used in the derivation of the rate equations. The rate equation was robust in terms of being accurately derived, and in comparison with the rates determined with PySCeS. Addition of more elongation steps to the mechanism allowed the generalisation of the rate equation to an arbitrary number of elongations steps and an arbitrary number of monomer types. To test the regulatory design of the system we incorporated the generic rate equation in a computational model describing a metabolic system consisting of multiple monomer supplies linked by a template-directed demand reaction. Rate characteristics were chosen to demonstrate the utility of the simplified generic rate equation. The rate characteristics provided a visual representation of the control and regulation profile of the system and showed how this profile changes under varying conditions.

Opsomming

Die beskikbaarheid van generiese snelheidsvergelykings wat die gedrag en regulering van gekataliseerde prosesse akkuraat oor 'n wye reeks omstandighede beskryf is van kardinale belang vir vooruitgang in rekenaarmatige sisteembiologie. Sulke vergelykings is in ons groep ontwikkel vir gewone ensiem-gekataliseerde reaksies en blyk uiters nuttig te wees vir die modellering van metaboliese netwerke. Hierdie netwerke skakel egter deur templaat-gerigte sintese van makromolekule soos polinukleotiede en polipeptiede aan groei- en voorplantingsprosesse. Die gebrek aan vergelykings wat sulke verwantskappe beskryf het ons genoop om 'n generiese snelheidsvergelyking af te lei wat gekataliseerde, templaatgerigte polimerisasie-reaksies met wisselende monomeerstoigiometrie en kettinglengte beskryf. 'n Model wat die meganisme van 'n generiese templaat-gerigte polimerisasie-proses in terme van elementêre reaksies met massa-aksiekinetika beskryf is ontwikkel. Maxima, 'n rekenaarmatige algebraïese oplosser, is gebruik om analitiese uitdrukkings vir die bestendige-toestand konsentrasies van die spesies in die vergelyking-stelsel te vind. Hierdie uitdrukkings is gebruik om 'n bestendige-toestand snelheidsvergelyking af te lei. Ons het die tyd-afhanklike progressie en die bestendige toestande bereken van die spesies in die katalitiese meganismes wat gebruik is in die afleiding van die snelheidsvergelykings. Die rekenaarprogram PySCeS is 'n numeriese simulasieplatform wat in ons groep ontwikkel is. Die snelheidsvergelyking blyk akkuraat afgelei te wees en is in ooreenstemming met snelhede deur PySCeS bereken. Die toevoeging van verdere verlengingstappe tot die meganisme het dit moontlik gemaak om die snelheidsvergelyking te veralgemeen tot 'n arbitrêre hoeveelheid verlengingstappe en monomeertipes. Om die regulatoriese ontwerp van die sisteem te toets het ons die generiese snelheidsvergelyking in 'n rekenaarmatige model geïnkorporeer wat 'n metaboliese sisteem bestaande uit verskeie monomeer-aanbodblokke en 'n templaatgerigte aanvraagblok beskryf. Snelheidskenmerkanalise is gekies om die nut van die vereenvoudigde generiese snelheidsvergelyking te demon-

streer. Met hierdie snelheidskenmerke kon ons die kontrole- en reguleringsprofiel van die stelsel visualiseer en wys hoe hierdie profiel verander onder wisselende omstandighede.

Chapter 1

Introduction

Metabolism has been conventionally studied using a reductionistic approach in which metabolic pathways have been regarded as isolated modules. This is also the way that metabolic pathways have traditionally been depicted in biochemistry textbooks. Due to the complexity of metabolic organisation this approach has of course been necessary for the identification of the individual reactions and their substrates, products and cofactors. However, to gain an understanding of the integrated nature of metabolism it is necessary to consider the coupling of metabolic pathways with each other, not only between pathways within intermediary metabolism, but also between intermediary metabolism as a whole with processes such as the synthesis of proteins, polynucleotides and complex lipids, i.e., macromolecular biosynthetic processes that produce the polymers associated with growth and maintenance of the cellular machinery and structure. Metabolites such as amino acids, nucleotides and fatty acids, which are usually described as 'end-products' of metabolism, are actually metabolites that link intermediary metabolism with the synthesis of biopolymers. Such a point of view leads one to consider the functional organisation of cellular processes depicted in Fig. 1.1.

Hofmeyr and Cornish-Bowden [2] developed a quantitative framework called metabolic supply-demand analysis to study the control and regulation of the coupled metabolic 'factories' of catabolism, anabolism, and macromolecular synthesis. They used this analysis to study, for example, the control distribution between the biosynthetic supply of a metabolic product such as an amino acid and the demand for such a product in a macromolecular biosynthetic process such as protein synthesis [2, 3]. They were able to show how the supply and demand become functionally differentiated with regard to the control of flux and the homeostatic maintenance of the concentration of the product that

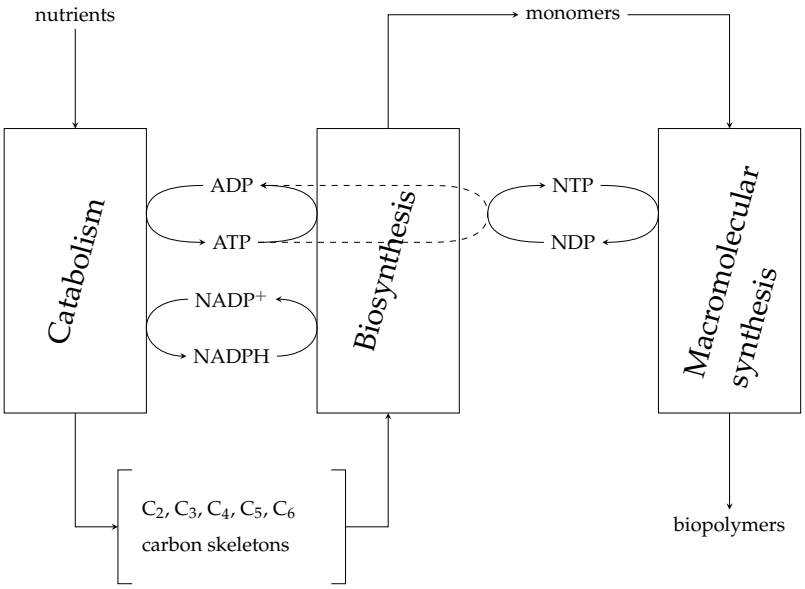

Figure 1.1: The functional organisation of intermediary metabolism. The primary carbon and energy sources are degraded by catabolic pathways to form ATP, reducing equivalents (NADPH), and C_3–C_6 metabolic intermediates (e.g., sugar phosphates, activated CoA-intermediates, PEP, pyruvate, and the intermediates of the citric acid cycle such as oxaloacetate, 2-oxoglutarate and citrate) that act as carbon skeletons for biosynthetic (anabolic) processes that produce monomers for the synthesis of biopolymers (proteins from amino acids, nucleic acids from nucleotides, lipids from fatty acids) and higher-order cellular structures; these processes also require an input of free energy (NTP, nucleotide triphosphates) (Adapted from [1]).

links supply and demand. For example, when the demand controls the flux, the supply takes over the role of maintaining the concentration of the linking metabolic within a narrow concentration range. Feedback by end-product inhibition of the supply pathway determines both the range of variation in concentration (the degree of homeostasis) and the distance from the equilibrium concentration that the product would reach at a fixed supply substrate concentration. Hofmeyr [4] subsequently showed how the addition of a genetic level to the regulation of the concentration of the linking metabolite (by adding a repressor to which this metabolite can bind as co-repressor) and of a catabolic sink for the linking metabolite enriches the regulatory behaviour of the system. In particular, he was able to show which parameters of the different modules must be matched to each other to ensure that the integrated system behaves harmoniously.

Whereas the supply-analysis of a single biosynthetic supply pathway coupled to its demand provided deep insight into the regulatory design of such systems, the really interesting problem is how the cell integrates biopolymer synthesis with the pathways that supply its individual monomers. Fig. 1.2 depicts such a (hypothetical) situation for the synthesis of a polymer from five different monomers, each of which is synthesised by its own biosynthetic pathway, which is subject to feedback regulation both on the metabolic and the genetic level.

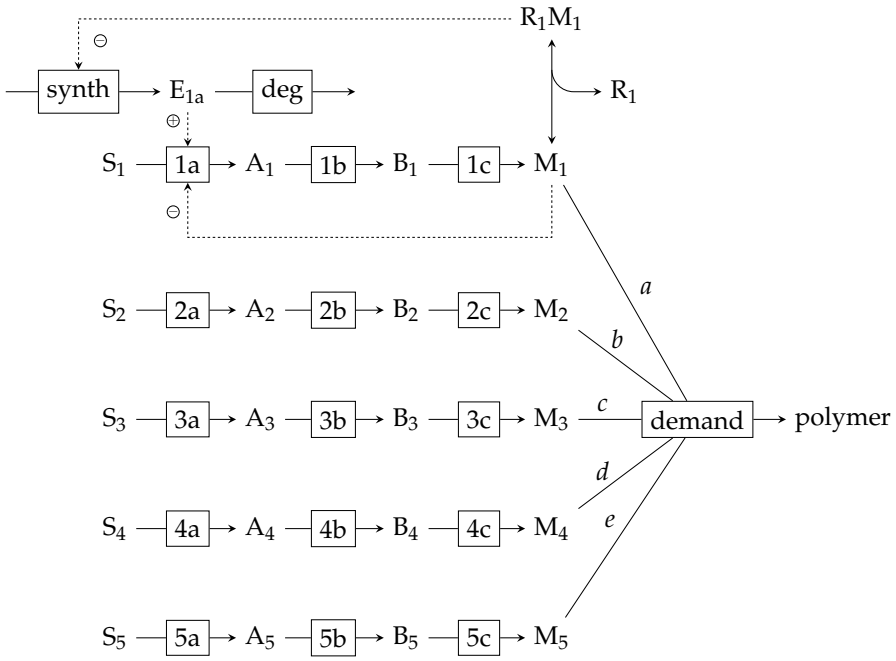

Figure 1.2: Scheme of a supply-demand metabolic system consisting of five biosynthetic (supply) blocks that each produce a monomer, and one demand block that consumes these monomers with the indicated stoichiometries (a to e) to yield a polymer product with monomer composition $(M_1)_a(M_2)_b(M_3)_c(M_4)_d(M_5)_e$. All five supply blocks are regulated both by allosteric feedback and by regulation of expression of the first enzyme; for simplicity sake this is only shown for the first supply block. R_1 is a repressor protein, which, when bound to M_1 (the corepressor), forms a R_1M_1 complex; the latter prevents expression of the structural gene that encodes E_{1a}.

The insight into regulatory design and behaviour described in the previous paragraphs was obtained mostly via computational studies in

which the steady-state behaviour of model pathways was numerically simulated. The field that comprises such studies is now known as computational systems biology [5]. One serious problem that hampered the construction of realistic models was the lack of enzyme rate equations that take account of the reversibility of reactions and phenomena such as cooperativity and allosteric effects. The rate equations of classical enzyme kinetics were generated from studies aimed at probing the mechanisms of catalysis and inhibition/activation and were almost always carried out under conditions that, for instance, ensured that no product was present—this led to irreversible rate equations. Even those rate equations that were developed by, for example, Monod, Wyman and Changeux [6] and Koshland, Nemethy and Filmer [7] to describe cooperativity and allosteric effects were irreversible. It was only in 1997 that the first serious effort was made by Hofmeyr and Cornish-Bowden [8] to remedy this situation; they developed the so-called reversible Hill equation, which incorporated the requirements of reversibility, cooperativity and allosteric effects. In their original paper they only consider single substrate–single product reactions, but the reversible Hill equation has since been generalised to multi-substrate–multi-product reactions [9, 10, 11].

This thesis confronts a similar problem: in order to construct a computational model of a system such as the one depicted in Fig. 1.2 one needs a general rate equation that can account for a catalysed, template-directed polymerisation process that can produce from a specified number of monomer types a polymer with a given monomer composition. Template-directed polymerisation reactions require a tightly coordinated regulation of the pathways that synthesise the monomers that serve as constituents of the polymers. This is because the monomer composition of the polymers varies considerably with conditions. The envisaged rate equation must therefore be able to handle conditions in which there is a varying demand for the monomers that constitute the biopolymers.

There have of course been attempts to study the kinetics of these polymerisation reactions, but they all aim at modelling the details of the complicated mechanistic processes that characterise the synthesis of a particular polymer, usually by either ribosomal polypeptide synthesis or the synthesis of polynucleotides such as DNA or RNA. As is the case with classical enzyme kinetics, the aim of these studies was to understand mechanism, not to understand the integration of these processes with the biosynthesis of the monomers. The type of rate equation required for our purposes is of a different nature, namely that of a single rate equation that describes the whole process and allows for varying monomer stoichiometry.

1.1 Aim and outline of this study

The main aim of this study was to derive a generic rate equation that describes catalysed, template-directed polymerisation reactions with varying monomer stoichiometry. For this purpose we intentionally simplified the extremely complicated details of processes such as protein and polynucleotide synthesis, especially with regard to the initiation reactions. We were able to develop such an equation and show how it can be used in a supply-demand analysis of the system in Fig. 1.2 through the use of rate characteristics. It must be emphasised, however, that this demonstration of its use served purely to show its utility. We did not aim to do an extensive supply-demand analysis of the regulatory design of such systems; it was felt that such an extension of the study would far exceed the scope of an M.Sc.-thesis.

Chapter 2 is an overview of the surveyed literature on available kinetic models that describe the synthesis of macromolecules.

Chapter 3 describes the derivation of a generic rate equation for template-directed polymerisation and forms the bulk of the thesis. Our initial strategy was to derive a rate equation for an irreversible Michaelis-Menten mechanism in which the enzyme first binds to a template before a single monomer is converted into a product. This allowed us to formulate conditions under which a steady-state could be established. Subsequently, we included the binding of a second and a third monomer so that we could incorporate dimerisation and elongation to produce a trimer. We obtained a rate equation to which we added additional elongation steps to provide a pattern from which we could generalise the equation to account for an arbitrary number of monomer types with arbitrary stoichiometry. Chapter 3 also deals with the validation of the derived rate equation and possible simplifications.

In Chapter 4 we use the derived equation in a computational supply-demand analysis of the system in Fig. 1.2.

Finally, in Chapter 5, we discuss our results in general and speculate on future studies.

Chapter 2

Literature review

Template-directed polymerization reactions, such as DNA replication, transcription and translation, form the basis of the 'central dogma' of molecular biology articulated by Crick [12]. It states that once sequence information is transferred into proteins it cannot be transferred back [12]. This transfer of sequence information is central to cellular function in living organisms [13, 14]. Synthesis of biopolymer molecules, DNA, RNA and proteins, is tightly regulated by complex machinery [13]. Translation displays the highest degree of complexity as a result of the large number of reacting molecules and individual steps involved in the production of proteins [13, 15, 16].

This chapter reviews a number of studies that had as aim the description of the detailed kinetics of biopolymer synthesis in the processes of transcription and translation. The aim of these kinetic models was to gain a better understanding of the overall reaction mechanisms as well as determining crucial components in the system that have an effect on the rate of biopolymer production. These studies had to deal with the issue of complex rate equations consisting of many parameters, and had to make simplifying assumptions, such as the rapid equilibrium [17] and steady-state assumptions [18, 19, 20].

2.1 Polynucleotide synthesis: Transcription

Transfer of genetic information from the primary genetic material, DNA, to RNA encompasses the process of transcription. The process consists of initiation, elongation and termination phases. The details of this complex process differ considerably between prokaryotes and eukaryotes [13].

The following discusses a few of the kinetic models that have been

developed to explain various aspects of the transcription mechanism: *in vitro* transcription by T7 RNA polymerase [21], the stochastic nature of transcription [22, 23], and gene transcription kinetics mediated by dimeric transcription factors [24].

Kinetic modelling of transcription by T7 RNA polymerase

Bacteriophage T7 RNA polymerase drives the promoter-specific DNA-directed RNA synthesis both *in vivo* and *in vitro* [25, 26]. The T7 RNA polymerase enzyme consists as a single subunit, has a low error rate, and requires Mg^{2+} ions that function as cofactors [25]. These properties and the 'uncomplicated' nature of this enzyme have assisted in the development of kinetic models of the transcription mechanism [27].

Following the development of a Michaelis-Menten-type equation by Pozhitkov *et al.* [27] for transcription kinetics, Arnold *et al.* [21] developed a kinetic model of *in vitro* transcript polymerisation. The model of Arnold *et al.* uses linear genomic sequence data to derive a rate equation characterising the overall mechanism of transcription. In constructing the model, they described initiation as a random-order binding mechanism between the T7 promoter, D, and GTP, the initiator nucleotide, therefore assuming rapid equilibrium to occur [17, 21]. This assumption helped them reduce complexity in the derived rate equation by removing the squared terms $[GTP]^2$ and $[D]^2$. By representing initiation as a random-order binding mechanism, they forced initiation to be the rate-limiting step in the mechanism [28]. Translocation of the enzyme along the template was modelled as an irreversible step. They assumed the addition of nucleotides to the growing RNA chain to be independent of the nucleotide sequence of the RNA chain. Elementary steps of competitive inhibition, i.e., competition of the free nucleotides for the RNA polymerase, the promoter-RNA polymerase complex and transcription complex, were defined in the model. Termination was defined as the disintegration of the transcription complex and the subsequent release of the transcript.

With the help of an automated algorithm and simulation experiments on the model, Arnold *et al.* derived the following rate equation describing the synthesis of RNA.

$$v = \frac{V_{\max}}{1+\sum_{j=1}^{N}\frac{K_{M,NTP,j}}{C_{NTP,j}}\left(1+\frac{C_{PPi}}{K_{I,PPi}}+\sum_{\substack{i=1\\ i\neq j}}^{N}\frac{C_{NTP,j}}{K_{M,NTP,i}}\right)+\frac{K_{M,D}}{C_D}\left[1+\frac{K_G^I}{C_{GTP}}\left(1+\frac{C_{PPi}}{K_{I,PPi}}+\sum_{i=1}^{N-1}\frac{C_{NTP,i}}{K_{I,NTP,i}}\right)\right]} \tag{2.1}$$

where the concentrations of nucleoside triphosphates, total promoter and the inhibitor inorganic pyrophosphate are denoted as C_{NTP}, C_D and C_{PPi}, respectively. N is the number of ribonucleotides that the product is composed of. Dissociation constants are denoted by K_{m}-values. This rate equation therefore covers transcript length, nucleotide composition and the rate constants for transcription initiation, elongation, and termination.

As is often done in the process of deriving rate equations, Arnold *et al.* made simplifying assumptions to reduce the complexity in eqn. 2.1. First, they assumed that the effect of competing nucleotide substrates may be significant only at concentrations above several millimolar of competing NTP and could therefore be neglected. Second, they assumed saturation by all nucleotides, so that the rate depended solely on promotor concentration C_D. This yielded an expression of the form of an irreversible Michaelis-Menten Eqn. 2.2:

$$v = \frac{V_{\max} C_D}{K_{M,D} + C_D} \tag{2.2}$$

The authors emphasised the capability to incorporate linear genomic sequence information for simulation of nonlinear *in vitro* transcription kinetics as a novel feature of their model.

Stochasticity of transcription

The processes that express genes, namely transcription and translation, are known to be tightly regulated, so ensuring the synthesis of particular proteins when required by the cell [16]. A consideration of the kinetics of transcription has provided significant insight in the regulation of these processes. Apart from this tight regulation, transcription has been shown to display stochasticity [23].

Stochastic systems originate from molecular interactions that involve small numbers of reacting molecules [23, 29]. In transcription these interactions occur as randomly occurring fluctuations that lead to an appreciable amount of molecular noise in the number of mRNA produced [23, 29]. Kinetic modelling studies investigating this feature in transcription have provided quantitative data [22, 23, 29, 30] that can be used in the ongoing quest to incorporate stochasticity into a quantitative model of the cell.

Jülicher and Bruinsma [22] developed a stochastic model based on classical chemical kinetics that describe polymerization reactions driven

by a free energy gain that depends on forces applied externally at the catalytic site. Their major interest was to compare the motion of RNA polymerase along the DNA chain with that of motor proteins such as kinesins that are used for fast transport in cells by moving along microtubules; in comparison RNA polymerase has to produce an RNA strand that is an exact copy of the DNA template. Their model will not be discussed in detail for stochastic modelling has little bearing on the deterministic type of rate equation developed in this thesis.

Different to the model of Jülicher and Bruinsma, Höfer and Rasch proposed a model of transcription that depicted initiation as a multi-step process [23]. In their model a promoter is activated by the binding of transcription factors making it competent for the recruitment, the subsequent binding of RNA polymerase, and the start of transcription. The evolution of this system was modelled with the help of the master equation [31].

Transcription factor mediated gene transcription

Classical gene transcription kinetic studies involved the empirical fitting of experimentally observed data with the Hill function [32] or S-system analysis [33]. Enzyme kinetics, on the other hand, has made extensive use of the mechanistic approach of Michaelis and Menten [34] to derive rate equations. This inspired Yang *et al.* [24] to draw an analogy between enzyme and transcription reactions, on the basis of which they derived analytical expressions for gene transcription rates that describe the kinetics of gene transcription mediated by dimeric transcription factors.

The model of Yang *et al.* focuses solely on the initiation stage of transcription and does not account for the stages of elongation and termination. In developing the model, the promoter sequence of the template molecule was assumed to always be exposed to the binding by transcription factors and polymerases. In their quest for a simple system Yang *et al.* ignored the intermediate reactions involved upon the binding by transcription factors. Adding on to the model of Cranz *et al.* [35], Yang *et al.* incorporated an irreversible step that accounts for the synthesis of the pre-initiation complex [24]. As this model does not account for the termination stage, i.e., the production of the final mRNA, it was assumed that the production of a copy of mRNA preceded the formation of the pre-initiation complex. Therefore, the transcription rate was assumed to be the rate of formation of the pre-initiation complex:

$$v = k_5[DT_2] \tag{2.3}$$

where k_5 denotes the rate constant and DT_2 the promoter and dimeric transcription factor complex (the original notation and numbering is retained).

Numerical simulations were performed on a set of ordinary differential equations that describe the time-dependent evolution in the concentrations of the species involved. Changes in the formation rates were also calculated.

On the basis of these results the derived analytical rate expression was simplified by reducing the number of variables using assumptions of mass balance, pre-equilibrium between the transcription factor forms and quasi-steady state:

$$V_{[T]_0} = k_5[DT]_2 = \frac{2k_1k_2k_5[D]_0[T]_0^2}{a[T]_0^2 + b[T]_0 + c} \tag{2.4}$$

where
a = $2k1k_2(K_D + 1)$
b = $8k_1K_N + k_2K_4K_p$
c = $2K_NK_p$
and $K_D = \frac{(k_5 + k_{-2'})}{k_{2'}}, K_N = k_{-2}K_D + k_5, K_4 = k_{-4}/k_4$ and $K_p = k_{-1} + \sqrt{k_{-1}^2 + 8k_1k{-}1[T]_0}$ where the k coefficients are rate constants and the K coefficients are dissociation constants.

Analytical expressions for the parameters of the Hill and S-system systems were derived from eqn. 2.4. This model focused only on the binding of Gcn4p (a homodimer molecule) to a promoter and can be applied to a heterodimer gene transcription system [24]. The results suggest that the derived expression shares similarities with the rate laws of enzyme reactions.

2.2 Polypeptide synthesis: Translation

The synthesis of polypeptides by translation of an mRNA is similar to the transcription process in that it occurs in three stages: initiation, elongation and termination. Initiation is the most complex part of translation and consists of four steps (in eukaryotes):

- the dissociation of ribosomes into 40S and 60S subunits,

- the formation of the pre-initiation complex that is made up of $tRNA^{Met}$ (the initiator tRNA), GTP as an energy source, the initiation factor eIF-2, and the 40S ribosomal subunit,
- the attachment of the pre-initiation complex to the mRNA,
- the attachment of the 60S ribosomal subunit to this complex to yield a 80S initiation complex.

The mRNA is initially attached to the ribosomal peptide site (P-site) of the 80S initiation complex. Free aminoacyl-tRNAs bind to the amino acid site (A-site) of the ribosome. In the elongation phase, addition of amino acids to the growing end of the polypeptide chain causes the 80S initiation complex to move along the mRNA to the next codon. Upon reaching a stop codon on the mRNA, the polypeptide chain is released and the tRNA dissociates from the ribosome [13].

The various steps involved in translation make it a highly complex process; theoretical and modelling studies therefore tended to focus only on selected features of the process.

Theoretical model on the kinetics of biopolymerisation

As part of a series of publications, MacDonald *et al.* [36] developed a theoretical model of polypeptide biosynthesis as an extension to the work of Pipkin and Gibbs [37]. MacDonald *et al.* incorporated the simultaneous synthesis of several polypeptide chains along a single template molecule. To this the feature of depolymerisation, i.e., a reverse reaction, was added.

MacDonald *et al.*'s model closely followed that of Pipkin and Gibbs, which represented the synthesis of polypeptides as the diffusion of a single point (the growing centre) along a one-dimensional lattice (i.e., template). The model was defined as an ensemble of systems, with each system made up of several segments that individually polymerise on a one-dimensional lattice of K sites, i.e., codons [36]. Non-overlapping of the segments was assumed to determine two sets of rates, uniform-density and steady-state solutions. Elongation was represented by the polymerisation centre moving along one lattice site j. On the basis of experimental evidence for ribosomal coverage of multiple lattice sites a parameter L was defined in the model to describe this feature [36].

The motion of the growing centre along the lattice was assumed to exist in the states of occupancy ($s = 1, 2, ...L$) and emptiness ($j = 0$). A probability term $n_j(t)$ describing the lattice in the j^{th} site occupied at

time t by a segment was defined. Solutions for $n_j^{(s)}(t)$ were determined. The segments were allowed to react either in forward (polymerisation) or backward (depolymerisation) directions, thus permitting derivation of the forward and backward fluxes. A flux equation was thus derived incorporating both the forward and backward reactions:

$$q_j(t) = k_f \frac{n_j(t)\left[1 - \sum_{s=1}^{L} n_{j+s}(t)\right]}{1 - \sum_{s=1}^{L} n_{j+s}(t) + n_{j+L}(t)} - k_b \frac{n_{j+1}(t)\left[1 - \sum_{s=1}^{L} n_{j-L+s}(t)\right]}{1 - \sum_{s=1}^{L} n_{j-L+s}(t) + n_{j-L+1}(t)} \tag{2.5}$$

To validate eqn. 2.5 it was used to determine the range over which the rates of polymerisation occur through uniform-density and steady-state cases. Results from these experiments indicated that initiation and termination determined the region(s) of uniformity [36].

Part III of this series of publications [38] attempted to bridge the gap between theory and experimental work on the biosynthesis of polypeptides by providing experimental kinetic information for subsequent studies. Hiernaux [39] performed a stability analysis on these results with respect to the rate constants involved in initiation, elongation and termination. Hiernaux's analysis agreed with results from MacDonald *et al.* [38] and later Vassart *et al.* [40], suggesting that translational control resides in the initiation and termination stages.

Model for the regulation of mRNA translation

The pioneering work of MacDonald and co-workers described in the previous section led to the derivation by Lodish [41] of a rate equation that describes the synthesis of polypeptide chains in multicellular organisms. Lodish's equation explained how initiation and elongation affect the rate at which proteins were synthesised. He then used his rate equation in a study of the regulation of the α and β-globin mRNAs in the reticulocytes [41].

Initiation was characterised by a single reaction between mRNA and the Met-tRNA-ribosome complex leading to the formation of the 80S initiation complex. The rate constant did not account for the several factors and steps known to be involved in this step [41]. Elongation and termination were defined as the addition of amino acids to the nascent chain and as the release of the completed polypeptide chain, respectively. Contrary to this approach, Bergmann and Lodish [42] constructed a more complex

model accounting for the many factors and steps involved in the process of protein synthesis. Lodish [41] assumed that the rate constant for the addition of amino acids and that of elongation were the same. Similarly to MacDonald *et al.* [36], Lodish defined the terms L, n_i. The even distribution of ribosomes on the mRNA was assumed to exist as it had been previously shown [43, 44]. Termination was assumed not to govern the rate of protein synthesis. These assumptions led to the derivation of a mathematical expression that accounted for the entire process of protein synthesis.

$$Q = mR^*K_1[1 - \frac{L}{\frac{K_e}{K_1R*} + L - 1}] \tag{2.6}$$

where m is the concentration of the mRNA and R^* the concentration of the Met-tRNA-ribosome complex.

Calculations on the parameters n, L, K_1, K_e were performed in terms of the concentration of the Met-tRNA$_f$-40S complex, R^*, and the effect of inhibition in the initiation stage. The rate of protein synthesis was shown to display a level of dependency on R^* and K_1.

Following Lodish's representation of the initiation stage as a single reaction between mRNA and the R^* complex, Godefroy-Colburn and Thach developed a kinetic model where initiation was characterised as a multi-step reaction [45]. Godefroy-Colburn and Thach introduced a 'discriminatory factor' that would bind mRNA prior to the pre-initiation complex. Elongation and termination were modelled similarly to that of Lodish's model [41, 42]. The model was applied amongst others in *in vitro* translational competition between α and β-globin, in the effect of elongation inhibitors, and in the effect of competition of the mRNAs for the discriminatory factor [45].

Model of the elongation step in protein synthesis

Mehra and Hatzimanikatis presented a genome wide mechanistic model for translation that aims to explain the lack of correspondence between mRNA and protein expression profiles shown by experimental studies. Their model, an augmented form of the models described previously [15, 36, 38], incorporated an additional feature of the initiation phase, i.e., the reversible attachment of the ribosome around the Shine-Dalgarno sequence [46]. This sequence allows for the recognition and backward binding of the ribosome [46]. Mehra and Hatzimanikatis developed a genome-wide algorithmic framework for subsequent models of transla-

tion. This study suggested that polysome sizes would give some insight on the rate at which proteins were synthesised.

Following this, Zouridis and Hatzimanikatis presented a deterministic, kinetic model of the protein synthesis process that is specific at the sequence level. Contrary to the models of MacDonald and Gibbs [36, 38] and of Heinrich and Rapoport [15] that modelled the elongation phase as a single step by means of k_e, the elongation rate constant, this model encompasses the fundamental steps involved in the elongation phase of the translation process [47]. The elongation factors Tu (Ef-Tu), Ts (Ef-Ts) and G (Ef-G), which act as cofactors in the process, were incorporated in this model [47]. The focus on the elongation phase was as a result of previous work that showed the codons on the mRNA to possess varying elongation kinetics [48, 49, 50]. This variation at the codon level has been shown to be a result of the competition for accurate tRNAs [48], codon-anticodon compatibility [49, 50], and the many elements involved in the steps of elongation. Later, Fluitt *et al.* [51] showed that at the codon level the accessibility to cognate, near-cognate and non-cognate charged tRNAs affected the rate of translation.

In formulating their model, Zouridis and Hatzimanikatis assumed the ribosomes at each codon to be in separate states, thus defining the elongation phase in terms of the different states of the ribosome. Similar to the model developed by Lodish [41], Zouridis and Hatzimanikatis modelled the initiation phase as a bimolecular reaction between the ribosome and initiator site on the mRNA. The ribosomes were set to cover 12 codons, all the free tRNAs were assumed to be in the ternary complex (elongation factor-aminoacyl-tRNA complex), and the reaction rate constants involved in the elongation phase were defined to be the same. The concentration of near and non-cognate tRNAs was assumed to be negligible. First order binding kinetics was assumed for the elongation factors and the states of the ribosomes. The release step was also assumed to follow first order kinetics. The model was characterised by flux expressions.

Sensitivity analysis was performed on the model to determine the effects of the constituents of the translation process on the rate of translation. The model was applied in the investigation of the steady-state behaviour of translation of the *trpR* gene in *Escherichia coli*. These researchers investigated the relationship between the rate at which proteins are synthesised with varying polysome sizes and it was shown that the rate of translation dependended on a certain size of the polysomes, i.e., translation was shown to possess a proportional relationship with polysome size. The kinetics of the translation process were found to be initiation or elongation-limited for low or intermediate polysome sizes,

while termination-limited at high polysome sizes [47]. As with previous studies, the ribosomes were shown to be evenly distributed along the mRNA with respect to codon positions in the initiation and elongation-limited regions. Zouridis and Hatzimanikatis therefore concluded that when polysome sizes agreed with certain elongation rate constants, translation rates were influenced [47, 51]. This study presented evidence of the effects of ribosome crowding and served as an adequate reference for subsequent studies.

Fluitt *et al.* [51] proposed a mathematical model for ribosomal kinetics that results from the competition at the codon level between cognate, near and non-cognate aminoacyl-tRNAs. The Fluitt *et al.* model formulation required far fewer assumptions than those made previously by Zouridis and Hatzimanikatis, therefore making this model a more useful tool for studying the kinetics of translation. Fluitt *et al.* assumed the pool of tRNAs to be constant and that the hampering caused by other ribosomes on a mRNA was negligible. The transport of the charged tRNAs was defined as a random diffusion process. To obtain the kinetics of this process, the times at which the charged tRNAs arrived at the ribosomes and the diffusion coefficients were defined in the model. This model showed that the availability of tRNAs influenced the rate at which the polypeptide chain was formed, i.e., tRNAs affected elongation rates.

As mentioned in the beginning of this chapter the studies reviewed here all focussed on particular aspects and details of the mechanism of transcription and translation. Not one of the mathematical models or, where specifically derived, rate equations that were developed can serve our purposes as we outlined them in Chapter 1. The next chapter describes how we developed, from basic principles, a suitably generic rate equation for template-directed polymerisation that ignores most of the intricacies of the previous models but instead focusses on accounting for the polymerisation rate response to enzyme, template, and monomer concentrations, and, most importantly, polymer length and composition.

Chapter 3

Derivation of a generic rate equation for catalysed, template-directed polymerisation reactions

3.1 Introduction

This chapter presents the derivation of a generic rate equation for a catalysed, template-directed polymerisation reaction. The derivation is built up gradually, starting with a simple mechanism that is identical to the irreversible Michaelis-Menten mechanism, except that the enzyme first binds to a template molecule. Before handling the added complexity of a polymerisation reaction, we wanted to study a mechanism which contains a binding step that is allowed to fully equilibrate without fixing any of the enzyme or template forms. This analysis suggested a way of handling the complexities that binding of template to enzyme introduces. We then progressively added elongation steps into the mechanism and were able to derive a generic steady-state rate equation for template-directed polymerisation.

3.2 Methods

We used the simulation platform PySCeS [52, 53] to calculate both the time-dependent evolution and the steady-states of the species in the catalytic mechanisms used in the derivation of the rate equation. Models were defined in a PySCeS input file in terms of reactions, species and pa-

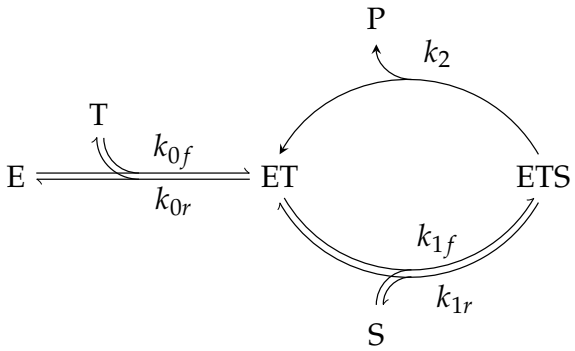

Figure 3.1: Reaction scheme of a classical Michaelis-Menten mechanism that converts S to P, but in which the enzyme E first binds to a template molecule T (which eventually will be the template that directs the sequence in which monomers bind and are ligated). ET and ETS are the intermediate complexes. P, the final product is released from ET. The half-headed arrows denote the reversible steps with the single-headed arrows denoting catalytic steps. k_{0f}, k_{0r}, k_{1f}, k_{1r}, and k_2 are rate constants.

rameters. Analytical steady-state solutions of the systems of differential equations that describe the reaction mechanisms were obtained using the 'Solve' function of the computer algebra software Maxima [54].

3.3 A preliminary model

As a point of departure we derived a steady-state rate equation for a uni-uni Michaelis-Menten type mechanism in which the enzyme first binds to a template molecule T (Fig. 3.1). Although T does not really play the role of template in this preliminary mechanism we shall already refer to it by this name. T binds to the enzyme E to yield an enzyme-template complex (ET). A substrate (S) subsequently binds to ET forming an enzyme-template-substrate complex (ETS). S is converted in product P, which is then released from ET.

The time-dependent evolution of the concentrations of species involving enzyme or template in this system was described by the following set of ordinary differential equations:

$$\frac{d[\mathrm{S}]}{dt} = k_{1\mathrm{r}}[\mathrm{ETS}] - k_{1\mathrm{f}}[\mathrm{ET}][\mathrm{S}] \tag{3.1}$$
$$\frac{d[\mathrm{P}]}{dt} = k_2[\mathrm{ETS}] \tag{3.2}$$
$$\frac{d[\mathrm{E}]}{dt} = k_{0\mathrm{r}}[\mathrm{ET}] - k_{0\mathrm{f}}[\mathrm{E}][\mathrm{T}] \tag{3.3}$$
$$\frac{d[\mathrm{T}]}{dt} = k_{0\mathrm{r}}[\mathrm{ET}] - k_{0\mathrm{f}}[\mathrm{E}][\mathrm{T}] \tag{3.4}$$
$$\frac{d[\mathrm{ET}]}{dt} = k_{0\mathrm{f}}[\mathrm{E}][\mathrm{T}] + (k_{1\mathrm{r}} + k_2)[\mathrm{ETS}] - (k_{0\mathrm{r}} + k_{1\mathrm{f}}[\mathrm{S}])[\mathrm{ET}] \tag{3.5}$$
$$\frac{d[\mathrm{ETS}]}{dt} = k_{1\mathrm{f}}[\mathrm{ET}][\mathrm{S}] - (k_{1\mathrm{r}} + k_2)[\mathrm{ETS}] \tag{3.6}$$

where [species] denotes concentrations.

There are two linear dependencies in this set of differential equations. The first is the sum of eqns. 3.3, 3.5 and 3.6, which leads to the conservation equation for enzyme:

$$[\mathrm{E}]_\mathrm{t} = [\mathrm{E}] + [\mathrm{ET}] + [\mathrm{ETS}] \tag{3.7}$$

where $[\mathrm{E}]_\mathrm{t}$ denotes the total concentration of the enzyme.

The second is the the sum of eqns. 3.4, 3.5 and 3.6, which leads to the conservation equation for template T:

$$[\mathrm{T}]_\mathrm{t} = [\mathrm{T}] + [\mathrm{ET}] + [\mathrm{ETS}] \tag{3.8}$$

where $[\mathrm{T}]_\mathrm{t}$ denotes the total concentration of template T.

The rate of the production of P depends on the concentration of ETS:

$$v = \frac{d[\mathrm{P}]}{dt} = k_2[\mathrm{ETS}] \tag{3.9}$$

At *steady-state* (assuming constant [S] and [P]), eqns. 3.3–3.6 are equal to zero and are referred to as balance equations:

$$k_{0\mathrm{r}}[\mathrm{ET}] - k_{0\mathrm{f}}[\mathrm{E}][\mathrm{T}] = 0 \tag{3.10}$$
$$k_{0\mathrm{f}}[\mathrm{E}][\mathrm{T}] + k_{1\mathrm{r}}[\mathrm{ETS}] + k_2[\mathrm{ETS}] - (k_{0\mathrm{r}} + k_{1\mathrm{f}}[\mathrm{S}])[\mathrm{ET}] = 0 \tag{3.11}$$
$$k_{1\mathrm{f}}[\mathrm{ET}][\mathrm{S}] - (k_{1\mathrm{r}} + k_2)[\mathrm{ETS}] = 0 \tag{3.12}$$

Eqn. 3.10 expresses the fact that in steady state the enzyme-template dissociation reaction is in equilibrium, and could therefore be rewritten as:

$$K_0 = \frac{k_{0r}}{k_{0f}} = \frac{[E][T]}{[ET]} \tag{3.13}$$

where K_0 denotes the dissociation constant for the enzyme-template complex.

Similarly, eqn. 3.12 was rewritten as:

$$K_m = \frac{k_{1r} + k_2}{k_{1f}} = \frac{[ET][S]}{[ETS]} \tag{3.14}$$

Time-dependency behaviour of the system

In order to obtain a mental picture of how the mechanism in Fig. 3.1 behaves dynamically, a kinetic model was defined in a PySCeS [52] input file (see Appendix 6.1). S was clamped at a constant concentration of 10.0 and all rate constants were arbitrarily set to a value of 1.0. The total concentration of E was 10-fold higher than that of T ($[E]_t = 10 \cdot [T]_t$). This choice was based on the rather arbitrary assumption that the template concentration would be the limiting factor in physiological conditions (however, whether this assumption is justified is irrelevant to the derivation that follows, because the roles of E and T in the mechanism are symmetric, and therefore interchangeable).

The time-dependent changes in concentrations of E, T, ET, ETS and P were calculated (Fig. 3.2). The concomitant changes in the rates of the three reactions as a function of time are shown in Fig. 3.3.

E and T equilibrated with ET, which initially increased, but then decreased as it was converted to ETS through the binding of S. Eventually, for this set of parameters, most of the template accumulated in the form of ETS as the system approached a steady state where the net reaction rate (rate of change of [P] with time) became constant.

The rate profile in Fig. 3.3 also clearly shows how the rate of reaction R0 fell to zero as the reaction approached equilibrium, while the rates of R1 and R2 approached each other to become equal in the steady state.

A steady-state rate equation

From the rate expression $v = k_2[ETS]$ (eqn. 3.9) it is clear that in order to obtain a steady-state rate equation for the scheme in Fig. 3.1 we needed to derive an expression for [ETS].

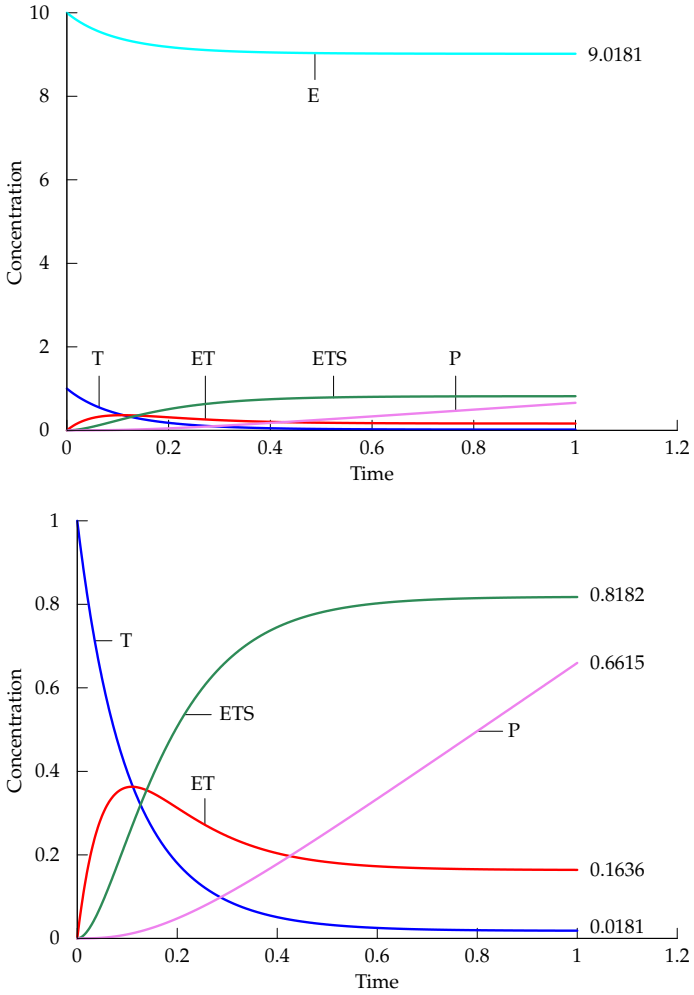

Figure 3.2: Time-dependent concentration changes of E, T, ET, ETS and P in Scheme 3.1 shown on two different concentration scales. The decrease in the concentration change of E from a value of 10.0 tracks that of T from a value of 1.0. The concentration of S was kept constant at a value of 10.0. All rate constants were set to 1.0 (see Appendix 6.1 for the PySCeS model file with initial conditions and parameter values). Numbers next to the curves indicate the steady-state concentrations (except for that of P, which does not reach a steady state but keeps accumulating).

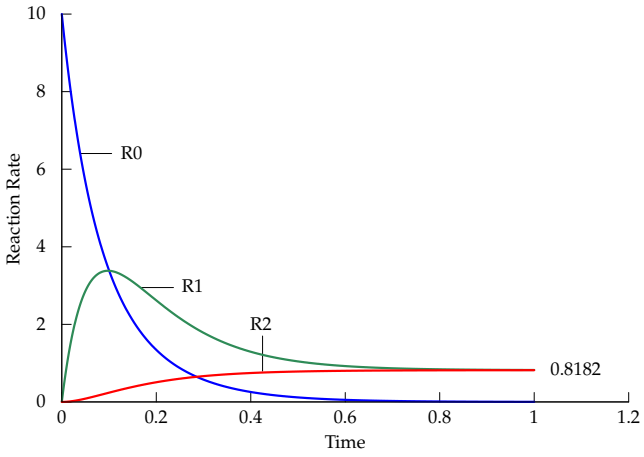

Figure 3.3: Time-dependent changes of rates of the reactions 1, 2 and 3 in Scheme 3.1. The number next to the R1 and R2 rate curves indicates the steady-state flux. The initial conditions and parameter values are described in Fig. 3.2.

We obtained the following analytical expression for [ETS] by solving eqns. 3.7, 3.8, 3.13, and 3.14, using the 'Solve' function of the computer algebra program Maxima [54]:

$$[\mathrm{ETS}] = \frac{\begin{array}{c}\frac{[\mathrm{S}]}{K_\mathrm{m}}\left(1+\frac{[\mathrm{S}]}{K_\mathrm{m}}\right)\left[K_0\left(2[\mathrm{T}]_\mathrm{t}+[\mathrm{E}]_\mathrm{t}\right)+[\mathrm{T}]_\mathrm{t}\left([\mathrm{T}]_\mathrm{t}-[\mathrm{E}]_\mathrm{t}\right)\left(1+\frac{[\mathrm{S}]}{K_\mathrm{m}}\right)\right] \\ \pm\frac{[\mathrm{S}]}{K_\mathrm{m}}\left[\left(1+\frac{[\mathrm{S}]}{K_\mathrm{m}}\right)[\mathrm{T}]_\mathrm{t}+K_0\right]X\end{array}}{\left(1+\frac{[\mathrm{S}]}{K_\mathrm{m}}\right)^2\left[\left([\mathrm{T}]_\mathrm{t}-[\mathrm{E}]_\mathrm{t}\right)\left(1+\frac{[\mathrm{S}]}{K_\mathrm{m}}\right)+K_0\pm X\right]} \tag{3.15}$$

where

$$X = \sqrt{\left([\mathrm{T}]_\mathrm{t}-[\mathrm{E}]_\mathrm{t}\right)^2\left(1+\frac{[\mathrm{S}]}{K_\mathrm{m}}\right)^2+2K_0\left([\mathrm{T}]_\mathrm{t}+[\mathrm{E}]_\mathrm{t}\right)\left(1+\frac{[\mathrm{S}]}{K_\mathrm{m}}\right)+K_0^2} \tag{3.16}$$

This expression was far too complex to be of any practical use. We therefore made the additional assumption that the concentration of free enzyme, [E], is constant (clamped). We could just as well have considered a clamped free [T]; the two situations are symmetrical. This removed the conservation equation 3.7 for $[\mathrm{E}]_\mathrm{t}$ from the system, which then reduced to eqns. 3.8, 3.13, and 3.14. This may seem too restricting an assumption, but if it is taken into account that usually there is much less template than enzyme, i.e., $[\mathrm{E}]_\mathrm{t} \gg [\mathrm{T}]_\mathrm{t}$, then this would imply that $[\mathrm{E}] \approx [\mathrm{E}]_\mathrm{t}$. However,

in what follows we did not assume that $[E] \approx [E]_t$, only that free enzyme concentration $[E]$ was fixed.

Solving for ETS allowed us to construct the rate equation as:

$$v = k_2[ETS] = \frac{k_2[T]_t \frac{[S]}{K_m}}{1 + \frac{K_0}{[E]} + \frac{[S]}{K_m}} \tag{3.17}$$

Symmetrically, if we assumed a fixed $[T]$ and a variable $[E]$, we obtained an analogous expression:

$$v = k_2[ETS] = \frac{k_2[E]_t \frac{[S]}{K_m}}{1 + \frac{K_0}{[T]} + \frac{[S]}{K_m}} \tag{3.18}$$

These equations exhibit an additional positive term ($K_0/[E]$ or $K_0/[T]$) in the denominator, as compared to the usual irreversible Michaelis-Menten equation in the absence of binding of T.

When we made the assumption of *near-equilibrium* in the ETS $\rightleftharpoons$ ET + S dissociation reaction, i.e., $k_{1r} \gg k_2$, eqn. 3.14 simplified to

$$K_s = \frac{k_{1r}}{k_{1f}} = \frac{[ET][S]}{[ETS]} \tag{3.19}$$

Under this assumption eqn. 3.17

$$v = k_2[ETS] = \frac{k_2[T]_t \frac{[S]}{K_s}}{1 + \frac{K_0}{[E]} + \frac{[S]}{K_s}} \tag{3.20}$$

In this section we have established that allowing both enzyme and template to vary freely yielded too complex a rate equation; we needed to assume either a fixed $[E]$ (as was done above) or a fixed $[T]$. As the main aim of this study was to generate a rate equation for catalysed, template-directed polymerisation reactions, we now extended the enzyme mechanism of the simple catalysed, template-directed system to cater for a dimerisation of two monomers on the template and one subsequent elongation step.

3.4 Extended Model

We extended the reaction scheme in Fig. 3.1 by incorporating a template-directed polymerisation process consisting of an initial dimerisation step followed by one elongation step and a final product release step (see Fig. 3.4A). Two monomers, M_1 and M_2, bind sequentially to the enzyme-template complex (ET) and are then coupled. A third monomer M_3 binds and is coupled to the dimer ETM_1–M_2 to yield a trimer ETM_1–M_2–M_3. Finally, a polymer product M_1–M_2–M_3 is released from ET. Binding steps were considered to be reversible, while the condensation and product release steps were considered to be irreversible (we assumed that the monomers of template-directed condensation reactions are usually activated by the attachment of a good leaving group, so that the catalytic reactions have a large equilibrium constant).

To avoid later confusion we note here that M_1, M_2, M_3, etc. refer specifically to the positions the monomers occupy in the polymer sequence (or, equivalently, the positions where the monomers enter the reaction mechanism). They do not refer to the identities of the monomers. Accordingly, $[M_3]$, for example, refers to the concentration of the monomer that occupies position 3 in the polymer sequence.

In Fig. 3.4A there is an explicit product release step with rate constant k_6. If it is assumed that the release of product is must faster than the catalytic elongation step, the reaction mechanism can be simplified to the scheme in Fig. 3.4B. In what follows this simplified scheme is used as the basis for the derivation of a steady-state rate equation. We discuss the difference between the two mechanisms in Section 3.4.

The system in Fig. 3.4 could be expressed in terms of ordinary differential equations:

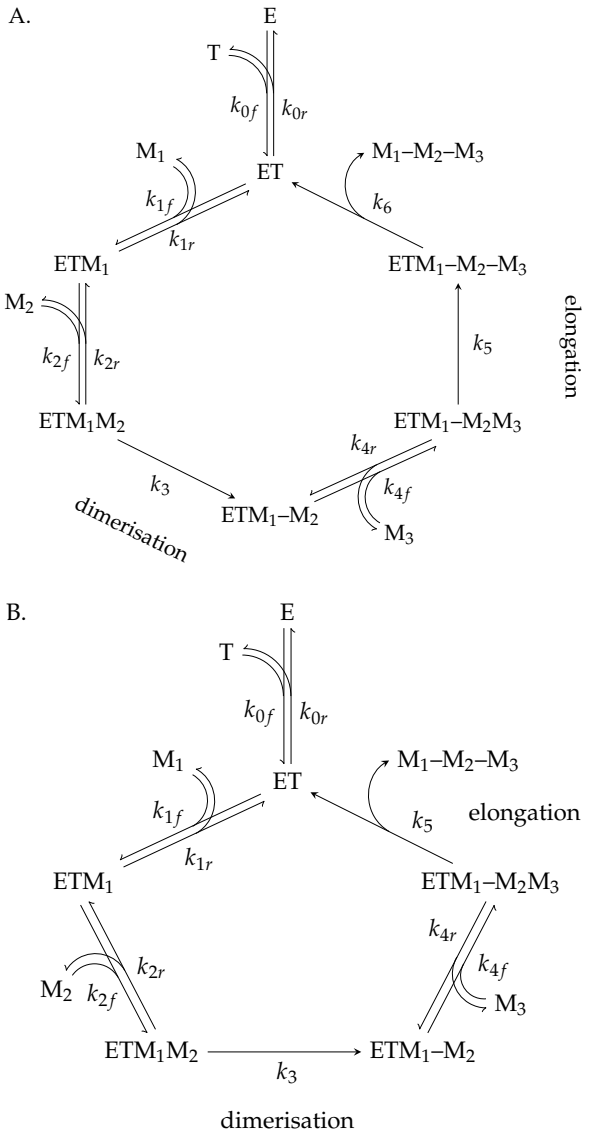

Figure 3.4: Reaction schemes of a catalysed, template-directed polymerisation reaction. Scheme A has an explicit elongation step with rate constant k_5 and product release step with rate constant k_6. In Scheme B the elongation and product release steps have been combined into one step with rate constant k_5 (see text for explanation). M_1, M_2, M_3 denote the monomers, E the free enzyme, T the free template, ET the enzyme-template complex, ETM_1 the ET–monomer complex, ETM_1M_2 the complex of ET with two unligated monomers, ETM_1–M_2 the ET–dimer complex, ETM_1–M_2M_3 the complex of ET–dimer with the next monomer, ETM_1–M_2–M_3 the ET–trimer complex, and M_1–M_2–M_3 the final trimer product. The half-headed arrows denote the reversible binding steps, and the single-headed arrows denote irreversible catalytic steps.

$$\frac{d[\mathrm{T}]}{dt} = \frac{d[\mathrm{E}]}{dt} = k_{0\mathrm{r}}[\mathrm{ET}] - k_{0\mathrm{f}}[\mathrm{E}][\mathrm{T}] \tag{3.21}$$

$$\frac{d[\mathrm{ET}]}{dt} = k_{0\mathrm{f}}[\mathrm{E}][\mathrm{T}] + k_{1\mathrm{r}}[\mathrm{ETM_1}] + k_5[\mathrm{ETM_1\text{–}M_2M_3}] - (k_{0\mathrm{r}} + k_{1\mathrm{f}}[\mathrm{M_1}])[\mathrm{ET}] \tag{3.22}$$

$$\frac{d[\mathrm{ETM_1}]}{dt} = k_{1\mathrm{f}}[\mathrm{ET}][\mathrm{M_1}] + k_{2\mathrm{r}}[\mathrm{ETM_1M_2}] - (k_{1\mathrm{r}} + k_{2\mathrm{f}}[\mathrm{M_2}])[\mathrm{ETM_1}] \tag{3.23}$$

$$\frac{d[\mathrm{ETM_1M_2}]}{dt} = k_{2\mathrm{f}}[\mathrm{ETM_1}][\mathrm{M_2}] - (k_{2\mathrm{r}} + k_3)[\mathrm{ETM_1M_2}] \tag{3.24}$$

$$\frac{d[\mathrm{ETM_1\text{–}M_2}]}{dt} = k_3[\mathrm{ETM_1M_2}] + k_{4\mathrm{r}}[\mathrm{ETM_1\text{–}M_2M_3}] - k_{4\mathrm{f}}[\mathrm{ETM_1\text{–}M_2}][\mathrm{M_3}] \tag{3.25}$$

$$\frac{d[\mathrm{ETM_1\text{–}M_2M_3}]}{dt} = k_{4\mathrm{f}}[\mathrm{ETM_1\text{–}M_2}][\mathrm{M_3}] - (k_{4\mathrm{r}} + k_5)[\mathrm{ETM_1\text{–}M_2M_3}] \tag{3.26}$$

Time-dependency behaviour of the extended model

A kinetic model describing the dynamic behaviour of the mechanism in Fig. 3.4B was defined in a PySCeS input file (see Appendix 6.4). M_1, M_2, M_3 and E were clamped at constant concentrations (E was clamped in the light of the results of Section 3.3). The total concentration of E was again assumed to be 10-fold higher than that of T. To assign values to the rate constants we used the dissociation rate constants as reference, setting $k_{1\mathrm{r}} = k_{2\mathrm{r}} = k_{4\mathrm{r}} = 1.0$. Strong and fast binding was then ensured by setting $k_{1\mathrm{f}} = k_{2\mathrm{f}} = k_{4\mathrm{f}} = 10^3$. The initial binding of template to enzyme was arbitrarily assigned an equilibrium constant of 1.0 with rate constants set to 10^4, which ensured very rapid equilibration. The rate constants of catalytic steps 3 and 5 were assumed to be much slower than binding (a typical assumption in enzyme kinetics) and were set to 14 and 12 respectively, so that we could distinguish between the rates of the two condensation steps (in the derivation to be discussed shortly we assumed them to be equal).

The time-dependent changes in the concentrations of T, ET, ETM_1, ETM_1M_2, ETM_1–M_2, ETM_1–M_2M_3 and M_1–M_2–M_3 were calculated (see Figs. 3.5 and 3.6). Changes in the rates of the reactions involved in the system as a function of time are shown in Fig. 3.7.

In the initial *fast phase* up to 0.0001 time units, reactions R0, R1 and R2 equilibrated and enzyme-template accumulated as ETM_1M_2, in which

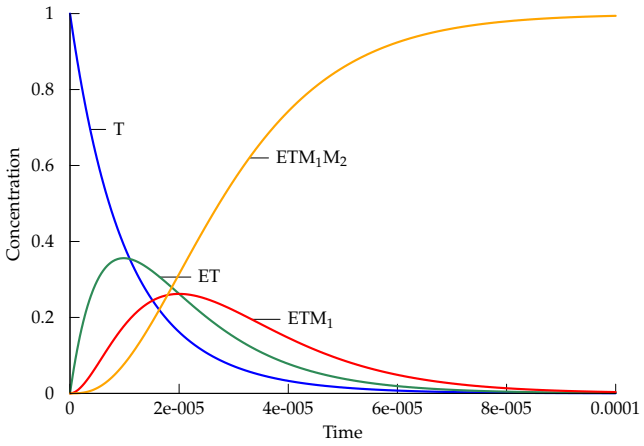

Figure 3.5: Time-dependent concentration changes of the intermediates involved in the fast binding equilibria (reactions 0, 1 and 2) of Scheme 3.4B. The species ET and ETM_1 decreased to low concentration levels, with most of the enzyme accumulating as ETM_1M_2. The initial conditions and parameter values are listed in Appendix 6.4.

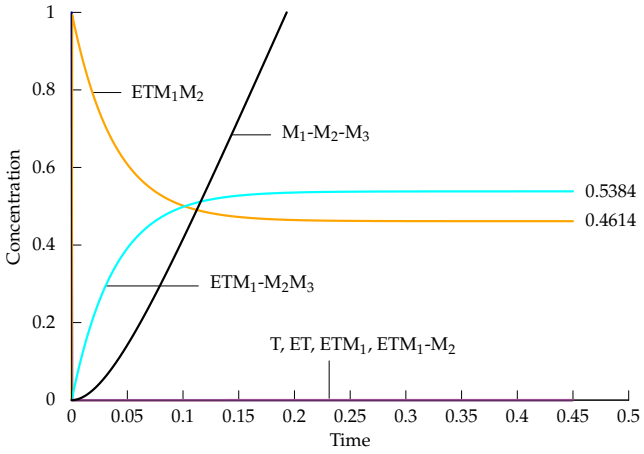

Figure 3.6: Time-dependent concentration changes of the intermediates involved in reactions 3, 4 and 5 of Scheme 3.4B, which occurred on a much slower time-scale because of the relatively slow catalytic rate constants of reactions 3 and 5. The species ETM_1M_2 and ETM_1–M_2M_3 reached steady-state, while the rate of production of the final polymeric product M_1–M_2–M_3 became constant. The concentrations of T, ET, ETM_1, ETM_1–M_2 remained very low relative to the concentrations of ETM_1M_2 and ETM_1–M_2M_3 throughout the time course of the reaction. The initial conditions and parameter values are listed in Appendix 6.4.

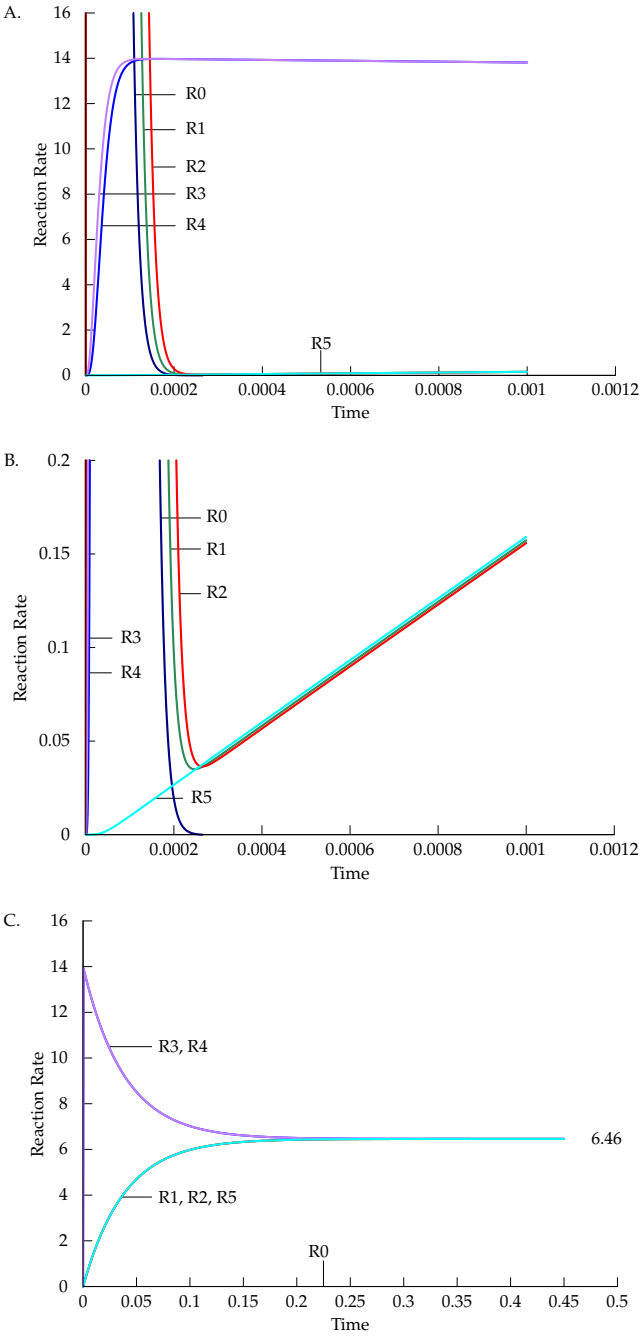

Figure 3.7: Time-dependent changes of the rates of the reactions in Scheme 3.4. A and B show the initial fast phase with two different rate scales, while C shows rate changes in the slow phase. The number next to the converging rate curves indicates the steady-state flux. The initial conditions and parameter values are listed in Appendix 6.4.

both monomers are bound (see Fig. 3.5). The rate changed up to 0.001 time units as shown in Fig. 3.7: A. shows how R0, R1 and R2 rapidly approached equilibrium, while the rates of R3 and R4 increased to a maximum. B. provides deeper insight, showing that the binding of template to enzyme, R0, being 10-fold faster than the other binding steps, reached and remained in quasi equilibrium with near zero net rate. As ETM_1–M_2M_3 started forming R5 came into play. The rates of reactions R1 and R2 tracked the slowly increasing rate of R5.

The subsequent *slow phase* comprised dimerisation, binding of M_3, and the second condensation step. A steady state was established in which enzyme-template occurred in the form of ETM_1M_2 and ETM_1–M_2M_3 (see Figs. 3.6 and 3.7C). Because the equilibrium constant of binding reaction 4 was large (1000) and the forward rate constant was about 100-fold larger than the catalytic constants, the concentration of ETM_1–M_2 remained very low throughout the time course of the reaction. As the steady state became established the rate of M_1–M_2–M_3 production became constant.

Solving for a rate equation using the steady-state assumption

We introduced the following definitions:

$$\sigma_1 = \frac{[M_1]}{K_{d_1}}, \quad \sigma_2 = \frac{[M_2]}{K_{d_2}}, \quad \sigma_3 = \frac{[M_3]}{K_{d_3}}$$

where

$$K_{d_1} = \frac{k_{1r}}{k_{1f}}, \quad K_{d_2} = \frac{k_3 + k_{2r}}{k_{2f}}, \quad K_{d_3} = \frac{k_5 + k_{4r}}{k_{4f}}$$

K_{d_1} is the dissociation constant for the complex of ET with the first monomer in the polymer sequence, while K_{d_2} and K_{d_3} represent the Michaelis constants for the monomers that occur in positions 2 and 3 of the polymer sequence.

Using these definitions, we derived the steady-state equations for this system by setting eqns. 3.22–3.26 to zero and transforming them as follows:

1. As before, eqn. 3.21 expresses the fact that in steady state the enzyme-template dissociation reaction is in equilibrium, and could therefore be rewritten as:

$$K_0 = \frac{k_{0r}}{k_{0f}} = \frac{[E][T]}{[ET]} \tag{3.27}$$

where K_0 denotes the dissociation constant for the enzyme-template complex.

2. Eqns. 3.22 and 3.23 were divided by k_{1r}:

$$\left(\frac{k_{0f}}{k_{1r}}\right)[E][T] + [ETM_1] + \left(\frac{k_5}{k_{1r}}\right)[ETM_1\text{–}M_2M_3] - \left(\frac{k_{0r}}{k_{1r}} + \sigma_1\right)[ET] = 0 \tag{3.28}$$

$$\sigma_1[ET] + \left(\frac{k_{2r}}{k_{1r}}\right)[ETM_1M_2] - \left(1 + \left(\frac{k_3 + k_{2r}}{k_{1r}}\right)\sigma_2\right)[ETM_1] = 0 \tag{3.29}$$

3. Eqn. 3.24 was divided by $(k_3 + k_{2r})$:

$$\sigma_2[ETM_1] - [ETM_1M_2] = 0 \tag{3.30}$$

4. Eqn. 3.25 was divided by $(k_5 + k_{4r})$:

$$\left(\frac{k_3}{k_5 + k_{4r}}\right)[ETM_1M_2] + \left(\frac{k_{4r}}{k_5 + k_{4r}}\right)[ETM_1\text{–}M_2M_3] - \sigma_3[ETM_1\text{–}M_2] = 0 \tag{3.31}$$

5. Eqn. 3.26 was divided by $(k_5 + k_{4r})$:

$$\sigma_3[ETM_1\text{–}M_2] - [ETM_1\text{–}M_2M_3] = 0 \tag{3.32}$$

The two conservation equations for enzyme species and template species are:

$$[E]_t = [E] + [ET] + [ETM_1] + [ETM_1M_2] + [ETM_1\text{–}M_2] + [ETM_1\text{–}M_2M_3] \tag{3.33}$$

$$[T]_t = [T] + [ET] + [ETM_1] + [ETM_1M_2] + [ETM_1\text{–}M_2] + [ETM_1\text{–}M_2M_3] \tag{3.34}$$

The rate of the polymerisation reaction is the rate at which the trimer M_1–M_2–M_3 is released from the enzyme-template complex ET, and is given by

$$v = \frac{d[M_1\text{–}M_2\text{–}M_3]}{dt} = k_5[ETM_1\text{–}M_2M_3] \tag{3.35}$$

As in the case of the simple scheme described in Section 3.3 we assumed the free enzyme concentration [E] to be fixed. Using the 'Solve'

function of Maxima [54], we obtained solutions to the steady-state concentrations of the species in the equation system eqn. 3.27 and eqns. 3.29–3.33. Using the expression for $[\mathrm{ETM_1–M_2M_3}]$ the following rate equation was obtained:

$$v = \frac{k_3 k_5 k_{1r} \sigma_1 \sigma_2 \sigma_3 [\mathrm{T}]_t}{\frac{K_0}{[\mathrm{E}]}\left(k_3 k_5 \sigma_2 \sigma_3 + k_{1r} k_5 \sigma_3\right) + k_{1r} k_5 \sigma_1 \sigma_2 \sigma_3 + k_{1r} k_3 \sigma_1 \sigma_2 \sigma_3 + k_3 k_5 \sigma_2 \sigma_3 + k_{1r} k_5 \sigma_1 \sigma_3 + k_{1r} k_3 \sigma_1 \sigma_2 + k_{1r} k_5 \sigma_3} \tag{3.36}$$

It was assumed that the catalytic rate constants are identical, i.e., $k_3 = k_5$, and so these rate constants were denoted by k_{cat}. Dividing by $k_{1r} k_{cat}$ yielded:

$$v = \frac{k_{cat} \sigma_1 \sigma_2 \sigma_3 [\mathrm{T}]_t}{\frac{K_0}{[\mathrm{E}]}\left(\frac{k_{cat}}{k_{1r}} \sigma_2 \sigma_3 + \sigma_3\right) + \sigma_3 + \frac{k_{cat}}{k_{1r}} \sigma_2 \sigma_3 + \sigma_1 \sigma_2 + \sigma_1 \sigma_3 + 2\sigma_1 \sigma_2 \sigma_3} \tag{3.37}$$

Eqn. 3.37 could be simplified further by assuming that the dissociation half-reactions occur much faster than the catalytic steps, that is $k_{1r}, k_{2r}, k_{4r} \gg k_{cat}$. This also simplified the expressions for Michaelis constants for $\mathrm{M_2}$ and $\mathrm{M_3}$ to:

$$K_{d_2} = \frac{k_{2r}}{k_{2f}}, \qquad K_{d_3} = \frac{k_{4r}}{k_{4f}}$$

Eqn. 3.37 now became:

$$v = \frac{k_{cat} [\mathrm{T}]_t \sigma_1 \sigma_2 \sigma_3}{\left(1 + \frac{K_0}{[\mathrm{E}]}\right) \sigma_3 + \sigma_1 \left(\sigma_2 + \sigma_3\right) + 2\sigma_1 \sigma_2 \sigma_3} \tag{3.38}$$

Dividing the numerator and denominator by $\sigma_1 \sigma_2 \sigma_3$ yielded a particularly useful form of the rate equation that we subsequently used:

$$v = \frac{k_{cat} [\mathrm{T}]_t}{\left(1 + \frac{K_0}{[\mathrm{E}]}\right) \frac{1}{\sigma_1 \sigma_2} + \frac{1}{\sigma_2} + \frac{1}{\sigma_3} + 2} \tag{3.39}$$

Alternatively, if $[\mathrm{T}]$ was regarded as fixed instead of $[\mathrm{E}]$, the rate equation became:

$$v = \frac{k_{cat} [\mathrm{E}]_t}{\left(1 + \frac{K_0}{[\mathrm{T}]}\right) \frac{1}{\sigma_1 \sigma_2} + \frac{1}{\sigma_2} + \frac{1}{\sigma_3} + 2} \tag{3.40}$$

In summary, to obtain these forms of the steady-state rate equation we had to assume (i) that the concentration of either the free enzyme or the free template was fixed, (ii) that the catalytic rate constants were equal, and (iii) that binding occurred much faster than catalysis. The second assumption presupposed that different monomers have similar chemical reactivity, which seemed reasonable. The third assumption is often made in enzymatic studies, and also seemed reasonable in this case.

When we introduced the reaction scheme that formed the basis for the derivation of rate eqn. 3.39 we made the assumption that product release is much faster than catalytic elongation, i.e., $k_6 \gg k_{cat}$. If we did not make this assumption and derived the steady-state rate equation for the reaction scheme in Fig. 3.4A we obtained

$$v = \frac{k_{cat}[T]_t}{\left(1 + \frac{K_0}{[T]}\right)\frac{1}{\sigma_1\sigma_2} + \frac{1}{\sigma_2} + \frac{1}{\sigma_3} + 2\left(1 + \frac{k_{cat}}{k_6}\right)} \tag{3.41}$$

The assumption that product release is faster than the rate of catalysis is often made in enzyme kinetics and we continued to use it.

3.5 Validation

In order to validate the rate equations derived above we posed the following questions:

1. Are the rate values calculated with rate equation 3.37 (in which all catalytic condensation steps have equal rate constants) identical to the steady-state flux values of the mass-action model in Fig. 3.4 (calculated with PySCeS) on which the derivation of the rate equation is based?

2. How does the assumption that the dissociation steps occur faster than the catalytic steps, i.e., that $k_{cat} \ll k_{1r}, k_{2r}, k_{4r}$, affect the rate values calculated with eqn. 3.38 when k_{cat} is varied relative to k_{1r}, k_{2r} and k_{4r}?

To answer these questions we varied k_{cat} in a range of 0.01–100.0, i.e. from 100 times smaller to 100 times larger than the dissociation rate constants, k_{1r}, k_{2r}, k_{4r} which were all set to 1.0 (see Appendix 6.4). The net rate of polymerisation was calculated for each k_{cat} value using the mass-action model, eqn. 3.37 and eqn. 3.38. The PySCeS script used for this

Table 3.1: A comparison of steady-state and reaction rate values at different values of k_{cat}. The % error was calculated as $100(v_{simp} - v)/v$.

k_{cat}	J	v (Eqn. 3.37)	v_{simp} (Eqn. 3.38)	% error
0.01	4.99995×10^{-3}	4.99995×10^{-3}	4.99995×10^{-3}	1.55×10^{-5}
0.1	4.99994×10^{-2}	4.99994×10^{-2}	4.99995×10^{-2}	1.55×10^{-4}
1.0	4.99987×10^{-1}	4.99987×10^{-1}	4.99995×10^{-1}	1.55×10^{-3}
10	4.99918	4.99918	4.99995	1.55×10^{-2}
100	4.99221×10^{1}	4.99221×10^{1}	4.99995×10^{1}	1.55×10^{-1}

purpose is given in Appendix 6.8. The calculation results are given in Table 3.1.

Table 3.1 shows that the steady-state flux values (denoted by J) and the rate values calculated from eqn. 3.37 (denoted v) yielded identical results at all values of k_{cat} (up to 12 significant figures, not shown). This demonstrated the correctness of the derivation of eqn. 3.37.

The simplified rate eqn. 3.38 gave surprisingly accurate results. As expected, when k_{cat} was 100 times smaller than the dissociation rate constants, the error was negligible. However, even if the rate constants were all of comparable magnitude (here 1.0), the percentage error was still only about 0.002%. What was surprising was that when k_{cat} was considerably larger than the dissociation rate constants, the percentage error was still quite acceptable, i.e., about 0.2% when k_{cat} was 100 times larger than the binding rate constants.

From these results we therefore concluded that our derivation was correct and that the simplified forms of the rate equations (eqns. 3.38–3.40), or, their generalised forms (eqns. 3.45 and 3.46) that are derived in the next section could be used in metabolic models to represent template-directed polymerisation reactions.

3.6 Generalising the rate equation

To generalise our rate equation we had to consider two aspects:

1. Extension to an arbitrary length n of the polymer sequence.
2. The constraint of a fixed set of m monomers. For example, polypeptides consist of 20 different monomers, polynucleotides of four, etc.

Extension to sequence length n

Section 3.4 focused on the derivation of a rate equation for a simple catalysed, template-directed polymerisation reaction. However, this rate equation is specifically for the formation of a trimer. In this section we show how we generalised the rate equation to a sequence length of n monomers, still assuming that either [T] or [E] was constant. Our strategy was to extend the system in Fig. 3.4 by successively incorporating additional elongation steps, i.e., incrementally increasing the length of the polymer. We hoped that a pattern would emerge that would allow us to construct a generic rate equation for a polymer of sequence length n.

For a system with *two elongation steps* (addition of a fourth monomer) the rate is given by:

$$v = \frac{d[\mathrm{M_1{-}M_2{-}M_3{-}M_4}]}{dt} = k_{\mathrm{cat}}[\mathrm{ETM_1{-}M_2{-}M_3M_4}] \tag{3.42}$$

Inserting the expression for $[\mathrm{ETM_1{-}M_2{-}M_3M_4}]$ yielded the following rate equation for the situation where [E] is constant:

$$v = \frac{k_{\mathrm{cat}}[\mathrm{T}]_{\mathrm{t}}}{\left(1 + \dfrac{K_0}{[\mathrm{E}]}\right)\dfrac{1}{\sigma_1\sigma_2} + \dfrac{1}{\sigma_2} + \dfrac{1}{\sigma_3} + \dfrac{1}{\sigma_4} + 3} \tag{3.43}$$

Similarly, a system with *three elongation steps*, that is with the addition of a fifth monomer, produced the following rate equation:

$$v = \frac{k_{\mathrm{cat}}[\mathrm{T}]_{\mathrm{t}}}{\left(1 + \dfrac{K_0}{[\mathrm{E}]}\right)\dfrac{1}{\sigma_1\sigma_2} + \dfrac{1}{\sigma_2} + \dfrac{1}{\sigma_3} + \dfrac{1}{\sigma_4} + \dfrac{1}{\sigma_5} + 4} \tag{3.44}$$

A clear pattern emerged from the above rate equations. This pattern allowed us to generalise to n monomers to yield the following *generic* rate equations. When [E] is constant:

$$v = \frac{k_{\mathrm{cat}}[\mathrm{T}]_{\mathrm{t}}}{\left(1 + \dfrac{K_0}{[\mathrm{E}]}\right)\dfrac{1}{\sigma_1\sigma_2} + \displaystyle\sum_{j=2}^{n}\frac{1}{\sigma_j} + (n-1)} \tag{3.45}$$

where n is the number of monomers and $n-1$ the number of catalytic steps.

When [T] is constant:

$$v = \frac{k_{\mathrm{cat}}[\mathrm{E}]_{\mathrm{t}}}{\left(1 + \dfrac{K_0}{[\mathrm{T}]}\right)\dfrac{1}{\sigma_1\sigma_2} + \displaystyle\sum_{j=2}^{n}\frac{1}{\sigma_j} + (n-1)} \tag{3.46}$$

Constrain to fixed set of m monomers

We assumed that the generic polymer in question was constructed from m different monomer types. In order to distinguish the identity of the monomer from the position it occupies in the sequence we denoted monomer types by M_A, M_B, M_C,..., while M_1, M_2, M_3,..., referred to positions in the polymer sequence.

Consider eqn. 3.45. From the first denominator term it is clear that the monomers occupying positions 1 and 2 have a distinguished role in the rate equation and that their identities need to be known. The middle denominator term is a sum and here all that we need to know is how the $1/\sigma_j$ terms (where j ranges over position 2 to n) partition between the m monomers. These two conditions imply that all that we need to know about our polymer is the *initial dimeric sequence* and the monomer *composition* of the sequence from position 2 onwards.

As the above may not be immediately obvious we illustrate with a specific example. Let the polymer have length $n = 7$. The generic rate equation is

$$v = \frac{k_{cat}[T]_t}{\left(1 + \frac{K_0}{[E]}\right)\frac{1}{\sigma_1\sigma_2} + \frac{1}{\sigma_2} + \frac{1}{\sigma_3} + \frac{1}{\sigma_4} + \frac{1}{\sigma_5} + \frac{1}{\sigma_6} + \frac{1}{\sigma_7} + 6} \tag{3.47}$$

Let this polymer now be constructed from a set of three monomers M_A, M_B, and M_C, and let the monomer sequence arbitrarily be

$$M_B M_A M_C M_A M_A M_B M_C.$$

with composition $(M_A)_3(M_B)_2(M_C)_2$. The rate equation now becomes

$$v = \frac{k_{cat}[T]_t}{\left(1 + \frac{K_0}{[E]}\right)\frac{1}{\sigma_B\sigma_A} + \frac{1}{\sigma_A} + \frac{1}{\sigma_C} + \frac{1}{\sigma_A} + \frac{1}{\sigma_A} + \frac{1}{\sigma_B} + \frac{1}{\sigma_C} + 6} \tag{3.48}$$

or, simpler,

$$v = \frac{k_{cat}[T]_t}{\left(1 + \frac{K_0}{[E]}\right)\frac{1}{\sigma_B\sigma_A} + \frac{3}{\sigma_A} + \frac{1}{\sigma_B} + \frac{2}{\sigma_C} + 6} \tag{3.49}$$

The coefficients i in the i/σ_i-terms, namely 3, 1, and 2, reflect the total number of each monomer type in the sequence from position 2 onwards. They are of course also correct for the monomer composition of the full sequence, except for the monomer in position 1 (here M_B) which is one less than the total number in the full sequence (i.e., 1 instead of 2).

The fully generalised rate equation

We could now finally construct the generic rate equation for a polymer with sequence length n constructed from a set of m monomer types. Let c_i be the number of monomers of type i from position 2 onwards in the monomer sequence. Then the generic rate equation when [E] is constant could be written as:

$$v = \frac{k_{\text{cat}}[\text{T}]_\text{t}}{\left(1 + \frac{K_0}{[\text{E}]}\right)\frac{1}{\sigma_1\sigma_2} + \sum_{i=1}^{m}\frac{c_i}{\sigma_i} + (n-1)} \tag{3.50}$$

where σ_1 refers to the first monomer in the sequence, and σ_2 to the second.

When [T] is constant

$$v = \frac{k_{\text{cat}}[\text{E}]_\text{t}}{\left(1 + \frac{K_0}{[\text{T}]}\right)\frac{1}{\sigma_1\sigma_2} + \sum_{i=1}^{m}\frac{c_i}{\sigma_i} + (n-1)} \tag{3.51}$$

3.7 Simplifications of the generic rate equation

There were two aspects of the generic rate equations that needed further consideration. The first was the degree to which the $K_0/[\text{E}]$ (or $K_0/[\text{T}]$) term influences the rate, and the second was whether it is possible to adapt the rate equation for the general case where only the composition of the polymer is known without any sequence information.

Consider the $K_0/[\text{E}]$ term. From the definition of K_0 it follows that

$$\frac{K_0}{[\text{E}]} = \frac{[\text{T}]}{[\text{ET}]} = \frac{[\text{free template}]}{[\text{bound template}]} \tag{3.52}$$

It should therefore be clear that the generic rate equations could be simplified further under the assumption that the free enzyme concentration [E] (in eqn. 3.50) is much larger than K_0, which implies that all the template is bound to enzyme, i.e., $[\text{ET}] \approx [\text{T}]_\text{t}$. Strong binding of template to enzyme would ensure a small dissociation constant K_0. We therefore needed to ask which additional condition would make it possible for $[\text{E}] \gg K_0$.

As discussed in section 3.3 we had to remove one of the two conservation equations (for E or for T) in order to obtain a usable analytical expression for [ETS]. To do this we had to assume that either the free

concentration of E or that of T is kept constant (clamped)—we clamped [E]. We made the point that if there is much less template than enzyme, i.e., $[E]_t \gg [T]_t$, then this would imply that $[E] \approx [E]_t$, this assumption would be justified. Therefore, the two conditions that would ensure that the $K_0/[E]$ term tends to zero are $[E]_t \gg [T]_t$ and $[E]_t \gg K_0$.

If these conditions were satisfied the generic rate equation would simplify to

$$v = \frac{k_{cat}[T]_t}{\frac{1}{\sigma_1\sigma_2} + \sum_{i=1}^{m} \frac{c_i}{\sigma_i} + (n-1)} \tag{3.53}$$

for the situation where $[E] \gg K_0$. For the other situation where $[T]_t \gg [E]_t$ and $[T]_t \gg K_0$, which ensures that $[T] \gg K_0$, the $[T]_t$ in the numerator is replaced by $[E]_t$.

$$v = \frac{k_{cat}[E]_t}{\frac{1}{\sigma_1\sigma_2} + \sum_{i=1}^{m} \frac{c_i}{\sigma_i} + (n-1)} \tag{3.54}$$

The above theoretical analysis provides conditions under which the $K_0/[E]$ term in itself tends to zero and becomes negligible, but it may be that, due to the functional form of the rate equation, these conditions could be relaxed without making much of a difference to the calculated rate. It may be that an increase in the length of the monomer overshadows any contribution that the $K_0/[E]$ term makes.

In addition, if the $K_0/[E]$ is negligible, another simplification of the generalised rate equation suggested itself. If the $1/\sigma_1\sigma_2$ term is changed to $1/\sigma_1$ the equation simplifies to

$$v = \frac{k_{cat}[T]_t}{\sum_{i=1}^{m} \frac{c_i}{\sigma_i} + (n-1)} \tag{3.55}$$

a form which is particularly attractive because it only requires a knowledge of the monomer composition of the polymer, avoiding the necessity of knowing the sequence and identity of the first two monomers. *Note that the coefficients c_i in eqn. 3.55 now reflect the total number of each monomer type in the full sequence, in contrast to c_i in eqns. 3.50 and 3.51 and eqns. 3.53 and 3.54 where they reflect the total number of each monomer type from position 2 in the polymer onwards.*

The behaviour of all of these possible forms of the denominator of eqn. 3.50 was explored by calculating the value of the denominator and

its simplifications under conditions of varying $K_0/[\mathrm{E}]$ and varying number of monomers. It was assumed that the polymer was a homopolymer, i.e., consisting of only one monomer. Fig. 3.8 shows how the following forms of the denominator varied with monomer concentration (the Gnuplot-plotfile used to generate this figure is given in Appendix 6.9; Gnuplot [55] is a multi-platform a portable command-line driven graphing utility that was extensively used in the research described in thesis):

- The full denominator of eqn. 3.50

$$\left(1+\frac{K_0}{[\mathrm{E}]}\right)\frac{1}{\sigma^2}+\frac{n-1}{\sigma}+(n-1) \tag{3.56}$$

- When $[\mathrm{E}] \gg K_0$

$$\frac{1}{\sigma^2}+\frac{n-1}{\sigma}+(n-1) \tag{3.57}$$

- When, in addition, $1/\sigma_1\sigma_2$ is changed to $1/\sigma_1$

$$\frac{n}{\sigma}+(n-1) \tag{3.58}$$

- Also included in the figure is the

$$\left(1+\frac{K_0}{[\mathrm{E}]}\right)\frac{1}{\sigma^2}$$

  term by itself.

The graphs show clearly that when $K_0/[\mathrm{E}]$ is small (0.01) there is, no matter the polymer size, no discernable difference between the full form of the denominator (red) and the form (green) that assumes that $K_0/[\mathrm{E}]$ is zero (on the top three graphs the red line overlays the green). When $n = 50$ this also holds for the simplest form of the denominator (black), except at very low levels of saturation ($\sigma < 0.01$). When the size of the polymer decreases ($n = 50$ and $n = 5$ on the top three graphs) the deviation becomes larger, but even for the shortest polymer the simplest denominator form is indistinguishable from the full form at levels above half-saturation ($\sigma > 1.0$).

This profile changes very little when $K_0/[\mathrm{E}]$ is increased to 1.0, except that the denominator form that assumes that $K_0/[\mathrm{E}]$ is zero is slightly offset from the full form, but is nevertheless an excellent approximation.

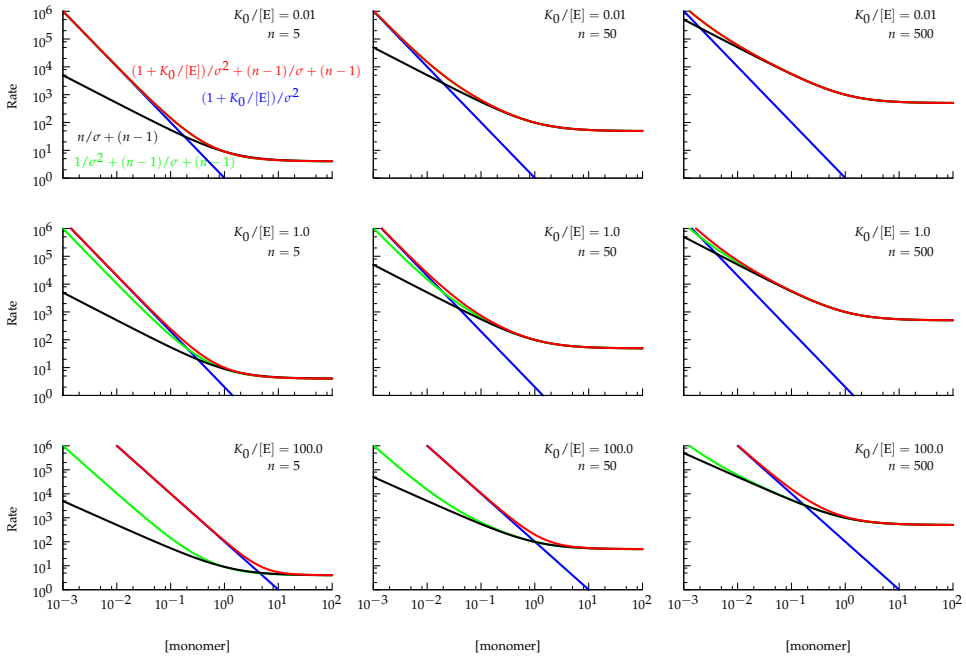

Figure 3.8: Variation in the value of different forms of the denominator of eqn. 3.50 for a homopolymer with n monomers as a function of monomer concentration. The different graphs show combinations of different values of $K_0/[E]$ and n. The monomer dissociation constant is 1.0.

It is only when $K_0/[E]$ is very large (100.0) that the simplified forms of the denominator deviate substantially from the full form. Nevertheless, for longer polymers the simplified forms are still good approximations at $\sigma > 1.0$, and it is only for the shorter polymers that the level of saturation needs to be higher for the approximation to hold.

In all cases the $(1 + K_0/[E])/\sigma^2$ term dominates the value of the full denominator at low monomer concentrations while the other terms dominate at high monomer concentrations, the switch-over point depending on the value of $K_0/[E]$ and n.

From these graphs we can conclude that for $K_0/[E]$ values up to 1.0 the denominator can be simplified by assuming that $K_0/[E]$ is zero. This weakens the condition derived theoretically earlier in this section considerably, and implies that eqns. 3.53 is usable under most conditions. Furthermore, if the monomer concentrations are all at least half-saturating the simplest form of the denominator is also a good approximation for the full form.

3.8 Exploring the rate behaviour of the derived rate equations

Variation in V_{max} with number of monomers, n

When all monomer concentrations approach saturation values, i.e., all $\sigma_i \gg 1$, the reaction rate of eqn. 3.45 approaches the limiting rate $V_{max} = k_{cat}[T]_t/(n-1)$ (when $[E]_t \gg [T]_t$), whereas eqn. 3.46 approaches the limiting rate $V_{max} = k_{cat}[E]_t/(n-1)$ (when $[T]_t \gg [E]_t$).

The variation of V_{max} with n of course reflects the time it takes to synthesise a polymer consisting of n subunits—the larger n the longer it takes to synthesise one polymer molecule. The reason why V_{max} varies with $n-1$ instead of with n is that $n-1$ reflects the number of catalytic steps (one could also think of it as due to the first monomer actually forming part of the initiation complex, i.e., two monomers must bind before a condensation reaction can take place).

Dependence of reaction rate on the concentrations of monomers

For the purposes of this exploration of the behaviour of our derived rate equations with varying monomer concentrations, we used the rate equation for a pentamer (eqn. 3.44, $n = 5$) in the form of eqn. 3.53 under the assumptions explained in Section 3.7. Under these conditions eqn. 3.44 simplifies to

$$v = \frac{k_{cat}[T]_t}{\frac{1}{\sigma_1\sigma_2} + \frac{1}{\sigma_2} + \frac{1}{\sigma_3} + \frac{1}{\sigma_4} + \frac{1}{\sigma_5} + 4} \tag{3.59}$$

We assumed that the pentamer consists of 5 different monomer types, with monomer M1 in position 1, M2 in position 2, etc.

We also compared this equation with the simplified form in eqn. 3.55, namely

$$v = \frac{k_{cat}[T]_t}{\frac{1}{\sigma_1} + \frac{1}{\sigma_2} + \frac{1}{\sigma_3} + \frac{1}{\sigma_4} + \frac{1}{\sigma_5} + 4} \tag{3.60}$$

in order to gain an idea of the conditions under which this form can be used.

We explored the behaviour of these rate equations to changes in monomer concentration by varying the concentration of one monomer while keeping all the other monomer concentrations equal at concentrations of

either 0.1, 0.5. 1.0, 2.0, 5.0, 10.0, 50.0 or 100.0. All parameters were set to 1.0, which means that the maximum rate that can be achieved under such conditions is 0.25 rate units ($k_{\text{cat}}[\text{T}]_t/(n-1)$). The results are depicted in Figs. 3.9 and 3.10 (the Gnuplot-plotfile used to generate these figures is given in Appendix 6.10).

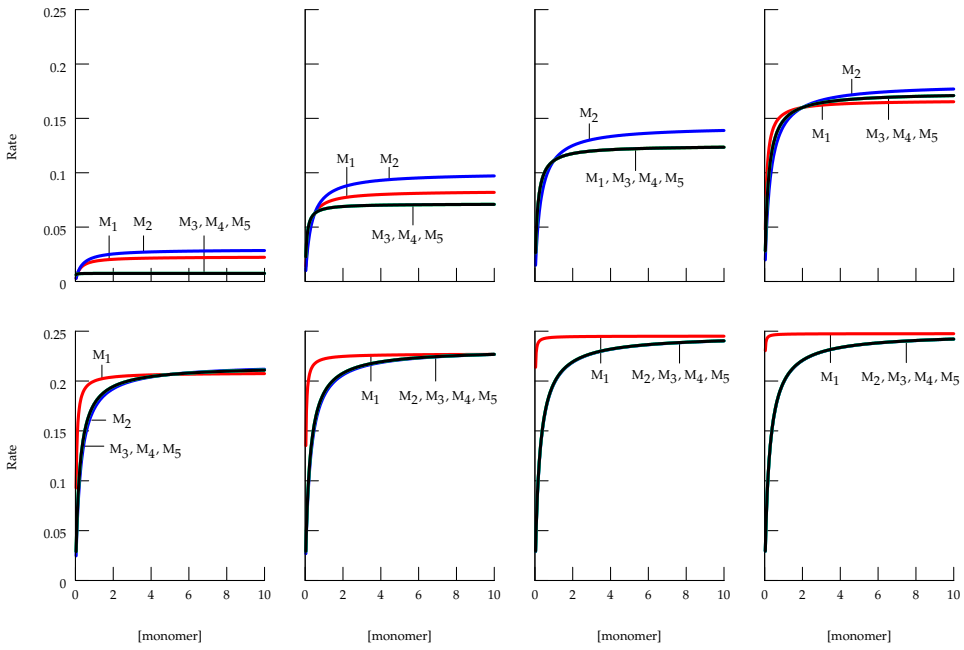

Figure 3.9: Variation of the reaction rate of eqn. 3.59 with monomer concentration. Each curve represents the variation in reaction rate when the indicated monomer is varied while the concentrations of all the other monomers are kept constant and equal at 0.1, 0.5. 1.0, 2.0 (top row) and 5.0, 10.0, 50.0 or 100.0 (bottom row).

We also calculated the apparent K_{m} and V_{max} values for the two forms of the rate equations by transforming, for each monomer in turn, the rate equation into the form of the irreversible Michaelis-Menten equation

$$v = \frac{V_{\text{max}} s}{K_{\text{m}} + s}$$

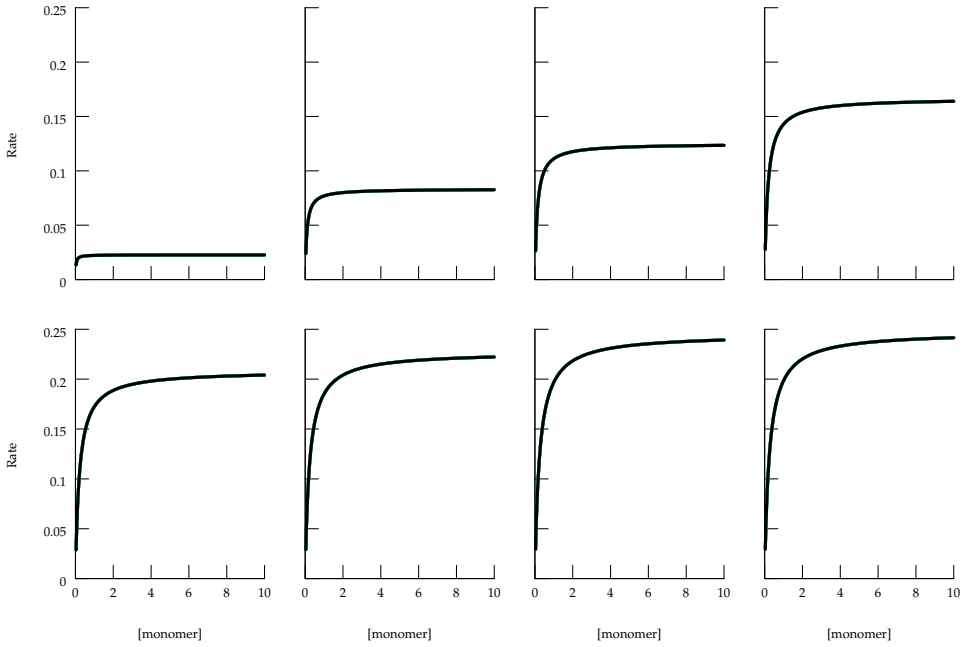

Figure 3.10: Variation of the reaction rate of the modified derived rate equation, eqn. 3.60 with monomer concentration. Conditions are identical to those in Fig. 3.9.

For example, if M_1 is the variable monomer then

$$\begin{aligned} v &= \frac{k_{cat}[T]_t}{\frac{1}{\sigma_1\sigma_2}+\frac{1}{\sigma_2}+\frac{1}{\sigma_3}+\frac{1}{\sigma_4}+\frac{1}{\sigma_5}+4} \\ &= \frac{k_{cat}[T]_t}{\frac{1}{\sigma_1 x}+\frac{4}{x}+4} \\ &= \frac{k_{cat}[T]_t\sigma_1}{\frac{1}{x}+\sigma_1\left(\frac{4}{x}+4\right)} \\ &= \frac{k_{cat}[T]_t x\sigma_1}{1+\sigma_1\left(4+4x\right)} \\ &= \frac{\left(k_{cat}[T]_t\cdot\frac{x}{4+4x}\right)\sigma_1}{\left(\frac{1}{4+4x}\right)+\sigma_1} \end{aligned}$$

The bracketed terms in the numerator and denominator are the expressions for the apparent V_{max} and K_m. Similar expressions were derived for the other monomers and are given in Table 3.2. The actual values for these parameters at different values of the fixed monomer concentration x are given in Table 3.3.

Table 3.2: Expressions used to calculate apparent K_m and V_{max}-values at different constant monomer concentrations, all set to x. For example, if M_1 is the variable monomer, all other monomers as fixed at concentration x.

Variable monomer	app. K_m	app. V_{max}
eqn. 3.59		
M_1	$\frac{1}{4+4x}$	$\frac{k_{cat}[T]_t x}{4+4x}$
M_2	$\frac{1+x}{3+4x}$	$\frac{k_{cat}[T]_t x}{3+4x}$
M_3, M_4, M_5	$\frac{x^2}{1+3x+4x^2}$	$\frac{k_{cat}[T]_t x^2}{1+3x+4x^2}$
eqn. 3.60		
M_i	$\frac{x}{4+4x}$	$\frac{k_{cat}[T]_t x}{4+4x}$

For eqn. 3.59 the reaction rate, as expected from the form of the rate equation, responds differently to M_1 and M_2 than to the other three monomers, which all have the same effect on the reaction rate. As the concentration of the constant monomers increase M_2 starts to behave the same as M_3, M_4, and M_5. At saturating concentrations of the constant monomers the rate responds much more sensitively to changes in M_1 concentration than to changes in the concentration of the other monomers. The apparent K_m-value of M_1 decreases dramatically as the constant monomer concentration increases, that of M_2 decreases slightly, while those of the other three monomers increase from a very low value. At high monomer concentrations all the apparent K_m-values are nearly the same, with the exception of the much lower value of M_1. V_{max}-values

Table 3.3: Apparent K_m and V_{max}-values for eqns. 3.59 and 3.60 at different monomer concentrations. The monomers in the first column are the ones that are considered to be variable.

Conc.	0.1		1.0		10.0		100.0	
eqn. 3.59								
	K_m	V_{max}	K_m	V_{max}	K_m	V_{max}	K_m	V_{max}
M_1	0.2273	0.0227	0.1250	0.1250	0.0227	0.2273	0.0025	0.2475
M_2	0.3235	0.0294	0.2857	0.1429	0.2558	0.2326	0.2506	0.2481
M_3	0.0074	0.0074	0.1250	0.1250	0.2320	0.2320	0.2481	0.2481
M_4	0.0074	0.0074	0.1250	0.1250	0.2320	0.2320	0.2481	0.2481
M_5	0.0074	0.0074	0.1250	0.1250	0.2320	0.2320	0.2481	0.2481
eqn. 3.60								
M_i	0.0227	0.0227	0.1250	0.1250	0.2272	0.2272	0.2475	0.2475

increase with increasing constant monomer concentration, approaching the limit of 0.25 at high values.

For eqn. 3.60 the reaction rate responds identically to all monomers, since they are functionally equivalent in the rate equation. The V_{max}-values are identical to that of M_1 in eqn. 3.59 (see Table 3.2), but the apparent K_m increases from low values to a value nearly identical to that of monomers 3–5 in eqn. 3.59.

These results show that, whereas the two forms of the rate equation behave differently at low concentration of the constant monomer concentration, their behaviour is nearly indistinguishable when the enzyme-template complex is more than half saturated. As expected from the form of rate equations, the difference at low concentrations of constant monomer is with respect to the first two monomers in the chain. However, as shown in section 3.7 these differences become less as the length of the polymer increases. We therefore are of the opinion that, for most purposes (in computational systems biology), the simple form of the rate equation as given in eqn. 3.55 suffices.

Chapter 4

Testing the generic rate equation in a supply-demand analysis of template-directed polymerisation

In this chapter we test the generic rate equation derived in Chapter 3 by inserting it into a computational model of the reaction scheme given in the introduction (Fig. 1.2 in Chapter 1). For easy referencing the reaction scheme is repeated here as Fig. 4.1.

The main aim of this exercise it to generate the rate characteristics [56] of the five supply subsystems as the monomer product of each varies with the polymerisation demand reaction and to show how variation in the monomer composition affects the steady-state fluxes through the different biosynthetic pathways and the steady-state concentrations of the monomers.

This chapter is structured as follows: First we review the theoretical background to supply-demand analysis through a metabolic control analysis of a simple supply-demand system, and then we show how the behaviour of a supply-demand system around a steady state can be visualised with log-log rate characteristics. Using a model of the system in Fig. 4.1 we then generate the full set of rate characteristics and show how they respond to changes in the monomer composition and length of the polymer.

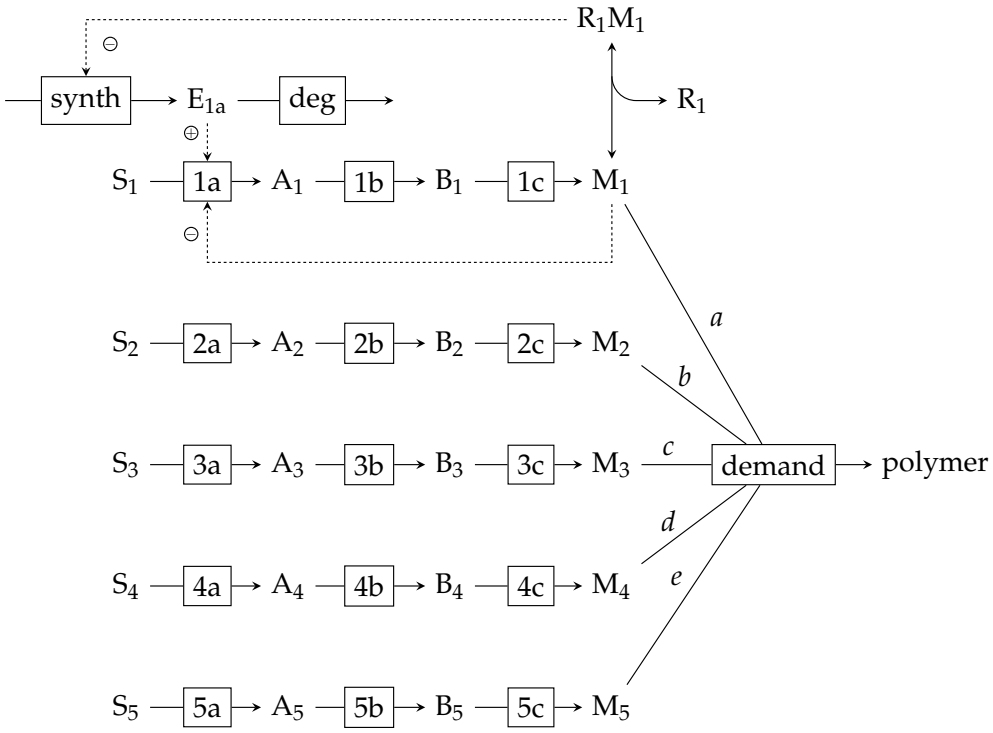

Figure 4.1: Scheme of a supply-demand metabolic system consisting of five biosynthetic (supply) blocks that each produce a monomer, and one demand block that consumes these monomers with the indicated stoichiometries (a to e) to yield a polymer product with monomer composition $(M_1)_a(M_2)_b(M_3)_c(M_4)_d(M_5)_e$. All five supply blocks are regulated by both allosteric feedback and regulation of expression of the first enzyme; for simplicity sake this is only shown for the first supply block. R_1 is a repressor protein, which, when bound to M_1 (the corepressor), forms a R_1M_1 complex; the latter prevents expression of the structural gene that encodes E_{1a}.

4.1 Metabolic control analysis of a supply-demand system

As mentioned in Chapter 1, Hofmeyr and Cornish-Bowden [2, 3, 4] developed a quantitative framework called supply-demand analysis to study the regulatory design of metabolism. This framework is based on a metabolic control analysis [57, 58] of a supply-demand system in steady state in which the degree of flux and concentration-control by the supply and demand blocks is related to their local properties, which are quantified as the elasticities of supply and demand.

Consider the biosynthesis of one of the monomers in Fig. 4.1. It can be regarded as a supply block that is linked by its product to the demand for that product as in Fig. 4.2.

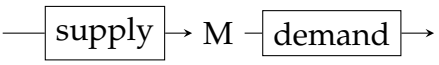

Figure 4.2: A metabolic supply-demand system around metabolite M

Metabolic control analysis defines measures, called control coefficients, for quantifying the degree to which a particular step in the system controls the steady-state fluxes and metabolite concentrations. For the supply-demand system in Fig. 4.2 they are defined as

$$C^J_{\text{supply}} = \frac{d\ln J}{d\ln v_{\text{supply}}}, \quad C^J_{\text{demand}} = \frac{d\ln J}{d\ln v_{\text{demand}}} \tag{4.1}$$

for *flux-control coefficients* (J is the steady-state flux; v_{supply} and v_{demand} are the local activities of the supply and demand subsystems) and

$$C^m_{\text{supply}} = \frac{d\ln m}{d\ln v_{\text{supply}}}, \quad C^m_{\text{demand}} = \frac{d\ln m}{d\ln v_{\text{demand}}} \tag{4.2}$$

for the *concentration-control coefficients* with respect to linking metabolite M with steady-state concentration m.

Flux-control and concentration-control coefficients obey the following summation relationships:

$$C^J_{\text{supply}} + C^J_{\text{demand}} = 1 \tag{4.3}$$

$$C^m_{\text{supply}} + C^m_{\text{demand}} = 0 \tag{4.4}$$

With regard to flux-control in a supply-demand system it is therefore appropriate to talk of the distribution of flux control. With regard to m there is no distribution of m-control because C^m_{supply} is always equal to $-C^m_{\text{demand}}$. Here it is only the magnitude of the variation in m that is of interest.

Control coefficients are related to properties of the supply and demand subsystems that quantify how sensitive the flux local to the subsystem (or the reaction rate, if it consists of only one reaction) is to perturbations in the concentration of any metabolite (here M) that directly affects that subsystem. These local properties are called *elasticity coefficients* and are defined as

$$\varepsilon_m^{v_{\text{supply}}} = \frac{d \ln v_{\text{supply}}}{d \ln m}, \quad \varepsilon_m^{v_{\text{demand}}} = \frac{d \ln v_{\text{supply}}}{d \ln m} \tag{4.5}$$

Note that $\varepsilon_m^{v_{\text{demand}}}$ is typically positive because M is a substrate of the demand; an increase in substrate concentration typically increases the reaction rate (except, of course, in the rare cases where it inhibits the rate). The product elasticity coefficient $\varepsilon_m^{v_{\text{supply}}}$ is typically negative because M is a product of the supply that inhibits the supply rate through product inhibition and mass action.

The *connectivity theorems* relate control coefficients to elasticity coefficients as follows:

$$C^J_{\text{supply}} \varepsilon_m^{v_{\text{supply}}} + C^J_{\text{demand}} \varepsilon_m^{v_{\text{demand}}} = 0 \tag{4.6}$$

$$C^m_{\text{supply}} \varepsilon_m^{v_{\text{supply}}} + C^m_{\text{demand}} \varepsilon_m^{v_{\text{demand}}} = -1 \tag{4.7}$$

Together, the summation and connectivity theorems allow the expression of control coefficients in terms of elasticities of supply and demand [3]. The flux-control coefficients are

$$C^J_{\text{supply}} = \frac{\varepsilon_m^{v_{\text{demand}}}}{\varepsilon_m^{v_{\text{demand}}} - \varepsilon_m^{v_{\text{supply}}}} \tag{4.8}$$

and

$$C^J_{\text{demand}} = \frac{-\varepsilon_m^{v_{\text{supply}}}}{\varepsilon_m^{v_{\text{demand}}} - \varepsilon_m^{v_{\text{supply}}}} \tag{4.9}$$

and the concentration-control coefficients:

$$C^m_{\text{supply}} = -C^m_{\text{demand}} = \frac{1}{\varepsilon_p^{v_{\text{demand}}} - \varepsilon_p^{v_{\text{supply}}}} \tag{4.10}$$

From eqns. 4.9 and 4.10 it follows that the ratio of elasticities determines the distribution of flux-control between supply and demand [2]. If $|\varepsilon_m^{v_{\text{supply}}}/\varepsilon_m^{v_{\text{demand}}}| > 1$ the demand has more control over the flux than the supply; if $|\varepsilon_m^{v_{\text{supply}}}/\varepsilon_m^{v_{\text{demand}}}| < 1$ the demand has less control over the flux than the supply. On the other hand it is the sum of the absolute values of the elasticities that determines the magnitude of the variation in m and, therefore, the degree to which it is homeostatically maintained: the larger $|\varepsilon_m^{v_{\text{demand}}} - \varepsilon_m^{v_{\text{supply}}}|$, the smaller the absolute values of both $C^m_{\text{supply}}$and C^m_{demand}, and the better the homeostatic regulation of m.

We now show how the behaviour of a supply-demand system around a steady state can be visualised with log-log rate characteristics.

4.2 Rate characteristic analysis

A rate characteristic is a graph that shows how the rate through a reaction (or the flux local to a reaction block) varies with the concentration of a chemical species that affects that reaction (such as a substrate, a product, or an effector). If the rate characteristic is plotted in double logarithmic space the slope of the tangent to the rate characteristic at a particular species concentration is equal to the elasticity coefficient that obtains at that concentration [56].

If the rate characteristics for the supply and demand blocks are plotted on the same graph they intersect at a point that represents the steady state, which is characterised by a flux, J, and concentration [M]. Rate characteristics therefore also illustrate the result from control analysis that the response in the steady state to small perturbations in the activities of supply or demand depends completely on the slopes of the tangents to the rate characteristics at the steady-state point, i.e., their elasticity coefficients [2]. The supply-demand rate characteristics for the supply of and the demand for M_1 is given in Fig. 4.3. However, before this graph is discussed we first describe the computational model that generated it.

The computational model

In order to generate the rate characteristics for the five biosynthetic supply pathways and the demand reaction in Fig. 4.1 we defined a model of the system in a PySCeS input file (provided in Appendix 6.11). All reactions were modelled with realistic enzyme kinetic rate equations and arbitrary parameter values (as defined in the PySCeS-input file). In each

biosynthetic pathway the first enzyme was modelled using the reversible Hill equation [8], which exhibits both cooperativity and allosteric regulation.

$$v = \frac{[\mathrm{E}]_t \frac{k_{\mathrm{cat}}}{s_{0.5}} \left([\mathrm{S}] - \frac{[\mathrm{P}]}{K_{\mathrm{eq}}} \right) \left(\frac{[\mathrm{S}]}{s_{0.5}} + \frac{[\mathrm{P}]}{p_{0.5}} \right)^{h-1}}{\left(\frac{[\mathrm{S}]}{s_{0.5}} + \frac{[\mathrm{P}]}{p_{0.5}} \right)^{h} + \frac{1 + \left(\frac{[\mathrm{M}]}{m_{0.5}} \right)^{h}}{1 + \alpha \left(\frac{[\mathrm{M}]}{m_{0.5}} \right)^{h}}} \tag{4.11}$$

where [S] is the substrate concentration, [P] the product concentration, [M] the allosteric modifier concentration, $s_{0.5}$, $p_{0.5}$, and $m_{0.5}$ are the half-saturating concentrations in the absence of other ligands, h is the Hill coefficient, α is the interaction factor (inhibitory when < 1; activating when > 1), k_{cat} and K_{eq} are the catalytic and equilibrium constants respectively, and $[\mathrm{E}]_t$ is the concentration of the enzyme.

Enzymes 2 and 3 were modelled using the reversible Michaelis-Menten equation:

$$v = \frac{[\mathrm{E}]_t \frac{k_{\mathrm{cat}}}{K_{\mathrm{s}}} \left([\mathrm{S}] - \frac{[\mathrm{P}]}{K_{\mathrm{eq}}} \right)}{\left(1 + \frac{[\mathrm{S}]}{K_{\mathrm{s}}} + \frac{[\mathrm{P}]}{K_{\mathrm{p}}} \right)} \tag{4.12}$$

where K_{s} and K_{p} denote the Michaelis constants for the substrate S and the product P respectively, k_{cat} and K_{eq} are the catalytic and equilibrium constants respectively, and $[\mathrm{E}]_t$ is the concentration of the enzyme.

The template-directed polymerisation reaction catalysed by $\mathrm{E}_{\mathrm{dem}}$ and T was modelled with the simplified generic rate eqn. 3.55 derived in Chapter 3 for a system with three elongation steps. Because we wanted to study the effects of changes in monomer composition and polymer length without having to worry about the identity of the first two monomers in the sequence, we chose to use the simplified generic rate equation that depends only on the monomer composition.

$$v_{\mathrm{demand}} = \frac{k_{\mathrm{cat}}[\mathrm{T}]_{\mathrm{t}}}{\frac{a}{\sigma_1} + \frac{b}{\sigma_2} + \frac{c}{\sigma_3} + \frac{d}{\sigma_4} + \frac{e}{\sigma_5} + (n-1)} \tag{4.13}$$

where k_{cat} is the catalytic rate constant, $[\mathrm{T}]_{\mathrm{t}}$ is the total template concentration, and the σ terms refer to the monomer concentration/dissociation

constant ratios. The coefficients a, b, c, d, and e are the number of monomers of each monomer type that occur in the polymer so that the total number of monomers (the length of the polymer) $n = a + b + c + d + e$.

Rate chacteristics of the supply and demand for M_1

The rate characteristics in Fig. 4.3 were generated by fixing the concentration of M_1, scanning it over a wide concentration range, and calculating the changes in the flux local to the supply block and the changes in the demand rate. Before the scan, the steady state of the system with all monomers variable was calculated and the initial concentrations of the monomers were set to their steady-state values. During the $[M_1]$-scan all other monomers remained fixed at these values. The PySCeS-script that generated the results is provided in Appendix 6.12 and the Gnuplot file that generated the graph is provided in Appendix 6.13.

Although there is only one demand process the actual demand on each supply differs with the stoichiometry with which its monomer product M_x participates in the polymerisation reaction. The stoichiometric coefficient of each monomer is of course equal to the number of units of that monomer in the polymer that is synthesised. For the reaction scheme given in Fig. 4.1 the monomer composition is $(M_1)_a(M_2)_b(M_3)_c(M_4)_d(M_5)_e$, so that the stoichiometric coefficient for M_1 is a, for M_2 is b, etc. The calculated demand rate was therefore multiplied with the stoichiometric coefficient for M_1 (here 10) to produce the actual production rate of M_1 (this was done in the Gnuplot file used to generate the plot, rather than in the PySCeS-script)

The supply rate characteristic in Fig. 4.3 has distinct regions that are numbered on the graph. Let us first consider the situation where there is no feedback via repression of E_{1a} synthesis: the light blue line at region 3 then represents the maximum flux-carrying capacity of the supply when the concentration of E_{1a} remains constant.

When E_{1a} is allowed to vary the situation at regions 1 and 2 obtains: in region 2 the concentration of M_1 is so low that the repressor-corepressor complex (R_1M_1) starts to dissociate, relieving inhibition and allowing the synthesis of additional E_{1a} to occur until it reaches a plateau (region 1) where the supply reaches a higher maximum flux-carrying capacity.

The parameters of E_{1a} have been chosen such that the concentration ranges in which M_1 acts as a repressor of E_{1a}-synthesis (region 2) and as an allosteric inhibitor of E_{1a}-activity (region 4) are distinct from each other (the relevant parameters are the dissociation constant of the repressor-corepressor complex and the half-saturation constant for the binding

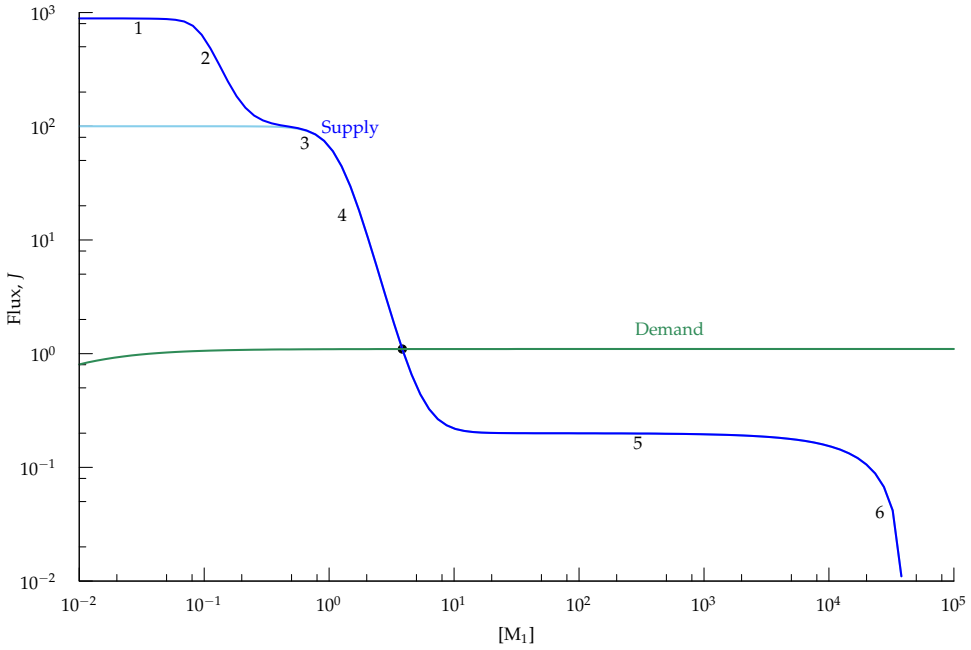

Figure 4.3: Log-log rate characteristics of the supply pathway from substrate S_1 to product M_1 and of the demand for M_1 with respect to changes in $[M_1]$. The steady state is obtained at the intersections of supply and demand rate characteristics (black dot). The light blue line represents the supply rate characteristic when the concentration of E_{1a} is clamped, i.e., when there is no genetic regulation of its concentration. The numbered regions of the supply rate characteristic are discussed in the text.

of M_1 to E_{1a}). Region 4 therefore represents the $[M_1]$-range where the flux responds sensitively to M_1 through kinetic regulation at the metabolic level.

Region 4 should be seen relative to region 6, where $[M_1]$ approaches its equilibrium value (the overall equilibrium constant of the supply block was set to $400 \times 10 \times 10 = 40000$ so that at the clamped value of 1 for S_1 the equilibrium value for $[M_1]$ is 40000). It is therefore clear that in this particular system kinetic regulation takes place at M_1-concentrations orders away from equilibrium (in which concentration range kinetic regulation occurs is a function of the binding strength of M_1 to E_{1a}). The steepness of the curve at region 4 is determined by the Hill coefficient, h, in eqn. 4.11. Changing the value of h changes the degree of cooperativity in the binding of M_1. The higher h, the steeper the response and the stronger the degree of cooperativity. Feedback inhibition is therefore es-

sential for maintaining homeostasis of $[M_1]$ far from its equilibrium value [2].

The plateau at region 5 represents the lower limit for kinetic regulation of the supply flux by M_1 and is a function of the interaction strength, α, in eqn. 4.11 [8]. The smaller α, the lower the flux at which the plateau occurs. When $\alpha = 0$, M_1 becomes an ordinary competitive inhibitor and there is no plateau and the supply curve continues downwards.

In the near-equilibrium region 6 the supply flux is again very sensitive to changes in $[M_1]$. Here we can speak of thermodynamic regulation of the supply flux, in contrast to kinetic regulation.

The point where the supply and demand rate characteristics intersect represents the steady state characterised by flux J and $[M_1]$ that obtain at that point. The slope of the demand curve at this point is effectively zero so that the demand has full control over the flux. As discussed in [2], the slope of the supply curve (the supply elasticity) determines the magnitude of the variation in $[M_1]$ under these conditions.

Rate characteristics of the full supply-demand system

This section describes five numerical experiments to produce the full set of supply and demand rate characteristics by repeating for the other four monomers the concentration scan described in the previous section. In all experiments the monomer supply pathways had the same reactions and identical kinetic parameters, except for the catalytic constants of the first reaction in each pathway ($k_{1a} = 200.0$, $k_{2a} = 20.0$, $k_{3a} = 10.0$, $k_{4a} = 5.0$, $k_{5a} = 1.0$). The differences between the experiments are listed in Table 4.1 and the rate characteristics are graphed in Figs. 4.4–4.7. Each figure contrasts the rate characteristics of experiment 1 with one of the other experiments. In all graphs the demand rate (the rate at which polymer is produced) was scaled with the stoichiometric coefficient for each monomer to yield the five demand rate characteristics. The flux-control coefficients and steady states for the four experiments are listed in Table 4.2 and Table 4.3. It should be emphasized that there is really only one flux, J, in this system, numerically equal to the rate at which the polymer is produced. It may seem as if there were five separate supply fluxes (each measured as the rate at which its pathway substrates is consumed), but they are of course all stoichiometrically linked to the demand flux and therefore stand in a fixed ratio to each other when the system is in steady state.

In section 4.1 we showed that the distribution of flux-control between supply and demand is determined by the ratio of supply and demand

Table 4.1: Values of parameters relevant to the numerical experiments. k_{5a} is the catalytic constant for reaction 5a and K_{d_x} represents all five monomer dissociation constants of the demand.

	k_{5a}	a, b, c, d, e	K_{d_x}	[Template]
Exp. 1	1.0	10, 20, 30, 40, 50	1.0	300.0
Exp. 2	50.0	10, 20, 30, 40, 50	1.0	300.0
Exp. 3	1.0	50, 40, 30, 20, 10	1.0	300.0
Exp. 4	1.0	1, 2, 3, 4, 5	1.0	300.0
Exp. 5	1.0	10, 20, 30, 40, 50	0.1	3.0

Table 4.2: Flux-control coefficients of the combined monomer supplies and the demand. The sum of flux-control coefficients were calculated from the non-truncated values. C^J_{demand} is the same for all 5 fluxes.

	Exp. 1	Exp. 2	Exp. 3	Exp. 4	Exp. 5
$C^J_{1a} + C^J_{1b} + C^J_{1c}$	0.000	0.000	0.007	0.000	0.000
$C^J_{2a} + C^J_{2b} + C^J_{2c}$	0.000	0.018	0.124	0.000	0.001
$C^J_{3a} + C^J_{3b} + C^J_{3c}$	0.000	0.078	0.077	0.000	0.002
$C^J_{4a} + C^J_{4b} + C^J_{4c}$	0.000	0.194	0.054	0.000	0.004
$C^J_{5a} + C^J_{5b} + C^J_{5c}$	0.991	0.043	0.076	0.991	0.087
C^J_{demand}	0.009	0.666	0.660	0.009	0.910
$C^J_{\text{all supplies}} + C^J_{\text{demand}}$	1.000	1.000	1.000	1.000	1.000

elasticities. When $|\varepsilon_m^{v_{\text{supply}}}/\varepsilon_m^{v_{\text{demand}}}| > 1$ the demand has more control over the flux than the supply; if $|\varepsilon_m^{v_{\text{supply}}}/\varepsilon_m^{v_{\text{demand}}}| < 1$ the demand has less control over the flux than the supply. These relationships allow us to understand the flux-control distribution in the rate characteristics in Figs. 4.4–4.6 at a glance (this is one of the most useful features of rate characteristics). Consider, for example, the set of supply and demand rate characteristics for experiment 1 (the top graphs in Figs. 4.4–4.6). Except for the supply elasticity of M_5, the demand elasticity at each steady state is much smaller than the supply elasticity. For the supply of M_5 the situation is reversed: the supply elasticity is effectively zero, and much less than the demand elasticity. This means that the supply for M_5 limits the demand reaction and prevents it from having any control over the rate of production of polymer. The calculated control coefficients listed in Table 4.2 confirm this reasoning: the supply for M_5 has complete control over the flux.

In experiment 2 the activity of the supply for M_5 was increased by increasing the value of k_{5a} from 1.0 to 50.0 (Fig. 4.4, bottom graph). This changed the steady state considerably and created a situation where the supply for M_5 was no longer limiting. The rate characteristics show that the limitation on the demand reaction now shifted mostly to the supply for M_4 where the elasticities of supply and demand were nearly equal, but the effect on the distribution of flux-control should not be so severe as in experiment 1. One expects flux-control to be split about evenly between the combined supplies and the demand. Again the calculated flux-control coefficients confirmed this: the demand had 67% control over the flux, while the supply for M_4 had the bulk (19%) of the rest.

Experiments 3 and 4 are the key experiments that show how the generic rate equation for template-directed polymerisation can be used to study the regulatory design and performance of the combined supply-demand system in the face of varying monomer composition and length of the polymer. In experiment 3 the monomer composition was changed (see Table 4.1) while retaining the length of the polymer, while in experiment 4 the monomer ratios were retained but the polymer was shortened from 150 to 15 monomer units. The rate characteristics of the two situations as compared to experiment 1 are given in Figs. 4.5 and 4.6. The rate characteristics for the situation in which the monomer composition has been changed within the same total number of units (Fig. 4.5, bottom graph) is more difficult to interpret because the supplies for M_2, M_3, M_4, and M_5 all share flux control between supply and demand, while the supply for M_1 clearly has little control over the flux. Because there is

no one clear limiting supply, one would expect the demand to have an appreciable degree of flux control because in all cases the demand elasticities are smaller than the supply elasticities. The calculated flux-control coefficients agree with this analysis.

At first glance the results of experiment 4, in which the relative monomer composition was retained but the polymer shortened by a factor of 10, were unexpected, because, despite the apparent lower demand on the monomer supplies due to the shorter polymer length, the rate characteristics in Fig. 4.6 (bottom graph) look virtually indistinguishable from those for the longer polymer in the top graph. Closer examination of the steady-state fluxes showed that for the short polymer the flux was nearly equal to 10 times the flux of the long polymer (see Table 4.3). However, the stoichiometric coefficients for the monomers also differed by a factor of 10 (those for the long polymer being 10 times those for the short polymer) so that the effects on the demand for the different supplies cancelled. This can be explained by examining the demand rate equation for the two situations. For the long polymer the rate equation is

$$v_{\text{demand}} = \frac{k_{\text{cat}}[\text{T}]_{\text{t}}}{\frac{10}{\sigma_1} + \frac{20}{\sigma_2} + \frac{30}{\sigma_3} + \frac{40}{\sigma_4} + \frac{50}{\sigma_5} + 149} \tag{4.14}$$

while for the shorter polymer the demand rate equation is

$$v_{\text{demand}} = \frac{k_{\text{cat}}[\text{T}]_{\text{t}}}{\frac{1}{\sigma_1} + \frac{2}{\sigma_2} + \frac{3}{\sigma_3} + \frac{4}{\sigma_4} + \frac{5}{\sigma_5} + 14} \tag{4.15}$$

That the demand rate for the short polymer is approximately equal to 10 times that of the long polymer follows from scaling both numerator and denominator by a factor of 10:

$$v_{\text{demand}} = \frac{10k_{\text{cat}}[\text{T}]_{\text{t}}}{\frac{10}{\sigma_1} + \frac{20}{\sigma_2} + \frac{30}{\sigma_3} + \frac{40}{\sigma_4} + \frac{50}{\sigma_5} + 140} \tag{4.16}$$

The only difference in the denominator is the constant factor which is 149 for the long polymer and 140 for the short polymer. This difference accounts for the small discrepancy between the two steady states. This experiment therefore shows that the length of the polymer does not make much of a difference to the steady state and the flux-control distribution if the relative monomer composition remains constant.

Finally, in experiment 5 the demand activity was decreased by decreasing the template concentration from 300.0 to 3.0 while the demand was also made 10 times more sensitive to the monomer concentrations by changing its monomer dissociation constants K_{d_1}, K_{d_2}, K_{d_3}, K_{d_4}, and K_{d_5} from 1.0 to 0.1. The rate characteristics are given in Fig. 4.7 (bottom graph). For all five supplies the demand elasticity was much smaller than the supply elasticity, so that the demand had a high degree (91%) of control over the flux. The situation for M_1 illustrates the problem of a demand that decreases to a point where kinetic regulation of the supply fails and the steady state jumps to a state close equilibrium, the concentration of M_1 in this case increasing by about three orders of magnitude. It is here that a catabolic sink for the monomer could act as an overflow valve and prevent the potentially catastrophic increase in concentration, providing it has the appropriate kinetic properties (this regulatory feature is discussed in [4]).

We believe that the experiments described in this section demonstrate forcefully the utility of the generic rate equation for template-directed polymerisation developed in this thesis, especially with regard to rate characteristic studies of monomer supply pathways integrated by a common demand in situations where different templates dictate different monomer sequences.

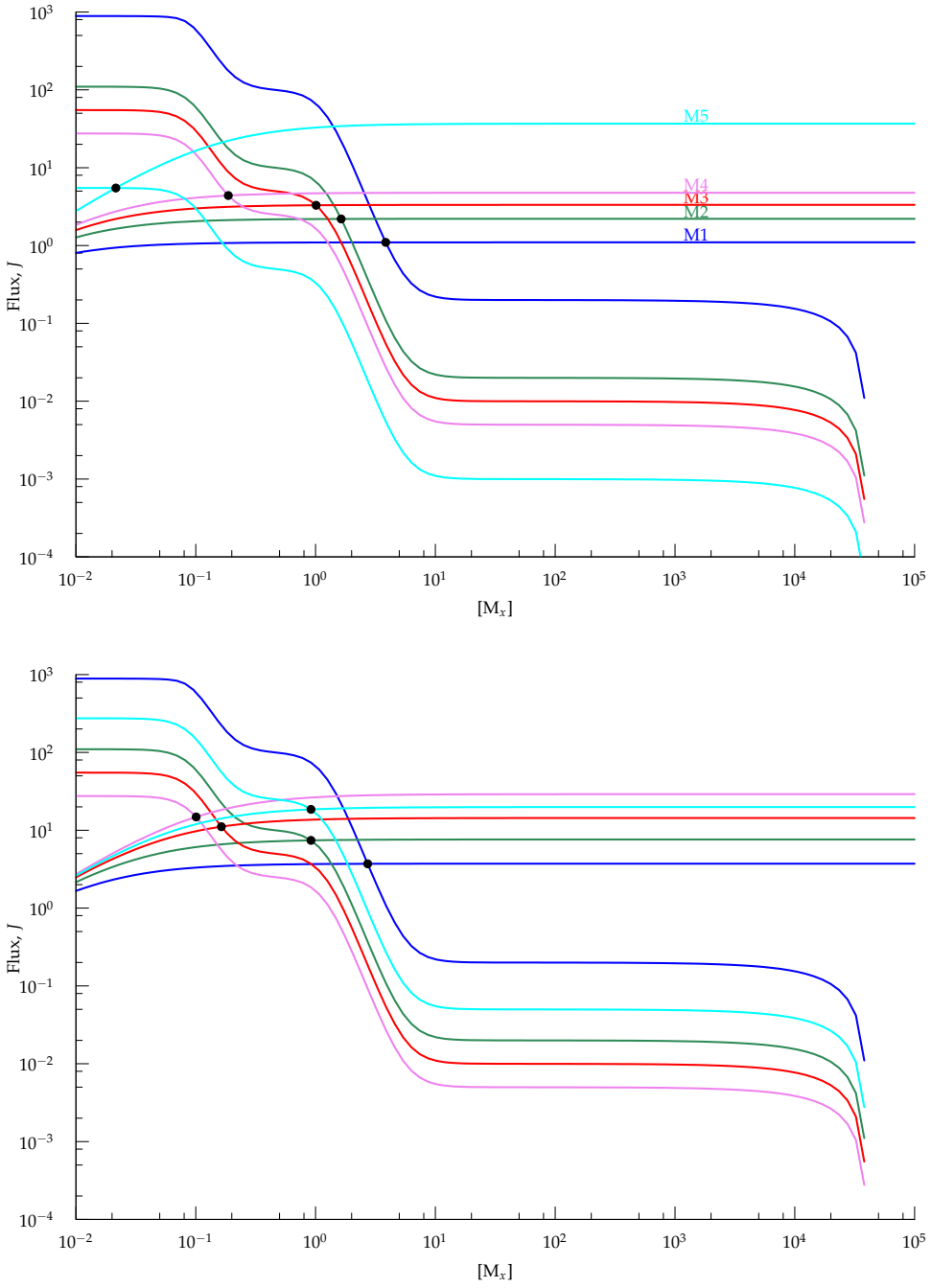

Figure 4.4: Log-log rate characteristics of the five supply pathways in Fig. 4.1 and of the demand for the five monomers M_1–M_5 for experiments 1 and 2. Each pair of supply and demand characteristics have their own colour. All monomers were clamped at their concentrations in the steady state calculated when the only fixed species were the pathway substrates S_1–S_5. Each of the five monomers were in turn scanned over the concentration range that spans the x-axis of the graph. The demand curves were generated by scaling the demand rate with the stoichiometric coefficients of the monomers. The black dots represent the calculated steady state for each monomer. The two graphs differ with respect to the catalytic constant of E_{5a}: in experiment 1 (top graph) $k_{5a} = 1.0$, while in experiment 2 (bottom graph) $k_{5a} = 50.0$.

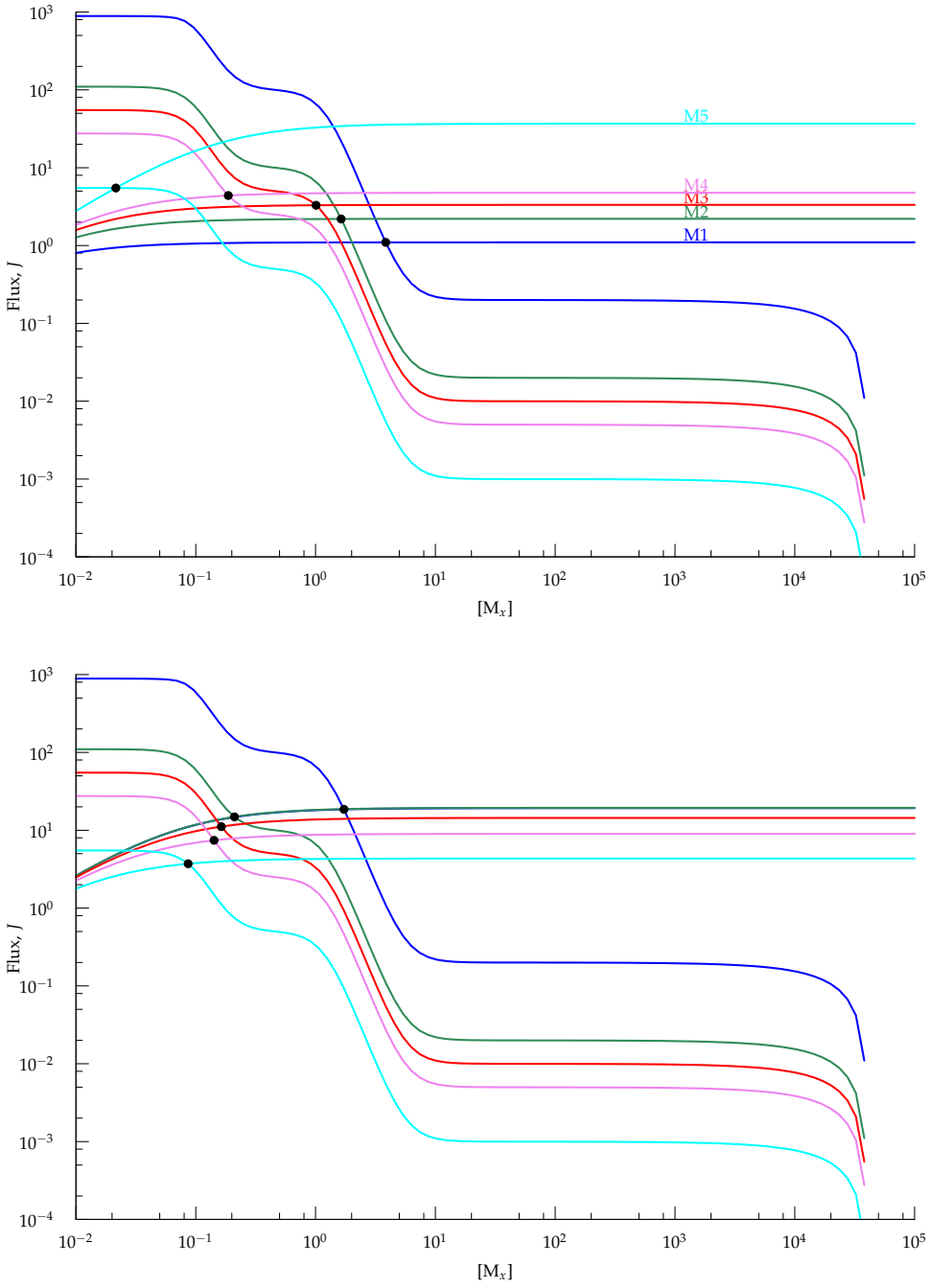

Figure 4.5: Log-log rate characteristics of the five supply pathways in Fig. 4.1 and of the demand for the five monomers M_1–M_5 for experiments 1 and 3. The two graphs differ with respect to monomer composition of the polymer: in experiment 1 (top graph) $(M_1)_{10}(M_2)_{20}(M_3)_{30}(M_4)_{40}(M_5)_{50}$, while in experiment 2 (bottom graph) $(M_1)_{50}(M_2)_{40}(M_3)_{30}(M_4)_{20}(M_5)_{10}$.

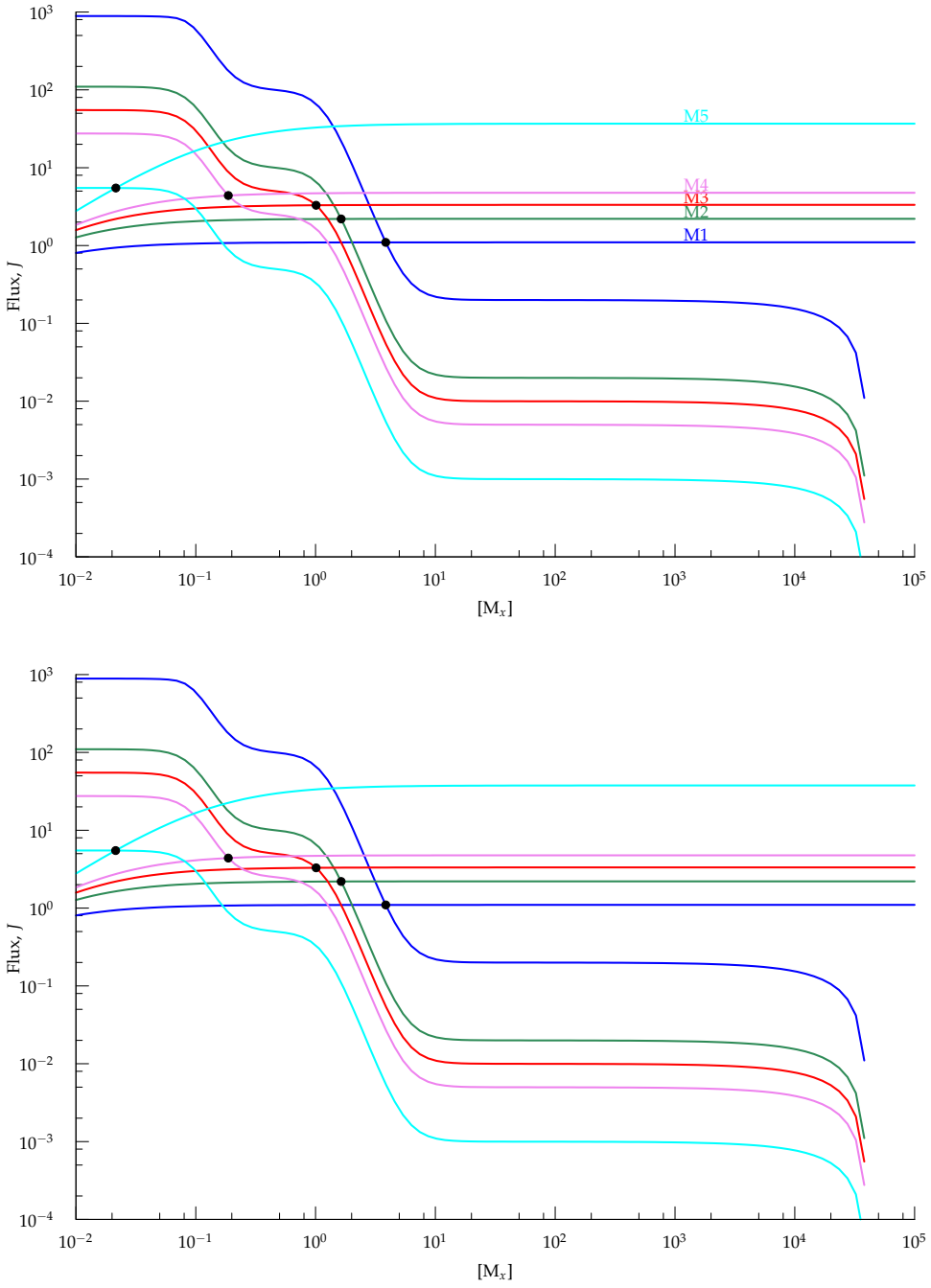

Figure 4.6: Log-log rate characteristics of the five supply pathways in Fig. 4.1 and of the demand for the five monomers M_1–M_5 for experiments 1 and 4. The two graphs differ with respect to polymer length while retaining the same monomer ratio: in experiment 1 (top graph) $(M_1)_{10}(M_2)_{20}(M_3)_{30}(M_4)_{40}(M_5)_{50}$, while in experiment 2 (bottom graph) $(M_1)_1(M_2)_2(M_3)_3(M_4)_4(M_5)_5$.

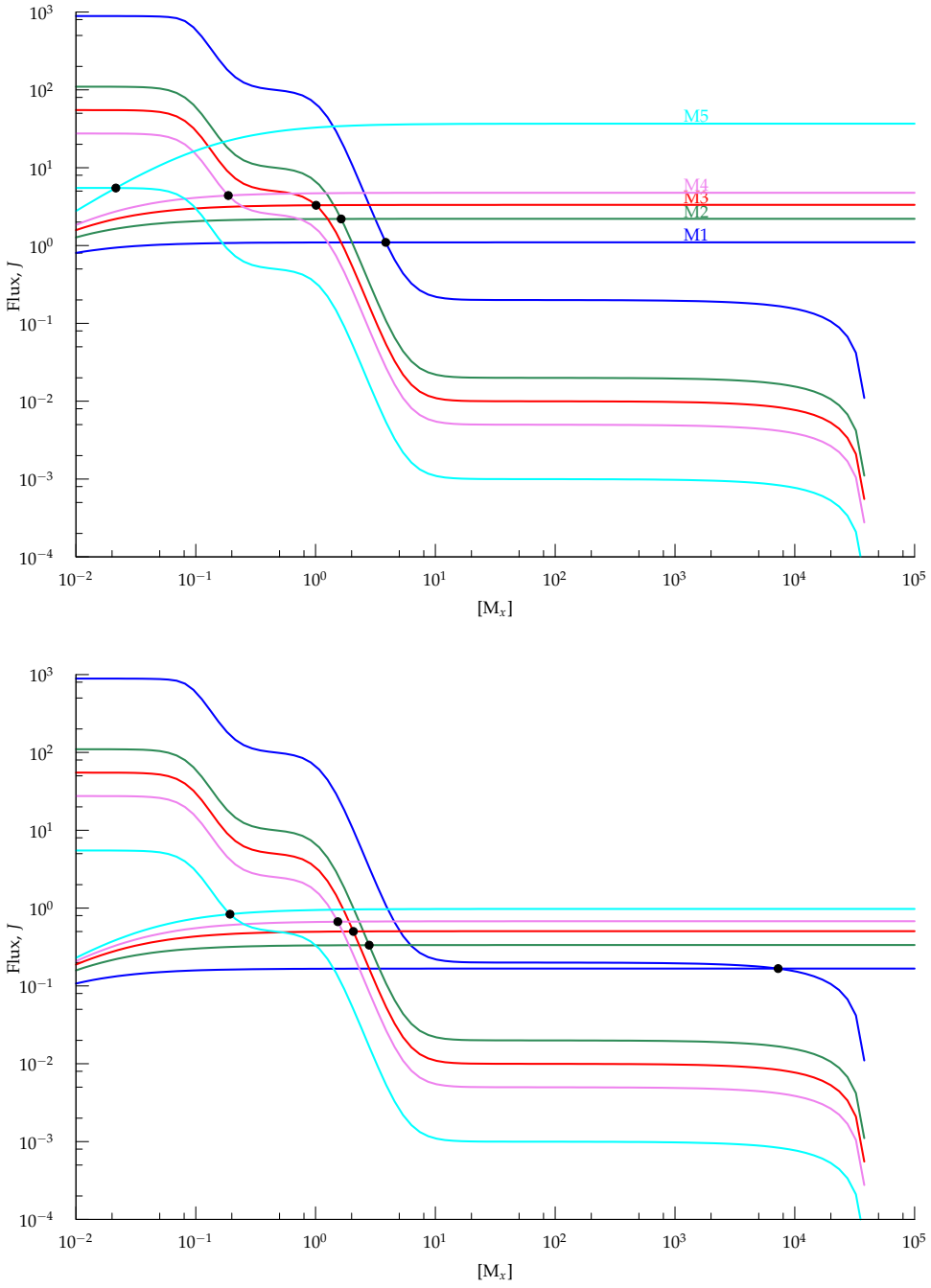

Figure 4.7: Log-log rate characteristics of the five supply pathways in Fig. 4.1 and of the demand for the five monomers M_1–M_5 for experiments 1 and 5. The two graphs differ with respect to the template concentration and monomer dissociation constant of the demand: In experiment 1 (top graph) [Template] = 300.0 and all $K_{d_x} = 1.0$, while in experiment 2 (bottom graph) [Template] = 3.0 and all $K_{d_x} = 0.1$.

Table 4.3: Steady-state fluxes and concentrations.

	Exp. 1	Exp. 2	Exp. 3	Exp. 4	Exp. 5
J_{dem}	1.0978e-01	3.7054e-01	3.7119e-01	1.0979e+00	1.6698e-02
J_{R1a}	1.0978e+00	3.7054e+00	1.8560e+01	1.0979e+00	1.6698e-01
J_{R2a}	2.1957e+00	7.4109e+00	1.4848e+01	2.1958e+00	3.3395e-01
J_{R3a}	3.2935e+00	1.1116e+01	1.1136e+01	3.2936e+00	5.0093e-01
J_{R4a}	4.3914e+00	1.4822e+01	7.4238e+00	4.3915e+00	6.6790e-01
J_{R5a}	5.4892e+00	1.8527e+01	3.7119e+00	5.4894e+00	8.3488e-01
J_{E1a}	1.0000e-02	1.0000e-02	1.0001e-02	1.0000e-02	1.0000e-02
J_{E2a}	1.0001e-02	1.0014e-02	1.4863e-02	1.0001e-02	1.0000e-02
J_{E3a}	1.0010e-02	2.2241e-02	2.2280e-02	1.0010e-02	1.0001e-02
J_{E4a}	1.7577e-02	5.9292e-02	2.9702e-02	1.7577e-02	1.0002e-02
J_{E5a}	1.0979e-01	1.0014e-02	7.4241e-02	1.0979e-01	1.6709e-02
$[M_1]$	3.8514e+00	2.7218e+00	1.7254e+00	3.8513e+00	7.2644e+03
$[M_2]$	1.6362e+00	9.1588e-01	2.1031e-01	1.6362e+00	2.8005e+00
$[M_3]$	1.0101e+00	1.6363e-01	1.6348e-01	1.0101e+00	2.0686e+00
$[M_4]$	1.8689e-01	1.0071e-01	1.4209e-01	1.8688e-01	1.5330e+00
$[M_5]$	2.1505e-02	9.1585e-01	8.6376e-02	2.1423e-02	1.9310e-01
$[A_1]$	4.0661e-02	3.3597e-02	4.6374e-02	4.0660e-02	7.2911e+01
$[A_2]$	1.9590e-02	1.8999e-02	1.9687e-02	1.9590e-02	2.8579e-02
$[A_3]$	1.4496e-02	1.4570e-02	1.4592e-02	1.4496e-02	2.1466e-02
$[A_4]$	6.9279e-03	1.8166e-02	9.9531e-03	6.9280e-03	1.6292e-02
$[A_5]$	6.3470e-03	3.4513e-02	5.0496e-03	6.3462e-03	2.8866e-03
$[B_1]$	3.9089e-01	2.8703e-01	2.2734e-01	3.9089e-01	7.2777e+02
$[B_2]$	1.6978e-01	1.0658e-01	3.9589e-02	1.6978e-01	2.8141e-01
$[B_3]$	1.0799e-01	2.9628e-02	2.9635e-02	1.0799e-01	2.0850e-01
$[B_4]$	2.4006e-02	2.6782e-02	2.2857e-02	2.4006e-02	1.5510e-01
$[B_5]$	7.8006e-03	1.2948e-01	1.2717e-02	7.7920e-03	2.0323e-02
$[E_{1a}]$	1.0000e+00	1.0000e+00	1.0001e+00	1.0000e+00	1.0000e+00
$[E_{2a}]$	1.0001e+00	1.0014e+00	1.4863e+00	1.0001e+00	1.0000e+00
$[E_{3a}]$	1.0010e+00	2.2241e+00	2.2280e+00	1.0010e+00	1.0001e+00
$[E_{4a}]$	1.7577e+00	5.9292e+00	2.9702e+00	1.7577e+00	1.0002e+00
$[E_{5a}]$	1.0979e+01	1.0014e+00	7.4241e+00	1.0979e+01	1.6709e+00

Chapter 5

Discussion

As described in the introduction (Chapter 1), the main aim of this thesis was to derive a generic rate equation for template-directed, enzyme catalysed polymerisation reactions which could be used in computational studies of the regulatory design of the integrated biosynthetic pathways for all the monomers linked to the polymerisation reaction; it would thereby provide a bridge between models of intermediary metabolism and models of the processes of growth.

A survey of the literature showed that there was no precedent for a rate equation of this nature. Although there have been a number of kinetic studies of DNA-transcription and mRNA-translation (surveyed in Chapter 2), their focus was mainly on the detailed mechanism of these processes, especially with regard to the initialisation phase.

Chapter 3 described the derivation of the required rate equation. There were several initial hurdles to be overcome. The first was the complication of adding to the catalytic mechanism the reversible binding of template to enzyme. In order to solve this we added template binding to a simple, irreversible Michaelis-Menten mechanism, even though the "template" did not here act as a template but rather as an essential catalytic cofactor. In such a mechanism the net reaction rate depends on the concentration of the enzyme-template-substrate (ETS) complex; in order to derive a steady-state rate equation for this simple catalytic mechanism we obtained an analytical expression for ETS (eqn. 3.15), assuming the free enzyme and template concentrations to be variable. This equation was far too complex to be usable, and we therefore had to make our first important assumption, namely that either the free enzyme concentration or the free template concentration is constant, thereby removing the corresponding conservation equation. If one assumes that the template and enzyme concentrations differ considerably then this assumption is justi-

fied: if, say, there is much less template than enzyme then, even if all the template is complexed to enzyme, the free enzyme concentration is still very close to the total enzyme concentration. Which concentration, template or enzyme, is assumed to be constant depends on the physiological state of the cell. Using this assumption we could derive a much simplified steady-state rate equation for the simple mechanism (eqn. 3.17).

When we added a dimerisation and elongation step to the mechanism the time-dependent behaviour showed an initial fast phase in which all the template is bound into ETM_1M_2, the complex with enzyme and two unligated monomers; in the ensuing slower phase ETM_1M_2 decreased until a steady state was reached in which the enzyme-template was partitioned between ETM_1M_2 and ETM_1–M_2M_3 forms.

In deriving the steady-state rate eqn. 3.39 for the expanded mechanism the following assumptions were made:

1. Binding steps were reversible, while catalytic and product release steps were irreversible;

2. Dissociation was much faster than catalysis (dimerisation, elongation, product release);

3. Rate constants for dimerisation and elongation steps were considered equal.

The rates calculated with the derived steady-state rate equation were identical to those calculated with PySCeS for the detailed mass-action model of the catalytic mechanism. Our rate equation was surprisingly robust with respect to assumption 2 above: even when k_{cat} was 100 times *larger* than the dissociation rate constants, the percentage error was still only about 0.2%.

By adding more elongation steps to the mechanism we were able to generalise the equation to an arbitrary number of elongation steps. Assuming that the polymer is composed of a fixed number of monomer types led to the fully generalised rate eqn. 3.50. The information needed to construct this equation for a particular polymer was the identity of the monomers that made up the initial dimeric sequence, as well as the monomer composition of the polymer.

We then considered a number of ways in which the generic rate equation could be further simplified. The denominator for the form of the equation in which [E] was considered clamped contains a term $K_0/[E]$ which vanishes under the condition that $[E]_t \gg [T]_t$ and $[E]_t \gg K_0$. This

assumption could well be satisfied under cellular conditions. Furthermore, if in addition the $1/\sigma_1\sigma_2$ term in the denominator is changed to $1/\sigma_1$ a form of the rate equation (eqn. 3.55) is obtained in which only the monomer composition needs to be known. We analysed the effect of these assumptions on the numerical value of the denominator of the rate equation and found it was quite robust to variation in $K_0/[\mathrm{E}]$: up to values of 1.0 the denominator could be simplified by assuming that $K_0/[\mathrm{E}]$ is zero. Even the second assumption was seen to be justified if the monomer concentrations are all at least half-saturating. Therefore, whereas the two forms of the rate equation behave differently at low concentration of the constant monomer concentration, their behaviour is nearly indistinguishable when the enzyme-template complex is more than half saturated, a condition which may well be generally satisfied in the physiological situation.

In the introduction the point was made that the rate equations used in classical enzyme kinetics were aimed at probing the mechanisms of catalysis and usually did not take account of the reversibility of the reaction and inhibition by product, and that such equations had limited usefulness for computational systems biology. It may seem that the generic rate equation derived in this thesis suffers the same limitations. However, template-directed polymerisation reactions are generally irreversible and product-insensitive. The irreversibility is due to coupling with activating agents in the form of nucleoside triphosphates. This particular feature has been ignored in the mechanism that formed the basis of our derivation, and should be included in future refinements of the generic rate equation. Another feature that should be studied is the stochasticity introduced when concentrations of enzyme or template become very low.

It then remained to test the usefulness of our derived rate equation by inserting it into a computational model. We constructed a toy model of a polymer consisting of five monomer types, each monomer having its own biosynthetic pathway (the reaction scheme is given in Fig. 1.2). We chose rate characteristic analysis of the combined supply and demand for the monomers to demonstrate the utility of the rate equation. In a series of numerical experiments we changed a number of features of our system: the activity of one of the supply pathways, the monomer composition at constant sequence length, the sequence length at constant monomer composition, and a decrease in demand activity (the results of these experiments are discussed fully in Chapter 4). It was particularly gratifying that, as we had hoped, the rate characteristics gave a clear visual representation of the control and regulation profile of the system.

It was made clear in the introduction that the primary aim of this the-

sis was to derive a generic rate equation for enzyme-catalysed template-directed polymerisation reactions and to test its utility as just described. Our results now make possible a full study of the regulatory design of the integrated system of monomer biosynthetic pathway coupled to polymerisation, and can therefore serve as a platform for a future research project for our group.

There are a number of aspects that such a future study should address. One important omission from the model used in this study is the existence of a catabolic demand for the monomers in addition to the demand of polymerisation. Hofmeyr [4] showed that a catabolic demand can act as an 'overflow valve' when the polymerisation demand falls so low that the lower limits of kinetic regulation is reached and the monomer concentration jumps to near-equilibrium values (the situation shown for M_1 in Fig. 4.7). It is therefore important to expand the model by adding a catabolic demand to each monomer. While rate characteristic analysis as described in this thesis will form an important part of the study, they will have to go hand in hand with an analysis of the responses of the system to changes in system parameters such as those that determine demand activity, the nature and degree of end-product inhibition of the biosynthetic subsystem at both the metabolic and genetic level. As in [4] the central task is to gain an understanding of how the properties of all the different subprocesses are tuned to each other to allow the integrated system to function harmoniously.

Another possibility for a future study would be to adapt the rather simple mechanism that forms the basis for the generic rate equation described in this thesis to the intricacies of the transcription and translation processes. Here the published studies described in Chapter 2 could serve as useful references. A particularly useful extension would be the incorporation of multiple binding of enzymes to template, such as is found in polyribosomal binding to messenger RNA.

Chapter 6

Appendices

6.1 PySCeS input file: Simple reaction scheme 3.1

```
# A kinetic model of the enzyme mechanism in Fig. 3.1
# Filename: system_1.psc

FIX: S

R0: E + T = ET          k0f * E * T - k0r * ET

R1: ET + S = ETS        k1f * ET * S - k1r * ETS

R2: ETS = ET + P        k2 * ETS

# Fixed concentrations

S = 10.0

# Initial concentrations

T = 1.0
E = 10.0
ET = 0.0
ETS = 0.0
P = 0.0

# Parameters

k0f = 1.0
```

```
k0r = 1.0
k1f = 1.0
k1r = 1.0
k2  = 1.0
```

6.2 PySCeS script for time-dependent simulation of reaction scheme 3.1

```
import pysces

m = pysces.model('system_1.psc')

m.doSimPlot(end=1.0,points=1000, plot='species')
pysces.plt.setGraphTitle(title='')
pysces.plt.setGrid("off")
pysces.plt.setRange("y",min=0.0,max=1.0)
pysces.plt.setKey("off")
pysces.plt.setAxisLabel("x",label="Time")
pysces.plt.setAxisLabel("y",label="Concentration")
pysces.plt.save('System_1_species_fast.dat')
pysces.plt.export('System_1_species_fast.png')

m.doSimPlot(end=1.0,points=1000, plot='species')
pysces.plt.setGraphTitle(title='')
pysces.plt.setGrid("off")
pysces.plt.setRange("y",min=0.0,max=10.0)
pysces.plt.setKey("off")
pysces.plt.setAxisLabel("x",label="Time")
pysces.plt.setAxisLabel("y",label="Concentration")
pysces.plt.save('System_1_species_slow.dat')
pysces.plt.export('System_1_species_slow.png')

m.doSimPlot(end = 1.0, points = 1000, plot='rates')
pysces.plt.setGraphTitle(title='')
pysces.plt.setGrid("off")
pysces.plt.setRange("y",min=0.0,max=10.0)
pysces.plt.setKey("off")
pysces.plt.setAxisLabel("x",label="Time")
pysces.plt.setAxisLabel("y",label="Reaction Rate")
pysces.plt.save('System_1_rates.dat')
pysces.plt.export('System_1_rates.png')

pysces.plt.closeAll()
```

6.3 Maxima batch file: Reaction scheme 3.1

```
/* Steady-state solution of the reaction system in Fig. 3.1

Filename: fig3_1.mac

s = [S]
e = [E]
t = [T]
a = [ET]
b = [ETS]
E = [E]t
T = [T]t

*/

e + a + b = E;

t + a + b = T;

K0 = e*t/a;

Km = a*s/b;

solve([%o2,%o3,%o4,%o5],[a,b,e,t]);
```

6.4 PySCeS input file: Reaction scheme 3.4B

```
# A kinetic model of the enzyme mechanism in Fig. 3.4B
# Filename: system_3.psc

  FIX: M1 M2 M3 E          # For calculating time-dependent
                           # progress curves
# FIX: M1 M2 M3 E M1_M2_M3 # For calculating steady state


R0: E + T = ET                  k0f * E * T - k0r * ET

R1: ET + M1 = ETM1              k1f * ET * M1 - k1r * ETM1

R2: ETM1 + M2 = ETM1M2          k2f * ETM1 * M2 - k2r * ETM1M2

R3: ETM1M2 = ETM1_M2            k3 * ETM1M2

R4: ETM1_M2 + M3 = ETM1_M2M3    k4f * ETM1_M2 * M3 - k4r * ETM1_M2M3

R5: ETM1_M2M3 = ET + M1_M2_M3   k5 * ETM1_M2M3

# Fixed concentrations

T  = 1.0
M1 = 100.0
M2 = 100.0
M3 = 100.0

# Initial concentrations

E = 10.0
ET = 0.0
ETM1 = 0.0
ETM1M2 = 0.0
ETM1_M2 = 0.0
ETM1_M2M3 = 0.0
M1_M2_M3 = 0.0

# Parameters

k0f = 10000.0
k0r = 10000.0
```

```
k1f = 1000.0
k1r = 1.0
k2f = 1000.0
k2r = 1.0
k3  = 14.0
k4f = 1000.0
k4r = 1.0
k5  = 12.0
```

6.5 PySCeS script for time-dependent simulation of reaction scheme 3.4B

```
import pysces

m = pysces.model('system_3.psc')

m.doSimPlot(end=0.0001,points=1000, plot='species')
pysces.plt.setGraphTitle(title='')
pysces.plt.setGrid("off")
pysces.plt.setRange("y",min=0.0,max=1.0)
pysces.plt.setKey("off")
pysces.plt.setAxisLabel("x",label="Time")
pysces.plt.setAxisLabel("y",label="Concentration")
pysces.plt.save('ExtModel_species_fast.dat')
pysces.plt.export('ExtModel_species_fast.png')

m.doSimPlot(end=0.45,points=1000, plot='species')
pysces.plt.setGraphTitle(title='')
pysces.plt.setGrid("off")
pysces.plt.setRange("y",min=0.0,max=1.0)
pysces.plt.setKey("off")
pysces.plt.setAxisLabel("x",label="Time")
pysces.plt.setAxisLabel("y",label="Concentration")
pysces.plt.save('ExtModel_species_slow.dat')
pysces.plt.export('ExtModel_species_slow.png')

m.doSimPlot(end=0.001,points=1000, plot='rates')
pysces.plt.setGraphTitle(title='')
pysces.plt.setGrid("off")
pysces.plt.setRange("y",min=0.0,max=0.2)
pysces.plt.setKey("off")
pysces.plt.setAxisLabel("x",label="Time")
pysces.plt.setAxisLabel("y",label="Reaction Rate")
pysces.plt.save('ExtModel_rates_upto_02.dat')
pysces.plt.export('ExtModel_rates_upto_02.png')

m.doSimPlot(end=0.001,points=1000, plot='rates')
pysces.plt.setGraphTitle(title='')
pysces.plt.setGrid("off")
pysces.plt.setRange("y",min=0.0,max=16.0)
pysces.plt.setKey("off")
pysces.plt.setAxisLabel("x",label="Time")
```

```
pysces.plt.setAxisLabel("y",label="Reaction Rate")
pysces.plt.save('ExtModel_rates_upto_16.dat')
pysces.plt.export('ExtModel_rates_upto_16.png')

m.doSimPlot(end = 0.45, points = 1000, plot='rates')
pysces.plt.setGraphTitle(title='')
pysces.plt.setGrid("off")
pysces.plt.setRange("y",min=0.0,max=16.0)
pysces.plt.setKey("off")
pysces.plt.setAxisLabel("x",label="Time")
pysces.plt.setAxisLabel("y",label="Reaction Rate")
pysces.plt.save('ExtModel_rates_slow.dat')
pysces.plt.export('ExtModel_rates_slow.png')

pysces.plt.closeAll()
```

6.6 Maxima batch file: Reaction scheme 3.4A

```
/* Steady-state solution of the reaction system in Fig. 3.4A

Filename: fig3_4A.mac

y  = [E]
t  = [T]
x  = [ET]
a  = [ETM1]
b  = [ETM1M2]
c  = [ETM1-M2]
d  = [ETM1-M2M3]
e  = [ETM1-M2-M3]
s1 = [M1]/Kd1 where Kd1 =  k1r/k1f
s2 = [M2]/Kd2 where Kd2 = (k3 + k2r)/k2f
s3 = [M3]/Kd3 where Kd3 = (k5 + k4r)/k4f
Et = [E]t
K0 = k0r/k0f = [E][T]/[ET]

*/

y*t - x*K0 = 0;

s1*x + (k2r/k1r)*b - (1 + ((k3+k2r)/k1r)*s2)*a = 0;

a*s2 - b = 0;

(k3/(k5+k4r))*b + (k4r/(k5+k4r))*d - c*s3 = 0;

c*s3 - d = 0;

k5*d - k6*e = 0;

a + b + c + d + e + x + y = Et;

solve([%o2,%o3,%o4,%o5,%o6,%o7,%o8],[a,b,c,d,e,x,y]);
```

6.7 Maxima batch file: Reaction scheme 3.4B

```
/* Steady-state solution of the reaction system in Fig. 3.4B

Filename: fig3_4B.mac

y  = [E]
t  = [T]
x  = [ET]
a  = [ETM1]
b  = [ETM1M2]
c  = [ETM1-M2]
d  = [ETM1-M2M3]
s1 = [M1]/Kd1 where Kd1 =  k1r/k1f
s2 = [M2]/Kd2 where Kd2 = (k3 + k2r)/k2f
s3 = [M3]/Kd3 where Kd3 = (k5 + k4r)/k4f
Et = [E]t
K0 = k0r/k0f = [E][T]/[ET]

*/

y*t - x*K0 = 0;

s1*x + (k2r/k1r)*b - (1 + ((k3+k2r)/k1r)*s2)*a = 0;

a*s2 - b = 0;

(k3/(k5+k4r))*b + (k4r/(k5+k4r))*d - c*s3 = 0;

c*s3 - d = 0;

a + b + c + d + x + y = Et;

solve([%o2,%o3,%o4,%o5,%o6,%o7],[a,b,c,d,x,y]);
```

6.8 PySCeS script for validating rate equations

```
# Filename: validate_rate_equation.py

import pysces

m = pysces.model('system_3_fixed_product.psc')

K0 = m.k0r/m.k0f

E_tot = m.E + m.ET + m.ETM1 + m.ETM1M2 + m.ETM1_M2 + m.ETM1_M2M3

T_tot = m.T + m.ET + m.ETM1 + m.ETM1M2 + m.ETM1_M2 + m.ETM1_M2M3

m.M1 = 100.0
m.M2 = 100.0
m.M3 = 100.0

rFile = open('validate.txt', 'w')
rFile.write("k_cat \tm.J_R5 \tv \tv_simp\n\n")

for k_cat in [0.01,0.1,1.0,10.0,100.0]:
   m.k3 = k_cat
   m.k5 = k_cat
   m.doState()

   print k_cat
   print m.J_R5

   K_d1 = m.k1r/m.k1f
   K_d2 = (k_cat + m.k2r)/m.k2f
   K_d3 = (k_cat + m.k4r)/m.k4f

   K_d2_s = m.k2r/m.k2f
   K_d3_s = m.k4r/m.k4f

   sig_1 = m.M1/K_d1
   sig_2 = m.M2/K_d2
   sig_3 = m.M3/K_d3

   sig_2_s = m.M2/K_d2_s
   sig_3_s = m.M3/K_d3_s
```

```
   v = (k_cat*sig_1*sig_2*sig_3*T_tot) /       \
   (K0/m.E*(k_cat/m.k1r*(sig_2*sig_3) + sig_3) \
   + 2*sig_1*sig_2*sig_3                       \
   + k_cat/m.k1r*(sig_2*sig_3)                 \
   + sig_1*sig_3                               \
   + sig_1*sig_2 + sig_3)
   print v

   v_simp = (k_cat*sig_1*sig_2_s*sig_3_s*T_tot) / \
   (2*(sig_1*sig_2_s*sig_3_s)                     \
   + sig_1*(sig_2_s+sig_3_s)                      \
   + sig_3_s*(1 + (K0/m.E)))
   print v_simp

   rFile.write("%-7.5e\t%-7.5e\t%-7.5e\t%-7.5e\n"
% (k_cat,m.J_R5,v,v_simp))

rFile.close()
```

6.9 Gnuplot plotfile for producing Fig. 3.8

```
# Gnuplot script to produce Fig.3.8 (TikZ output)
# Filename: Figs_3.8.plt

set term lua "gnuplot-tikz.lua" solid font "\\tiny"

set border 3
set samples 300
set key default
set style line 1 lt -1 lw 2 lc rgbcolor "red"
set style line 2 lt -1 lw 2 lc rgbcolor "blue"
set style line 3 lt -1 lw 2 lc rgbcolor "green"
set style line 4 lt -1 lw 2 lc rgbcolor "cyan"
set style line 5 lt -1 lw 2 lc rgbcolor "black"

unset size
set tics nomirror scale 0.5
set format x "$10^{%T}$"  # log scale
set format y "$10^{%T}$"  # log scale
set logscale xy

set xtics offset 0,0.5
set ytics offset 1,0

# Rate equation for homopolymer

# v = (kdem*Template)/((1 + K0/Edem)/((x/KdemM1)*(x/KdemM1))
                        + (n-1)/(x/KdemM1)
                        + (n-1))

# Rate equation for homopolymer (simplified symmetric form)

# v = (kdem*Template)/(n/(x/KdemM1) + (n-1))

# where
# x = concentration of monomer
# n is the length of the polymer

# Denominator terms of rate equation for homopolymer

rate_eq_homopol_denom(x)    = (1 + K0/Edem)/((x/KdemM1)*(x/KdemM1))\
                                + (n-1)/(x/KdemM1)                \
```

```
                                    + (n-1)
rate_eq_homopol_denom_1(x)  = (1 + K0/Edem)/((x/KdemM1)*(x/KdemM1))
rate_eq_homopol_denom_23(x) = 1/((x/KdemM1)*(x/KdemM1))            \
                                    + (n-1)/(x/KdemM1)             \
                                    + (n-1)
rate_eq_sym_homopol_denom(x) = n/(x/KdemM1)                        \
                                    + (n-1)

#-------------------------

#Initialise all parameters and variables to 1.0

K0 = 1.0
Edem = 1.0
Template = 1.0
kdem = 1.0
KdemM1 = KdemM2 = KdemM3 = KdemM4 = KdemM5 = 1.0
M1 = M2 = M3 = M4 = M5 = 1.0
n = 1.0

set output 'Homopolymer_denom_eqns_1.tikz'

set lmargin 0

set multiplot layout 3,3 rowsfirst
set xrange [1e-3:1e2]
set yrange [1e0:1e6]

unset key
unset title
unset label
unset arrow

# Produce multiplot for different values of K0 and n

#-------
K0 = 0.01
n = 5.0

set label 1 "$K_{0}/\\mathrm{[E]} = 0.01$" at 1,10e5 left
set label 2 "$n = 5$"       at 4.25,20e4 left

set label 3 "$n/\\sigma + (n-1)$" at 0.00125,1e1+30 left
```

```
set label 4 "{\\color{green} $1/\\sigma^{2} + (n-1)/\\sigma \
                    + (n-1)$}" at 0.00110,1e1-5 left
set label 5 "{\\color{blue}$(1+K_{0}/\\mathrm{[E]})/\\sigma^{2}$}" \
                    at 0.25,1e3+50 left
set label 6 "{\\color{red} $(1+K_{0}/\\mathrm{[E]})/\\sigma^{2} \
                    + (n-1)/\\sigma + (n-1)$}" at 0.0125,1e4 left

set ylabel "Rate" offset 2,0
unset xlabel
set format x ""

plot rate_eq_homopol_denom_1(x) ls 2,   \
     rate_eq_homopol_denom_23(x) ls 3,  \
 rate_eq_sym_homopol_denom(x) ls 5, \
 rate_eq_homopol_denom(x) ls 1

#-------
K0 = 0.01
n = 50.0
unset  label
set label 1 "$K_{0}/\\mathrm{[E]} = 0.01$" at 1,10e5 left
set label 2 "$n = 50$"       at 4.25,20e4 left
unset ylabel
set format y ""
unset xlabel
set format x ""

plot rate_eq_homopol_denom_1(x) ls 2,   \
     rate_eq_homopol_denom_23(x) ls 3,  \
 rate_eq_sym_homopol_denom(x) ls 5, \
 rate_eq_homopol_denom(x) ls 1
#-------
K0 = 0.01
n = 500.0
set label 1 "$K_{0}/\\mathrm{[E]} = 0.01$" at 1,10e5 left
set label 2 "$n = 500$"       at 4.25,20e4 left
unset ylabel
set format y ""
unset xlabel
set format x ""

plot rate_eq_homopol_denom_1(x) ls 2,   \
     rate_eq_homopol_denom_23(x) ls 3,  \
```

```
 rate_eq_sym_homopol_denom(x) ls 5, \
 rate_eq_homopol_denom(x) ls 1

#-------
K0 = 1.0
n = 5.0
set label 1 "$K_{0}/\\mathrm{[E]} = 1.0$" at 1,10e5 left
set label 2 "$n = 5$"       at 4.25,20e4 left
unset ylabel
unset xlabel
set ylabel "Rate" offset 2,0
set format y "$10^{%T}$"

plot rate_eq_homopol_denom_1(x) ls 2,   \
     rate_eq_homopol_denom_23(x) ls 3,  \
 rate_eq_sym_homopol_denom(x) ls 5, \
 rate_eq_homopol_denom(x) ls 1

#-------
K0 = 1.0
n = 50.0
set label 1 "$K_{0}/\\mathrm{[E]} = 1.0$" at 1,10e5 left
set label 2 "$n = 50$"       at 4.25,20e4 left
unset ylabel
set format y ""
unset xlabel
set format x ""

plot rate_eq_homopol_denom_1(x) ls 2,   \
     rate_eq_homopol_denom_23(x) ls 3,  \
 rate_eq_sym_homopol_denom(x) ls 5, \
 rate_eq_homopol_denom(x) ls 1

#-------
K0 = 1.0
n = 500.0
set label 1 "$K_{0}/\\mathrm{[E]} = 1.0$" at 1,10e5 left
set label 2 "$n = 500$"       at 4.25,20e4 left
unset ylabel
set format y ""
unset xlabel
set format x ""
```

```
plot rate_eq_homopol_denom_1(x) ls 2,   \
     rate_eq_homopol_denom_23(x) ls 3,  \
 rate_eq_sym_homopol_denom(x) ls 5, \
 rate_eq_homopol_denom(x) ls 1

#-------
K0 = 100.0
n = 5.0
set label 1 "$K_{0}/\\mathrm{[E]} = 100.0$" at 1,10e5 left
set label 2 "$n = 5$"       at 4.25,20e4 left
unset ylabel
unset xlabel
set xlabel "[monomer]"
set ylabel "Rate" offset 2,0
set format x "$10^{%T}$"
set format y "$10^{%T}$"

plot rate_eq_homopol_denom_1(x) ls 2,   \
     rate_eq_homopol_denom_23(x) ls 3,  \
 rate_eq_sym_homopol_denom(x) ls 5, \
 rate_eq_homopol_denom(x) ls 1

#-------
K0 = 100.0
n = 50.0
set label 1 "$K_{0}/\\mathrm{[E]} = 100.0$" at 1,10e5 left
set label 2 "$n = 50$"       at 4.25,20e4 left
unset ylabel
set format y ""

plot rate_eq_homopol_denom_1(x) ls 2,   \
     rate_eq_homopol_denom_23(x) ls 3,  \
 rate_eq_sym_homopol_denom(x) ls 5, \
 rate_eq_homopol_denom(x) ls 1

#-------
K0 = 100.0
n = 500.0
set label 1 "$K_{0}/\\mathrm{[E]} = 100.0$" at 1,10e5 left
set label 2 "$n = 500$"       at 4.25,20e4 left
unset ylabel
set format y ""
```

```
plot rate_eq_homopol_denom_1(x) ls 2,   \
     rate_eq_homopol_denom_23(x) ls 3,  \
 rate_eq_sym_homopol_denom(x) ls 5, \
 rate_eq_homopol_denom(x) ls 1unset multiplot

set term wxt
```

6.10 Gnuplot plotfile for producing Figs. 3.9 and 3.10

```
# Gnuplot script to produce Figs. 3.9 and 3.10 (TikZ output)
# Filename: Figs_3.9_3.10.plt

set term lua "gnuplot-tikz.lua" solid font "\\tiny"

set border 3
set samples 300
set key default
set style line 1 lt -1 lw 3 lc rgbcolor "red"
set style line 2 lt -1 lw 3 lc rgbcolor "blue"
set style line 3 lt -1 lw 3 lc rgbcolor "green"
set style line 4 lt -1 lw 3 lc rgbcolor "cyan"
set style line 5 lt -1 lw 3 lc rgbcolor "black"
set style line 6 lt  2 lw 2 lc rgbcolor "black"

unset size
unset logscale
set tics nomirror
set format x "%g"
set format y "%g"

set xtics offset 0,0.5
set ytics offset 1,0

#Initialise all parameters and variables to 1.0

K0 = 0.0
Edem = 1.0
Template = 1.0
kdem = 1.0
KdemM1 = KdemM2 = KdemM3 = KdemM4 = KdemM5 = 1.0
M1 = M2 = M3 = M4 = M5 = 1.0

c1 = 1.0
c2 = 1.0
c3 = 1.0
c4 = 1.0
c5 = 1.0

n = c1 + c2 + c3 + c4 + c5
```

```
# Rate equation (eq. 3.44), in each one a different monomer is varied

# v = (kdem*Template) / ( (1 + K0/Edem)/((M1/KdemM1)*(M2/KdemM2)) \
      + 1/(M2/KdemM2) + 1/(M3/KdemM3) + 1/(M4/KdemM4) + 1/(M5/KdemM5) + 4)

rate_eq_m1(x) = (kdem*Template)/((1 + K0/Edem)/((x/KdemM1)*(M2/KdemM2))  \
      + 1/(M2/KdemM2) + 1/(M3/KdemM3) + 1/(M4/KdemM4) + 1/(M5/KdemM5) + 4)
rate_eq_m2(x) = (kdem*Template)/((1 + K0/Edem)/((M1/KdemM1)*(x/KdemM2))  \
      + 1/(x/KdemM2)  + 1/(M3/KdemM3) + 1/(M4/KdemM4) + 1/(M5/KdemM5) + 4)
rate_eq_m3(x) = (kdem*Template)/( (1 + K0/Edem)/((M1/KdemM1)*(M2/KdemM2))\
      + 1/(M2/KdemM2) + 1/(x/KdemM3)  + 1/(M4/KdemM4) + 1/(M5/KdemM5) + 4)
rate_eq_m4(x) = (kdem*Template)/((1 + K0/Edem)/((M1/KdemM1)*(M2/KdemM2)) \
      + 1/(M2/KdemM2) + 1/(M3/KdemM3) + 1/(x/KdemM4)  + 1/(M5/KdemM5) + 4)
rate_eq_m5(x) = (kdem*Template)/((1 + K0/Edem)/((M1/KdemM1)*(M2/KdemM2)) \
      + 1/(M2/KdemM2) + 1/(M3/KdemM3) + 1/(M4/KdemM4) + 1/(x/KdemM5)  + 4)

# Varying all of the monomers at the same time

rate_eq_all(x) = (kdem*Template)/((1 + K0/Edem)/((x/KdemM1)*(x/KdemM2)) \
      + 1/(x/KdemM2) + 1/(x/KdemM3) + 1/(x/KdemM4) + 1/(x/KdemM5)  + 4 )

# Modification of original rate equations
# (modified by inserting an M2/KdemM2 term in the first denominator term)

# v = (kdem*Template) / ( c1/(M1/KdemM1) + c2/(M2/KdemM2) \
                        + c3/(M3/KdemM3) + c4/(M4/KdemM4) \
                        + c5/(M5/KdemM5) + (n-1) )

rate_eq_sym_m1(x) = (kdem*Template) / (c1/(x/KdemM1) + c2/(M2/KdemM2) \
                    + c3/(M3/KdemM3) + c4/(M4/KdemM4) \
                    + c5/(M5/KdemM5) + (n-1))
rate_eq_sym_m2(x) = (kdem*Template) / (c1/(M1/KdemM1) + c2/(x/KdemM2) \
                    + c3/(M3/KdemM3) + c4/(M4/KdemM4) \
                    + c5/(M5/KdemM5) + (n-1))
rate_eq_sym_m3(x) = (kdem*Template) / (c1/(M1/KdemM1) + c2/(M2/KdemM2) \
                    + c3/(x/KdemM3) + c4/(M4/KdemM4) \
                    + c5/(M5/KdemM5) + (n-1)
rate_eq_sym_m4(x) = (kdem*Template) / (c1/(M1/KdemM1) + c2/(M2/KdemM2) \
                    + c3/(M3/KdemM3) + c4/(x/KdemM4) \
                    + c5/(M5/KdemM5) + (n-1) )
rate_eq_sym_m5(x) = (kdem*Template) / (c1/(M1/KdemM1) + c2/(M2/KdemM2) \
                    + c3/(M3/KdemM3) + c4/(M4/KdemM4) \
```

```
                    + c5/(x/KdemM5) + (n-1))

# Varying all of the monomers at the same time

rate_eq_sym_all(x) = (kdem*Template) / ( c1/(M1/KdemM1) \
                    + c2/(M2/KdemM2) + c3/(M3/KdemM3) + c4/(M4/KdemM4) \
                    + c5/(M5/KdemM5) + (n-1) )

# Settings
K0 = 0.0001  # Very strong binding of template
Edem = 100.0 # Edem effectively saturates E,
             # so that the free enzyme is effectively ET

Template = 1.0
kdem = 1.0
KdemM1 = 1.0
KdemM2 = 1.0
KdemM3 = 1.0
KdemM4 = 1.0
KdemM5 = 1.0

# All monomer concentrations equal

M1 = M2 = M3 = M4 = M5 = 1.0

# Experiment 1
# Original rate equations

set output 'Exp_1_orig_rate_eqs.tikz'

set lmargin 0

set multiplot layout 2,4 rowsfirst

set xrange [0:10]
set yrange [0:0.25]

unset key
unset title
unset label
unset arrow

set xlabel "[monomer]" offset 0,1
```

```
set ylabel "Rate" offset 2,0

unset xlabel
set format x ""

unset label
unset arrow
set label 1 "M$_{1}$" at 1.78, 0.058 center
set label 2 "M$_{2}$" at 3.6, 0.058 center
set label 3 "M$_{3}$, M$_{4}$, M$_{5}$" at  5.0,  0.058

set arrow 1 from 1.78,0.042 to 1.78,0.0206001 nohead
set arrow 2 from 3.6,0.042  to 3.6,0.0274194  nohead
set arrow 3 from 6.8,0.042  to 6.8,0.009      nohead

M1 = M2 = M3 = M4 = M5 = 0.1
plot rate_eq_m1(x) ls 1 title "M1", \
     rate_eq_m2(x) ls 2 title "M2", \
 rate_eq_m3(x) ls 3 title "M3", \
 rate_eq_m4(x) ls 4 title "M4", \
 rate_eq_m5(x) ls 5 title "M5"

unset ylabel
set format y ""

unset label
unset arrow
set label 1 "M$_{1}$" at 2.2,0.116 center
set label 2 "M$_{2}$" at 4.5,0.116 center
set label 3 "M$_{3}$, M$_{4}$, M$_{5}$" at 5.45,0.046 center

set arrow 1 from 2.2,0.105   to 2.2,0.079     nohead
set arrow 2 from 4.44, 0.105 to 4.44,0.095    nohead
set arrow 3 from 5.7,0.052   to 5.7,0.0706086 nohead

M1 = M2 = M3 = M4 = M5 = 0.5
plot rate_eq_m1(x) ls 1 title "M1", \
     rate_eq_m2(x) ls 2 title "M2", \
 rate_eq_m3(x) ls 3 title "M3", \
 rate_eq_m4(x) ls 4 title "M4", \
 rate_eq_m5(x) ls 5 title "M5"

unset label
```

```
unset arrow
set label 1 "M$_{2}$" at 2.90028, 0.158 center
set label 2 "M$_{1}$, M$_{3}$, M$_{4}$, M$_{5}$" at 5.32110,0.098 center

set arrow 1 from 2.87520,0.129994 to 2.87520,0.145    nohead
set arrow 2 from 5.32110,0.102    to 5.32110,0.122038 nohead

M1 = M2 = M3 = M4 = M5 = 1.0
plot rate_eq_m1(x) ls 1 title "M1", \
     rate_eq_m2(x) ls 2 title "M2", \
 rate_eq_m3(x) ls 3 title "M3", \
 rate_eq_m4(x) ls 4 title "M4", \
 rate_eq_m5(x) ls 5 title "M5"

unset label
unset arrow
set label 1 "M$_{1}$" at 3.05,0.139 center
set label 2 "M$_{2}$" at 4.63123,0.198 center
set label 3 "M$_{3}$, M$_{4}$, M$_{5}$" at 7.3,0.139 center

set arrow 1 from 3.05,0.149    to 3.05,0.161817    nohead
set arrow 2 from 4.60615,0.186 to 4.60615,0.171478 nohead
set arrow 3 from 6.55,0.149    to 6.55,0.1694898   nohead

M1 = M2 = M3 = M4 = M5 = 2.0
plot rate_eq_m1(x) ls 1 title "M1", \
     rate_eq_m2(x) ls 2 title "M2", \
 rate_eq_m3(x) ls 3 title "M3", \
 rate_eq_m4(x) ls 4 title "M4", \
 rate_eq_m5(x) ls 5 title "M5"

unset label
unset arrow
set label 1 "M$_{1}$" at 1.44,0.23 center
set label 2 "M$_{2}$" at 2.5,0.165  center
set label 3 "M$_{3}$, M$_{4}$, M$_{5}$" at 3.75,0.135 center

set arrow 1 from 1.4,0.203  to 1.4,0.216       nohead
set arrow 2 from 1.6,0.1608 to 0.868297,0.1608 nohead
set arrow 3 from 0.5,0.1347 to 1.5,0.1347      nohead

set format x "%g"
set format y "%g"
```

```
set xlabel "[monomer]" offset 0,1
set ylabel "Rate" offset 2,0

M1 = M2 = M3 = M4 = M5 = 5.0
plot rate_eq_m1(x) ls 1 title "M1", \
     rate_eq_m2(x) ls 2 title "M2", \
 rate_eq_m3(x) ls 3 title "M3", \
 rate_eq_m4(x) ls 4 title "M4", \
 rate_eq_m5(x) ls 5 title "M5"

unset ylabel
set format y ""

unset label
unset arrow
set label 1 "M$_{1}$" at 3.5,0.189 center
set label 2 "M$_{2}$, M$_{3}$, M$_{4}$, M$_{5}$" at 7.6,0.189 center

set arrow 1 from 3.47727,0.2 to 3.47727,0.225749 nohead
set arrow 2 from 6.9,0.2     to 6.9,0.222623 nohead

M1 = M2 = M3 = M4 = M5 = 10.0
plot rate_eq_m1(x) ls 1 title "M1", \
     rate_eq_m2(x) ls 2 title "M2", \
 rate_eq_m3(x) ls 3 title "M3", \
 rate_eq_m4(x) ls 4 title "M4", \
 rate_eq_m5(x) ls 5 title "M5"

unset label
unset arrow
set label 1 "M$_{1}$" at 3.5,0.210 center
set label 2 "M$_{2}$, M$_{3}$, M$_{4}$, M$_{5}$" at 7.74820,0.210 center

set arrow 1 from 3.48,0.218    to 3.48,0.244786   nohead
set arrow 2 from 7.64785,0.218 to 7.64785,0.238251 nohead

M1 = M2 = M3 = M4 = M5 = 50.0
plot rate_eq_m1(x) ls 1 title "M1", \
     rate_eq_m2(x) ls 2 title "M2", \
 rate_eq_m3(x) ls 3 title "M3", \
 rate_eq_m4(x) ls 4 title "M4", \
 rate_eq_m5(x) ls 5 title "M5"
```

```
unset label
unset arrow
set label 1 "M$_{1}$" at 3.5,0.208 center
set label 2 "M$_{2}$, M$_{3}$, M$_{4}$, M$_{5}$" at 7.74820,0.208 center

set arrow 1 from 3.48,0.2185    to 3.48,0.247343 nohead
set arrow 2 from 7.49106,0.2185 to 7.49106,0.240240 nohead

M1 = M2 = M3 = M4 = M5 = 100.0
plot rate_eq_m1(x) ls 1 title "M1", \
     rate_eq_m2(x) ls 2 title "M2", \
 rate_eq_m3(x) ls 3 title "M3", \
 rate_eq_m4(x) ls 4 title "M4", \
 rate_eq_m5(x) ls 5 title "M5"

unset multiplot

# Experiment 2
# Modified rate equations

set output 'Exp_2_rate_eq_sym.tikz'

set format x "%g"
set format y "%g"

# set lmargin 0

set multiplot layout 2,4 rowsfirst

set xrange [0:10]
set yrange [0:0.25]

unset key
unset title
unset label
unset arrow

set xlabel "[monomer]" offset 0,1
set ylabel "Rate" offset 2,0

unset xlabel
set format x ""
```

```
M1 = M2 = M3 = M4 = M5 = 0.1
plot rate_eq_sym_m1(x) ls 1 title "M1", \
     rate_eq_sym_m2(x) ls 2 title "M2", \
     rate_eq_sym_m3(x) ls 3 title "M3", \
     rate_eq_sym_m4(x) ls 4 title "M4", \
     rate_eq_sym_m5(x) ls 5 title "M5"

unset ylabel
set format y ""

M1 = M2 = M3 = M4 = M5 = 0.5
plot rate_eq_sym_m1(x) ls 1 title "M1", \
     rate_eq_sym_m2(x) ls 2 title "M2", \
     rate_eq_sym_m3(x) ls 3 title "M3", \
     rate_eq_sym_m4(x) ls 4 title "M4", \
     rate_eq_sym_m5(x) ls 5 title "M5"


M1 = M2 = M3 = M4 = M5 = 1.0
plot rate_eq_sym_m1(x) ls 1 title "M1", \
     rate_eq_sym_m2(x) ls 2 title "M2", \
     rate_eq_sym_m3(x) ls 3 title "M3", \
     rate_eq_sym_m4(x) ls 4 title "M4", \
     rate_eq_sym_m5(x) ls 5 title "M5"


M1 = M2 = M3 = M4 = M5 = 2.0
plot rate_eq_sym_m1(x) ls 1 title "M1", \
     rate_eq_sym_m2(x) ls 2 title "M2", \
     rate_eq_sym_m3(x) ls 3 title "M3", \
     rate_eq_sym_m4(x) ls 4 title "M4", \
     rate_eq_sym_m5(x) ls 5 title "M5"

set format x "%g"
set format y "%g"
set xlabel "[monomer]" offset 0,1
set ylabel "Rate" offset 2,0

M1 = M2 = M3 = M4 = M5 = 5.0
plot rate_eq_sym_m1(x) ls 1 title "M1", \
     rate_eq_sym_m2(x) ls 2 title "M2", \
     rate_eq_sym_m3(x) ls 3 title "M3", \
     rate_eq_sym_m4(x) ls 4 title "M4", \
```

```
     rate_eq_sym_m5(x) ls 5 title "M5"

unset ylabel
set format y ""

M1 = M2 = M3 = M4 = M5 = 10.0
plot rate_eq_sym_m1(x) ls 1 title "M1", \
     rate_eq_sym_m2(x) ls 2 title "M2", \
     rate_eq_sym_m3(x) ls 3 title "M3", \
     rate_eq_sym_m4(x) ls 4 title "M4", \
     rate_eq_sym_m5(x) ls 5 title "M5"


M1 = M2 = M3 = M4 = M5 = 50.0
plot rate_eq_sym_m1(x) ls 1 title "M1", \
     rate_eq_sym_m2(x) ls 2 title "M2", \
     rate_eq_sym_m3(x) ls 3 title "M3", \
     rate_eq_sym_m4(x) ls 4 title "M4", \
     rate_eq_sym_m5(x) ls 5 title "M5"


M1 = M2 = M3 = M4 = M5 = 100.0
plot rate_eq_sym_m1(x) ls 1 title "M1", \
     rate_eq_sym_m2(x) ls 2 title "M2", \
     rate_eq_sym_m3(x) ls 3 title "M3", \
     rate_eq_sym_m4(x) ls 4 title "M4", \
     rate_eq_sym_m5(x) ls 5 title "M5"

unset multiplot
set term wxt
```

6.11 PySCeS input file: Supply-demand system in Fig. 4.1

```
# Filename: olona_supdem.psc

FIX: S1 S2 S3 S4 S5 Dummy

# Common growth demand

Rdem: M1 + M2 + M3 + M4 + M5 > Dummy

# The generic rate equation

# (kdem*Template) / (((1 + (K0/Edem))/((M1/KdemM1)*(M2/KdemM2)))
#                         + b/(M2/KdemM2) + c/(M3/KdemM3) + d/(M4/KdemM4)
#                         + e/(M5/KdemM5) + (n-1))

# Here the identity of the monomers in position 1 and 2 must be specified.
# Coefficients a,b,c,d,e are the number of each monomer type from
# position 2 in the polymer onwards.

# Simplified rate equation

(kdem*Template) / (a/(M1/KdemM1) + b/(M2/KdemM2) + c/(M3/KdemM3)
                + d/(M4/KdemM4) + e/(M5/KdemM5) + (n-1))

# Coefficients a,b,c,d,e are the number of each monomer type from
# in the full monomer sequence.

# Supply Enzymes

R1a: S1 = A1
(k1a*E1a/K1aS1)*(S1-A1/Keq1a)*(S1/K1aS1 + A1/K1aA1)**(h1a-1) /
      ((S1/K1aS1 + A1/K1aA1)**h1a
   + (1 + (M1/K1aM1)**h1a)/(1 + alpha1a*(M1/K1aM1)**h1a))

R2a: S2 = A2
(k2a*E2a/K2aS2)*(S2-A2/Keq2a)*(S2/K2aS2 + A2/K2aA2)**(h2a-1) /
      ((S2/K2aS2 + A2/K2aA2)**h2a
     + (1 + (M2/K2aM2)**h2a)/(1 + alpha2a*(M2/K2aM2)**h2a))

R3a: S3 = A3
(k3a*E3a/K3aS3)*(S3-A3/Keq3a)*(S3/K3aS3 + A3/K3aA3)**(h3a-1) /
      ((S3/K3aS3 + A3/K3aA3)**h3a \
     + (1 + (M3/K3aM3)**h3a)/(1 + alpha3a*(M3/K3aM3)**h3a))

R4a: S4 = A4
(k4a*E4a/K4aS4)*(S4-A4/Keq4a)*(S4/K4aS4 + A4/K4aA4)**(h4a-1) /
      ((S4/K4aS4 + A4/K4aA4)**h4a
 + (1 + (M4/K4aM4)**h4a)/(1 + alpha4a*(M4/K4aM4)**h4a))

R5a: S5 = A5
(k5a*E5a/K5aS5)*(S5-A5/Keq5a)*(S5/K5aS5 + A5/K5aA5)**(h5a-1) /
      ((S5/K5aS5 + A5/K5aA5)**h5a
 + (1 + (M5/K5aM5)**h5a)/(1 + alpha5a*(M5/K5aM5)**h5a))

# Supply Enzymes b
```

```
R1b: A1 = B1
(k1b*E1b/K1bA1)*(A1-B1/Keq1b)/(1 + A1/K1bA1 + B1/K1bB1)

R2b: A2 = B2
(k2b*E2b/K2bA2)*(A2-B2/Keq2b)/(1 + A2/K2bA2 + B2/K2bB2)

R3b: A3 = B3
(k3b*E3b/K3bA3)*(A3-B3/Keq3b)/(1 + A3/K3bA3 + B3/K3bB3)

R4b: A4 = B4
(k4b*E4b/K4bA4)*(A4-B4/Keq4b)/(1 + A4/K4bA4 + B4/K4bB4)

R5b: A5 = B5
(k5b*E5b/K5bA5)*(A5-B5/Keq5b)/(1 + A5/K5bA5 + B5/K5bB5)

# Supply Enzymes c

R1c: B1 = M1
(k1c*E1c/K1cB1)*(B1-M1/Keq1c)/(1 + B1/K1cB1 + M1/K1cM1)

R2c: B2 = M2
(k2c*E2c/K2cB2)*(B2-M2/Keq2c)/(1 + B2/K2cB2 + M2/K2cM2)

R3c: B3 = M3
(k3c*E3c/K3cB3)*(B3-M3/Keq3c)/(1 + B3/K3cB3 + M3/K3cM3)

R4c: B4 = M4
(k4c*E4c/K4cB4)*(B4-M4/Keq4c)/(1 + B4/K4cB4 + M4/K4cM4)

R5c: B5 = M5
(k5c*E5c/K5cB5)*(B5-M5/Keq5c)/(1 + B5/K5cB5 + M5/K5cM5)

# Synthesis  of supply enzyme a

E1a_syn: Dummy > E1a
V_syn_const
+ V_syn_induced*(1-M1**h_rpr1/(K_rpr1**h_rpr1 + M1**h_rpr1))

E2a_syn: Dummy > E2a
V_syn_const
+ V_syn_induced*(1-M2**h_rpr2/(K_rpr2**h_rpr2 + M2**h_rpr2))

E3a_syn: Dummy > E3a
V_syn_const
+ V_syn_induced*(1-M3**h_rpr3/(K_rpr3**h_rpr3 + M3**h_rpr3))

E4a_syn: Dummy > E4a
V_syn_const
+ V_syn_induced*(1-M4**h_rpr4/(K_rpr4**h_rpr4 + M4**h_rpr4))

E5a_syn: Dummy > E5a
V_syn_const
+ V_syn_induced*(1-M5**h_rpr5/(K_rpr5**h_rpr5 + M5**h_rpr5))

# Degradation of supply enzyme a

E1a_degrad: E1a > Dummy
k_degrad_E1a*E1a
```

```
E2a_degrad: E2a > Dummy
k_degrad_E2a*E2a

E3a_degrad: E3a > Dummy
k_degrad_E3a*E3a

E4a_degrad: E4a > Dummy
k_degrad_E4a*E4a

E5a_degrad: E5a > Dummy
k_degrad_E5a*E5a

# External metabolites
S1 = 1.0 S2 = 1.0 S3 = 1.0 S4 = 1.0 S5 = 1.0
Dummy = 0.0

# Internal metabolites
E1a = 1.0 E2a = 1.0 E3a = 1.0 E4a = 1.0 E5a = 1.0
A1  = 1.0 A2  = 1.0  A3 = 1.0  A4 = 1.0 A5  = 1.0
B1  = 1.0 B2  = 1.0  B3 = 1.0  B4 = 1.0 B5  = 1.0
M1  = 1.0 M2  = 1.0  M3 = 1.0  M4 = 1.0 M5  = 1.0

# Composition of the polymer string
a = 1.0 b = 1.0 c = 1.0 d = 1.0 e = 1.0

n = 5 # number of monomers

K0 = 1.0
Template = 1.0

# Rdem (common growth demand)
Edem   = 1.0
kdem   = 1.0
KdemM1 = 1.0
KdemM2 = 1.0
KdemM3 = 1.0
KdemM4 = 1.0
KdemM5 = 1.0

# R1a               # R2a               # R3a               # R4a               # R5a
k1a = 200.0         k2a = 200.0         k3a = 200.0         k4a = 200.0         k5a = 200.0
E1a = 1.0           E2a = 1.0           E3a = 1.0           E4a = 1.0           E5a = 1.0
Keq1a = 400.0       Keq2a = 400.0       Keq3a = 400.0       Keq4a = 400.0       Keq5a = 400.0
K1aS1 = 1.0         K2aS2 = 1.0         K3aS3 = 1.0         K4aS4 = 1.0         K5aS5 = 1.0
K1aA1 = 1.0e4       K2aA2 = 1.0e4       K3aA3 = 1.0e4       K4aA4 = 1.0e4       K5aA5 = 1.0e4
K1aM1 = 1.0         K2aM2 = 1.0         K3aM3 = 1.0         K4aM4 = 1.0         K5aM5 = 1.0
h1a = 4.0           h2a = 4.0           h3a = 4.0           h4a = 4.0           h5a = 4.0
alpha1a = 0.001     alpha2a = 0.001     alpha3a = 0.001     alpha4a = 0.001     alpha5a = 0.001

# R1b               # R2b               # R3b               # R4b               # R5b
k1b = 1.0           k2b = 1.0           k3b = 1.0           k4b = 1.0           k5b = 1.0
E1b = 1000.0        E2b = 1000.0        E3b = 1000.0        E4b = 1000.0        E5b = 1000.0
Keq1b = 10.0        Keq2b = 10.0        Keq3b = 10.0        Keq4b = 10.0        Keq5b = 10.0
K1bA1 = 1.0         K2bA2 = 1.0         K3bA3 = 1.0         K4bA4 = 1.0         K5bA5 = 1.0
K1bB1 = 1.0         K2bB2 = 1.0         K3bB3 = 1.0         K4bB4 = 1.0         K5bB5 = 1.0

# R1c               # R2c               # R3c               # R4c               # R5c
k1c = 1.0           k2c = 1.0           k3c = 1.0           k4c = 1.0           k5c = 1.0
```

```
E1c = 1000.0          E2c = 1000.0          E3c = 1000.0          E4c = 1000.0          E5c = 1000.0
Keq1c = 10.0          Keq2c = 10.0          Keq3c = 10.0          Keq4c = 10.0          Keq5c = 10.0
K1cB1 = 1.0           K2cB2 = 1.0           K3cB3 = 1.0           K4cB4 = 1.0           K5cB5 = 1.0
K1cM1 = 1.0           K2cM2 = 1.0           K3cM3 = 1.0           K4cM4 = 1.0           K5cM5 = 1.0

K_rpr1 = 0.1          K_rpr2 = 0.1          K_rpr3 = 0.1          K_rpr4 = 0.1          K_rpr5 = 0.1
h_rpr1 = 4.0          h_rpr2 = 4.0          h_rpr3 = 4.0          h_rpr4 = 4.0          h_rpr5 = 4.0
V_syn_const = 0.01    V_syn_const = 0.01    V_syn_const = 0.01    V_syn_const = 0.01    V_syn_const=0.01
V_syn_induced = 0.1   V_syn_induced = 0.1   V_syn_induced = 0.1   V_syn_induced = 0.1   V_syn_induced=0.1
k_degrad_E1a = 0.01   k_degrad_E2a = 0.01   k_degrad_E3a = 0.01   k_degrad_E4a = 0.01   k_degrad_E5a=0.01
```

6.12 PySCeS script for rate-characteristic analyses in Figs. 4.3 and 4.6

```
import pysces, scipy,  pylab, sushi

m1,m2 = sushi.model('olona_supdem', ['M1','M2','M3','M4','M5'], \
                    return_all=False)
m1,m3 = sushi.model('olona_supdem', ['M1','M2','M3','M4','M5','E1a'], \
                    return_all=False)

# There are 5 monomer types: M1, M2, M3, M4, M5

# Model m1 has FIXED: S1 S2 S3 S4 S5 Dummy (as in .psc file)
# Model m2 has FIXED: S1 S2 S3 S4 S5 Dummy M1 M2 M3 M4 M5
# Model m3 has FIXED: S1 S2 S3 S4 S5 Dummy M1 M2 M3 M4 M5 E1a

def experiment(exp, a, b, c, d, e, k1a, k2a, k3a, k4a, k5a, Kdem, template):

  m1.Stoich_nmatrix_SetValue('M1', 'Rdem', -a)
  m1.Stoich_nmatrix_SetValue('M2', 'Rdem', -b)
  m1.Stoich_nmatrix_SetValue('M3', 'Rdem', -c)
  m1.Stoich_nmatrix_SetValue('M4', 'Rdem', -d)
  m1.Stoich_nmatrix_SetValue('M5', 'Rdem', -e)

  m2.Stoich_nmatrix_SetValue('M1', 'Rdem', -a)
  m2.Stoich_nmatrix_SetValue('M2', 'Rdem', -b)
  m2.Stoich_nmatrix_SetValue('M3', 'Rdem', -c)
  m2.Stoich_nmatrix_SetValue('M4', 'Rdem', -d)
  m2.Stoich_nmatrix_SetValue('M5', 'Rdem', -e)

  m3.Stoich_nmatrix_SetValue('M1', 'Rdem', -a)
  m3.Stoich_nmatrix_SetValue('M2', 'Rdem', -b)
  m3.Stoich_nmatrix_SetValue('M3', 'Rdem', -c)
  m3.Stoich_nmatrix_SetValue('M4', 'Rdem', -d)
  m3.Stoich_nmatrix_SetValue('M5', 'Rdem', -e)

  m1.Stoichiometry_ReAnalyse()
  m2.Stoichiometry_ReAnalyse()
  m3.Stoichiometry_ReAnalyse()

  m1.a = m2.a = m3.a = a
  m1.b = m2.b = m3.b = b
  m1.c = m2.c = m3.c = c
```

```
m1.d = m2.d = m3.d = d
m1.e = m2.e = m3.e = e
m1.n = m2.n = m3.n = a + b + c + d + e

# Set the template concentration
m1.Template = m2.Template = m3.Template = template

# Set the demand dissociation constant for monomers
m1.KdemM1 = m2.KdemM1 = m3.KdemM1 = Kdem
m1.KdemM2 = m2.KdemM2 = m3.KdemM2 = Kdem
m1.KdemM3 = m2.KdemM3 = m3.KdemM3 = Kdem
m1.KdemM4 = m2.KdemM4 = m3.KdemM4 = Kdem
m1.KdemM5 = m2.KdemM5 = m3.KdemM5 = Kdem

# Set the catalytic constants

m1.k1a = m2.k1a = m3.k1a = k1a
m1.k2a = m2.k2a = m3.k2a = k2a
m1.k3a = m2.k3a = m3.k3a = k3a
m1.k4a = m2.k4a = m3.k4a = k4a
m1.k5a = m2.k5a = m3.k5a = k5a

# Calculate steady state for the model with variable Mx
m1.doState()
# Do a control analysis of this steady state
m1.doMca()

# Write out steady state and control analysis data

# Calculate summed flux-control coefficients
# for the 5 supply blocks
CJ1sup = m1.ccJR1a_R1a + m1.ccJR1a_R1b + m1.ccJR1a_R1c
CJ2sup = m1.ccJR2a_R2a + m1.ccJR2a_R2b + m1.ccJR2a_R2c
CJ3sup = m1.ccJR3a_R3a + m1.ccJR3a_R3b + m1.ccJR3a_R3c
CJ4sup = m1.ccJR4a_R4a + m1.ccJR4a_R4b + m1.ccJR4a_R4c
CJ5sup = m1.ccJR5a_R5a + m1.ccJR5a_R5b + m1.ccJR5a_R5c
CJsum  = CJ1sup + CJ2sup + CJ3sup + CJ4sup + CJ5sup + m1.ccJR1a_Rdem

F = open('C:\\pysces\\results\\SupDem_exp' + exp + '_mca.dat', 'w')
m1.showState(F)
F.write('\n')
m1.showCC(F)
F.write('\n')
```

```
m1.showElas(F)
F.write('\n')
F.write('ccJR1a_R1a  = ' + `m1.ccJR1a_R1a` + '\n')
F.write('ccJR1a_R1b  = ' + `m1.ccJR1a_R1b` + '\n')
F.write('ccJR1a_R1c  = ' + `m1.ccJR1a_R1c` + '\n')
F.write('ccJR1a_Rdem = ' + `m1.ccJR1a_Rdem` + '\n\n')
F.write('ccJR2a_R2a  = ' + `m1.ccJR2a_R2a` + '\n')
F.write('ccJR2a_R2b  = ' + `m1.ccJR2a_R2b` + '\n')
F.write('ccJR2a_R2c  = ' + `m1.ccJR2a_R2c` + '\n')
F.write('ccJR2a_Rdem = ' + `m1.ccJR2a_Rdem` + '\n\n')
F.write('ccJR3a_R3a  = ' + `m1.ccJR3a_R3a` + '\n')
F.write('ccJR3a_R3b  = ' + `m1.ccJR3a_R3b` + '\n')
F.write('ccJR3a_R3c  = ' + `m1.ccJR3a_R3c` + '\n')
F.write('ccJR3a_Rdem = ' + `m1.ccJR3a_Rdem` + '\n\n')
F.write('ccJR4a_R4a  = ' + `m1.ccJR4a_R4a` + '\n')
F.write('ccJR4a_R4b  = ' + `m1.ccJR4a_R4b` + '\n')
F.write('ccJR4a_R4c  = ' + `m1.ccJR4a_R4c` + '\n')
F.write('ccJR4a_Rdem = ' + `m1.ccJR4a_Rdem` + '\n\n')
F.write('ccJR5a_R5a  = ' + `m1.ccJR5a_R5a` + '\n')
F.write('ccJR5a_R5b  = ' + `m1.ccJR5a_R5b` + '\n')
F.write('ccJR5a_R5c  = ' + `m1.ccJR5a_R5c` + '\n')
F.write('ccJR5a_Rdem = ' + `m1.ccJR5a_Rdem` + '\n\n')
F.write('ccJR1a_R5a  = ' + `m1.ccJR1a_R5a` + '\n')
F.write('ccJR2a_R5a  = ' + `m1.ccJR2a_R5a` + '\n')
F.write('ccJR3a_R5a  = ' + `m1.ccJR3a_R5a` + '\n')
F.write('ccJR4a_R5a  = ' + `m1.ccJR4a_R5a` + '\n')
F.write('ccJR5a_R5a  = ' + `m1.ccJR5a_R5a` + '\n\n')
F.write('CJ1sup      = ' + `CJ1sup` + '\n')
F.write('CJ2sup      = ' + `CJ2sup` + '\n')
F.write('CJ3sup      = ' + `CJ3sup` + '\n')
F.write('CJ4sup      = ' + `CJ4sup` + '\n')
F.write('CJ5sup      = ' + `CJ5sup` + '\n')
F.write('CJsum       = ' + `CJsum`  + '\n')
F.close()

# Write the steady state [m1],Jsup pairs into a data file

F = open('C:\\pysces\\results\\SupDem_exp' + exp + '_ss.dat', 'w')
F.write(`a` + '  ' + `m1.M1_ss` + '  ' +   `m1.J_R1a` + '\n')
F.write(`b` + '  ' + `m1.M2_ss` + '  ' +   `m1.J_R2a` + '\n')
F.write(`c` + '  ' + `m1.M3_ss` + '  ' +   `m1.J_R3a` + '\n')
F.write(`d` + '  ' + `m1.M4_ss` + '  ' +   `m1.J_R4a` + '\n')
F.write(`e` + '  ' + `m1.M5_ss` + '  ' +   `m1.J_R5a` + '\n')
```

```
  F.close()

  scan_range = scipy.logspace(-2,5,101)

  # In turn, scan each monomer while keeping the
  # other at their steady-state concentrations

  for monomer in ['M1', 'M2', 'M3', 'M4', 'M5']:

    # Initialise the monomer concentrations of model m2
    # with fixed [Mi]) to steady-state values

    m2.M1 = m1.M1_ss
    m2.M2 = m1.M2_ss
    m2.M3 = m1.M3_ss
    m2.M4 = m1.M4_ss
    m2.M5 = m1.M5_ss

    m2.scan_in = monomer
    m2.scan_out = ['J_R1a','J_R2a','J_R3a','J_R4a','J_R5a','J_Rdem']

    m2.Scan1(scan_range)

    F = open('C:\\pysces\\results\\SupDem_Flux_'+ monomer \
                                  +'_exp'+exp+'.dat','w')
    m2.Write_array(m2.scan_res,F)
    F.close()

# Polymer composition
# a = for M1
# b = for M2
# c = for M3
# d = for M4
# e = for M5

# experiment(exp, a, b, c, d, e, k1a, k2a, k3a, k4a, k5a, Kdem, template):

# Experiment 1:
experiment('1', 10, 20, 30, 40, 50, 200.0, 20.0, 10.0, 5.0, 1.0, 1.0, 300.0)

# Experiment 2: make the M5-supply 50 times more active
experiment('2', 10, 20, 30, 40, 50, 200.0, 20.0, 10.0, 5.0, 50.0, 1.0, 300.0)
```

```
# Experiment 3: Same as exp 1, but reverse the monomer composition
experiment('3', 50, 40, 30, 20, 10, 200.0, 20.0, 10.0, 5.0, 1.0, 1.0, 300.0)

# Experiment 4: Same as exp 1, but shorter polymer, the same monomer ratios
experiment('4', 1, 2, 3, 4, 5, 200.0, 20.0, 10.0, 5.0, 1.0, 1.0, 300.0)

# Experiment 5: Same as exp 1, but decrease the demand
#               and make it more sensitive to [monomer]
experiment('5', 10, 20, 30, 40, 50, 200.0, 20.0, 10.0, 5.0, 1.0, 0.1, 3.0)
```

6.13 Gnuplot script for rate-characteristics in Figs. 4.3–4.6

```
# Filename: SupDem_ratechar.plt

set term lua "gnuplot-tikz.lua" solid font "\\scriptsize"

set palette
set border 3 front linetype -1 linewidth 1.000
set format x "$10^{%T}$"     # log scale
set format y "$10^{%T}$"     # log scale

set nokey
set logscale xy
set xtics border in scale 1,0.5 nomirror norotate offset character 0, 0, 0
set ytics border in scale 1,0.5 nomirror norotate offset character 0, 0, 0

# Supply-Demand model: Flux vs [M1]

set output 'C:\Pysces\fig_conversion\supdem_flux_M1.tikz'

a = 10.0
b = 20.0
c = 30.0
d = 40.0
e = 50.0

set xlabel "[M$_{1}$]"
set xrange [1e-2 : 1e5]  noreverse nowriteback
set ylabel "Flux, $J$" offset 2,0
set yrange [1e-2 : 1e3] noreverse nowriteback

unset label
unset arrow

set label 1 "1"      at 0.0233451,756.262
set label 2 "2"      at 0.08,408.866
set label 3 "3"      at 0.50,73.5
set label 4 "4"      at 0.99,17.2325
set label 5 "5"      at 230.367,0.169951
set label 6 "6"      at 20000.00,0.0419049
set label 7 "Demand" at 237.629,1.7     tc rgb "sea-green"
set label 8 "Supply" at 0.739330,101.00 tc rgb "blue"
```

```
set label 9 ""       at 3.851,1.098 point pointtype 7

plot 'C:\Pysces\results\SupDem_Flux_M1_fixE1a_exp1.dat' \
       u 1:2 w l lw 2 lt rgb "skyblue",                \
     'C:\Pysces\results\SupDem_Flux_M1_exp1.dat'       \
       u 1:2 w l lw 2 lt rgb "blue",                   \
     'C:\Pysces\results\SupDem_Flux_M1_exp1.dat'       \
       u 1:(a*$7) w l lw 2 lt rgb "sea-green"

unset ylabel

# Supply-Demand model: Flux vs [monomers]

set xlabel "[M$_{x}$]"
set xrange [1e-2 : 1e5]  noreverse nowriteback
set ylabel "Flux, $J$" offset 2,0
set yrange [1e-4 : 1e3] noreverse nowriteback

unset label
unset arrow

set label 1 "M1" at 1000,1.3*a*0.11 tc rgb "blue"
set label 2 "M2" at 1000,1.3*b*0.11 tc rgb "sea-green"
set label 3 "M3" at 1000,1.3*c*0.11 tc rgb "red"
set label 4 "M4" at 1000,1.3*d*0.12 tc rgb "violet"
set label 5 "M5" at 1000,1.3*e*0.74 tc rgb "cyan"

set output 'C:\Pysces\fig_conversion\supdem_flux_monomers_exp1.tikz'

plot 'C:\Pysces\results\SupDem_Flux_M1_exp1.dat' \
     u 1:2 w l lw 2 lt rgb "blue",               \
     'C:\Pysces\results\SupDem_Flux_M1_exp1.dat' \
     u 1:(a*$7) w l lw 2 lt rgb "blue",          \
     'C:\Pysces\results\SupDem_Flux_M2_exp1.dat' \
     u 1:3 w l lw 2 lt rgb "sea-green",          \
     'C:\Pysces\results\SupDem_Flux_M2_exp1.dat' \
     u 1:(b*$7) w l lw 2 lt rgb "sea-green",     \
     'C:\Pysces\results\SupDem_Flux_M3_exp1.dat' \
     u 1:4 w l lw 2 lt rgb "red",                \
     'C:\Pysces\results\SupDem_Flux_M3_exp1.dat' \
     u 1:(c*$7) w l lw 2 lt rgb "red",           \
     'C:\Pysces\results\SupDem_Flux_M4_exp1.dat' \
     u 1:5 w l lw 2 lt rgb "violet",             \
```

```
     'C:\Pysces\results\SupDem_Flux_M4_exp1.dat' \
     u 1:(d*$7) w l lw 2 lt rgb "violet",        \
     'C:\Pysces\results\SupDem_Flux_M5_exp1.dat' \
     u 1:6 w l lw 2 lt rgb "cyan",               \
     'C:\Pysces\results\SupDem_Flux_M5_exp1.dat' \
     u 1:(e*$7) w l lw 2 lt rgb "cyan",          \
     'C:\Pysces\results\SupDem_exp1_ss.dat'      \
     u 2:3 with points pt 7 lt rgb "black"

unset label

 set output 'C:\Pysces\fig_conversion\supdem_flux_monomers_exp2.tikz'

plot 'C:\Pysces\results\SupDem_Flux_M1_exp2.dat' \
     u 1:2 w l lw 2 lt rgb "blue",               \
     'C:\Pysces\results\SupDem_Flux_M1_exp2.dat' \
     u 1:(a*$7) w l lw 2 lt rgb "blue",          \
     'C:\Pysces\results\SupDem_Flux_M2_exp2.dat' \
     u 1:3 w l lw 2 lt rgb "sea-green",          \
     'C:\Pysces\results\SupDem_Flux_M2_exp2.dat' \
     u 1:(b*$7) w l lw 2 lt rgb "sea-green",     \
     'C:\Pysces\results\SupDem_Flux_M3_exp2.dat' \
     u 1:4 w l lw 2 lt rgb "red",                \
     'C:\Pysces\results\SupDem_Flux_M3_exp2.dat' \
     u 1:(c*$7) w l lw 2 lt rgb "red",           \
     'C:\Pysces\results\SupDem_Flux_M4_exp2.dat' \
     u 1:5 w l lw 2 lt rgb "violet",             \
     'C:\Pysces\results\SupDem_Flux_M4_exp2.dat' \
     u 1:(d*$7) w l lw 2 lt rgb "violet",        \
     'C:\Pysces\results\SupDem_Flux_M5_exp2.dat' \
     u 1:6 w l lw 2 lt rgb "cyan",               \
     'C:\Pysces\results\SupDem_Flux_M5_exp2.dat' \
     u 1:(e*$7) w l lw 2 lt rgb "cyan",          \
     'C:\Pysces\results\SupDem_exp2_ss.dat'      \
     u 2:3 with points pt 7 lt rgb "black"

a = 50.0
b = 40.0
c = 30.0
d = 20.0
e = 10.0

set output 'C:\Pysces\fig_conversion\supdem_flux_monomers_exp3.tikz'
```

```
plot 'C:\Pysces\results\SupDem_Flux_M1_exp3.dat' \
     u 1:2 w l lw 2 lt rgb "blue",                \
     'C:\Pysces\results\SupDem_Flux_M1_exp3.dat' \
     u 1:(a*$7) w l lw 2 lt rgb "blue",           \
     'C:\Pysces\results\SupDem_Flux_M2_exp3.dat' \
     u 1:3 w l lw 2 lt rgb "sea-green",           \
     'C:\Pysces\results\SupDem_Flux_M2_exp3.dat' \
     u 1:(b*$7) w l lw 2 lt rgb "sea-green",      \
     'C:\Pysces\results\SupDem_Flux_M3_exp3.dat' \
     u 1:4 w l lw 2 lt rgb "red",                 \
     'C:\Pysces\results\SupDem_Flux_M3_exp3.dat' \
     u 1:(c*$7) w l lw 2 lt rgb "red",            \
     'C:\Pysces\results\SupDem_Flux_M4_exp3.dat' \
     u 1:5 w l lw 2 lt rgb "violet",              \
     'C:\Pysces\results\SupDem_Flux_M4_exp3.dat' \
     u 1:(d*$7) w l lw 2 lt rgb "violet",         \
     'C:\Pysces\results\SupDem_Flux_M5_exp3.dat' \
     u 1:6 w l lw 2 lt rgb "cyan",                \
     'C:\Pysces\results\SupDem_Flux_M5_exp3.dat' \
     u 1:(e*$7) w l lw 2 lt rgb "cyan",           \
     'C:\Pysces\results\SupDem_exp3_ss.dat'       \
     u 2:3 with points pt 7 lt rgb "black"

a = 1.0
b = 2.0
c = 3.0
d = 4.0
e = 5.0

set output 'C:\Pysces\fig_conversion\supdem_flux_monomers_exp4.tikz'

plot 'C:\Pysces\results\SupDem_Flux_M1_exp4.dat' \
     u 1:2 w l lw 2 lt rgb "blue",                \
     'C:\Pysces\results\SupDem_Flux_M1_exp4.dat' \
     u 1:(a*$7) w l lw 2 lt rgb "blue",           \
     'C:\Pysces\results\SupDem_Flux_M2_exp4.dat' \
     u 1:3 w l lw 2 lt rgb "sea-green",           \
     'C:\Pysces\results\SupDem_Flux_M2_exp4.dat' \
     u 1:(b*$7) w l lw 2 lt rgb "sea-green",      \
     'C:\Pysces\results\SupDem_Flux_M3_exp4.dat' \
     u 1:4 w l lw 2 lt rgb "red",                 \
     'C:\Pysces\results\SupDem_Flux_M3_exp4.dat' \
```

```
     u 1:(c*$7) w l lw 2 lt rgb "red",           \
     'C:\Pysces\results\SupDem_Flux_M4_exp4.dat' \
     u 1:5 w l lw 2 lt rgb "violet",             \
     'C:\Pysces\results\SupDem_Flux_M4_exp4.dat' \
     u 1:(d*$7) w l lw 2 lt rgb "violet",        \
     'C:\Pysces\results\SupDem_Flux_M5_exp4.dat' \
     u 1:6 w l lw 2 lt rgb "cyan",               \
     'C:\Pysces\results\SupDem_Flux_M5_exp4.dat' \
     u 1:(e*$7) w l lw 2 lt rgb "cyan",          \
     'C:\Pysces\results\SupDem_exp4_ss.dat'      \
     u 2:3 with points pt 7 lt rgb "black"

a = 10.0
b = 20.0
c = 30.0
d = 40.0
e = 50.0

set output 'C:\Pysces\fig_conversion\supdem_flux_monomers_exp5.tikz'

plot 'C:\Pysces\results\SupDem_Flux_M1_exp5.dat' \
     u 1:2 w l lw 2 lt rgb "blue",               \
     'C:\Pysces\results\SupDem_Flux_M1_exp5.dat' \
     u 1:(a*$7) w l lw 2 lt rgb "blue",          \
     'C:\Pysces\results\SupDem_Flux_M2_exp5.dat' \
     u 1:3 w l lw 2 lt rgb "sea-green",          \
     'C:\Pysces\results\SupDem_Flux_M2_exp5.dat' \
     u 1:(b*$7) w l lw 2 lt rgb "sea-green",     \
     'C:\Pysces\results\SupDem_Flux_M3_exp5.dat' \
     u 1:4 w l lw 2 lt rgb "red",                \
     'C:\Pysces\results\SupDem_Flux_M3_exp5.dat' \
     u 1:(c*$7) w l lw 2 lt rgb "red",           \
     'C:\Pysces\results\SupDem_Flux_M4_exp5.dat' \
     u 1:5 w l lw 2 lt rgb "violet",             \
     'C:\Pysces\results\SupDem_Flux_M4_exp5.dat' \
     u 1:(d*$7) w l lw 2 lt rgb "violet",        \
     'C:\Pysces\results\SupDem_Flux_M5_exp5.dat' \
     u 1:6 w l lw 2 lt rgb "cyan",               \
     'C:\Pysces\results\SupDem_Flux_M5_exp5.dat' \
     u 1:(e*$7) w l lw 2 lt rgb "cyan",          \
     'C:\Pysces\results\SupDem_exp5_ss.dat'      \
     u 2:3 with points pt 7 lt rgb "black"
```

```
set term wxt
```

Bibliography

[1] Atkinson, D. E. (1977). *Cellular energy metabolism and its regulation*. Academic Press, New York.

[2] Hofmeyr, J.-H. S. and Cornish-Bowden, A. (2000). *FEBS Lett. 476*, 47–51.

[3] Hofmeyr, J.-H. S. and Cornish-Bowden, A. (1991). *Eur. J. Biochem. 200*, 223–236.

[4] Hofmeyr, J.-H. (2008). *Essays Biochem. 45*, 57–66.

[5] Kitano, H. (2002). *Nature 420*, 206–210.

[6] Monod, J., Wyman, J., and Changeux, J. P. (1965). *J. Mol. Biol. 12*, 88–118.

[7] Koshland, Jr., D. E., Nemethy, G., , and Filmer, D. (1966). *Biochemistry 5*, 365–385.

[8] Hofmeyr, J.-H. S. and Cornish-Bowden, A. (1997). *Comput. Appl. Biosci. 13*, 377–385.

[9] Hanekom, A. J. (2006). Generic kinetic equations for modelling multisubstrate reactions in computational systems biology. M.Sc. (Biochemistry), Univ. of Stellenbosch.

[10] Rohwer, J. M., Hanekom, A. J., and Hofmeyr, J.-H. S. (2007). A universal rate equation for systems biology. In Kettner, C. and Hicks, M. G., editors, *Proceedings of 2nd International ESCEC Symposium on Experimental Standard Conditions on Enzyme Characterizations, March 19th–23rd, 2006, Ruedesheim/Rhein, Germany*.

[11] Rohwer, J. M., Hanekom, A. J., Crous, C., Snoep, J. L., and Hofmeyr, J.-H. S. (2006). *IEE Proc.-Syst. Biol. 153*, 338–341.

[12] Crick., F. (1970). *Nature 227*, 561–563.

[13] Berg, J. M., Tymoczko, J. L., and Stryer, L. (2002). *Biochemistry*. Freeman, W.H., New York, 5th edition.

[14] Mehra, A., Lee, K. H., and Hatzimanikatis, V. (2003). *Biotechnol. Bioeng. 84*, 822–833.

[15] Heinrich, R. and Rapoport, T. A. (1980). *J. Theor. Biol. 86*, 279–313.

[16] Cosma, M. P. (2002). *Mol. Cell 10*, 227–236.

[17] Cha, S. (1968). *J. Biol. Chem. 243*, 820–825.

[18] Cleland, W. W. (1963). *Biochim. Biophys. Acta 67*, 104–137.

[19] Ishikawa, H., Maeda, T., Hikita, H., and Miyatake, K. (1988). *Biochem. J. 251*, 175–181.

[20] Kremling, A. (2007). *Biotechnol. Bioeng. 96*, 815–819.

[21] Arnold, S., Siemann, M., Scharnweber, K., Wener, M., Buamann, S., and Reuss, M. (2001). *Biotechnol. Bioeng. 72*, 548–561.

[22] Jülicher, F. and Bruinsma, R. (1998). *Biophys. J. 74*, 1169–1185.

[23] Höfer, T. and Rasch, M. (2005). *Genome Informatics 16*, 73–82.

[24] Yang, H. T., Hsu, C. P., and Hwang, M. J. (2007). *J. Biochem. 142*, 135–144.

[25] Sousa, R. and Mukherjee, S. (2003). *Prog. Nucleic Acid Res. Mol. Biol. 73*, 1–41.

[26] Martin, C., Esposito, E., Theis, K., and Gong, P. (2005). *Prog. Nucleic Acid Res. Mol. Biol. 80*, 323–347.

[27] Pozhitkov, A. E., Lavrik, I. N., Sergeev, M. M., and Kochetkov, S. N. (1998). *Mol. Biol. 32*, 78–82.

[28] Cornish-Bowden, A. (1995). *Fundamentals of enzyme kinetics*. Portland Press, London, 2nd edition.

[29] Roussel, M. R. and Zhu, R. (2006). *Phys. Biol. 3*, 274–284.

[30] Rempala, G. A., Ramos, K. S., and Kalbfleisch, T. (2006). *J. Theor. Biol. 242*, 101–116.

[31] Gillespie, D. T. (1977). *J. Phys. Chem. 8*, 2340–2361.

[32] Hill, A. (1910). *J. Physiol. 40*, 4–7.

[33] Savageau, M. A. (1976). *Biochemical systems analysis: A study of function and design in Molecular Biology*. Addison-Wesley Publishing Company, Reading, MA.

[34] Michaelis, L. and Menten, L. M. (1913). *Biochem. Z. 49*, 333–369.

[35] Cranz, S., Berger, C., Baici, A., Jelesarov, I., and Bosshard, H. R. (2004). *Biochemistry 43*, 718–727.

[36] MacDonald, C. T., Gibbs, J. H., and Pipkin, A. C. (1968). *Biopolymers 6*, 1–25.

[37] Pipkin, A. C. and Gibbs, J. H. (1966). *Biopolymers 4*, 3–15.

[38] MacDonald, C. T. and Gibbs, J. H. (1969). *Biopolymers 7*, 707–725.

[39] Hiernaux, J. (1974). *Biophys. Chem. 2*, 70–75.

[40] Vassart, G., Dumont, J. E., and Cantraine, F. R. (1971). *Biochim. Biophys. Acta 247*, 471–485.

[41] Lodish, H. F. (1974). *Nature 251*, 385–388.

[42] Bergmann, J. E. and Lodish, H. F. (1979). *J. Biol. Chem. 254*, 11927–11937.

[43] Hunt, T., Hunter, T., and Munro, A. (1968). *J. Mol. Biol. 36*, 31–45.

[44] Luppis, B., Bargellesi, A., and Conconi, F. (1970). *Biochemistry 9*, 4175–4179.

[45] Godefroy-Colburn, T. and Thach, R. E. (1981). *J. Biol. Chem. 256*, 11762–11773.

[46] Mehra, A. and Hatzimanikatis, V. (2006). *Biophys. J. 90*, 1136–1146.

[47] Zouridis, H. and Hatzimanikatis, V. (2007). *Biophys. J. 92*, 717–730.

[48] Varenne, S., Buc, J., Lloubes, R., and Lazdunski, C. (1984). *J. Mol. Biol. 180*, 549–576.

[49] Curran, J. F. and Yarus, M. (1989). *J. Mol. Biol. 209*, 65–77.

[50] Sorensen, M. A .and Pedersen, S. (1991). *J. Mol. Biol. 222*, 265–280.

[51] Fluitt, A., Pienaar, E., and Viljoen, H. (2007). *Comput. Biol. Chem. 31*, 335–346.

[52] Olivier, B. G., Rohwer, J. M., and Hofmeyr, J.-H. S. (2005). *Bioinformatics 21*, 560–561.

[53] PySCeS, the Python Simulator for Cellular Systems. http://maxima.sourceforge.net.

[54] Maxima, a computer algebra system. http://maxima.sourceforge.net.

[55] Gnuplot, a portable command-line driven graphing utility a portable command-line driven graphing utility. http://www.gnuplot.info.

[56] Hofmeyr, J.-H. (1995). *J. Bioenerg. Biomembr. 27*, 479–490.

[57] Kacser, H. and Burns, J. A. (1995). *Biochem. Soc. Trans. 23*, 341–366.

[58] Heinrich, R. and Rapoport, T. A. (1974). *Eur. J. Biochem. 42*, 89–95.